Fall 12-16-2017

Moving Bed Biofilm Reactors: Evaluation of Geometry, Attachment Surface Material and Biofilm Populations on the Uptake of Ammonia and Synthetic Organic Contaminants In Wastewater.

Patrick D. McLee

Patrick McLee
Candidate

Civil Engineering
Department

This dissertation is approved, and it is acceptable in quality and form for publication:

Approved by the Dissertation Committee:

Andrew Schuler, Chairperson

Kerry Howe

Bruce Thomson

Carlo Santoro

Moving Bed Biofilm Reactors: Evaluation of Geometry, Attachment Surface Material and Biofilm Populations on the Uptake of Ammonia and Synthetic Organic Contaminants In Wastewater.

By

Patrick McLee

B.S., Environmental Engineering, Manhattan College, 2011

M.E., Environmental Engineering, Manhattan College, 2013

DISSERTATION

Submitted in Partial Fulfillment of the

Requirements for the Degree of

Doctor of Philosophy

Engineering

The University of New Mexico

Albuquerque, New Mexico

May 2017

Acknowledgements

I would like to give special thanks to Dr. Andrew Schuler for facilitating my graduate school experience as a Lobo. His optimism, academic guidance, and willingness to share knowledge are invaluable to my positive growth as an individual.

I am also very grateful for the rest of my committee for their support and scientific passion that provided much of the inspiration towards this work. Equally, I would like that thank my friends, family, and dog for their patience and emotional support on this journey.

Finally, I would like to thank the National Science Foundation for providing funding to my research at the University of New Mexico.

Moving Bed Biofilm Reactors: Evaluation of Geometry, Attachment Surface Material and Biofilm Populations on the Uptake of Ammonia and Synthetic Organic Contaminants In Wastewater.

By
Patrick McLee
B.S., Environmental Engineering, Manhattan College, 2011
M.E., Environmental Engineering, Manhattan College, 2013
Ph.D., Civil Engineering, University of New Mexico, 2017

Abstract

Plastic biofilm carriers are used in biological wastewater treatment to encourage the attachment and retention of microorganisms that metabolize pollutants. The following research was conducted to better understand how different characteristics of the biofilm carrier affect the treatment performance of the attached biofilms in moving bed bioreactors. Lab scale reactors were used in this study to grow nitrifying biofilms in reactors with contrasting and controlled conditions. The effect of surface geometry on nitrification performance was evaluated by testing commercially available moving bed bioreactor media that contrast in physical design, and by varying operational parameters. Additionally, mature biofilm from a similar attachment media type were tested under nitrification-inhibited conditions to better understand microbial populations and metabolisms associated with organic microconstituent removal. Finally, the influence of surface chemistry on biofilm attachment and performance was tested by facilitating biofilm growth on freely floating nylon and high-density polyethylene. Results indicate that organisms grown on more protected, sheltered carrier media respond to changes in mixing more rapidly than those on open and exposed media design. Geometry of the carrier media in a well mixed freely floating reactor influences the environment of the biofilm as it determines the fluid dynamics experienced by the microorganisms. In

biofilm systems designed to remove organic microconstituents, the occurrence of nitrification appears to have benefits for the removal of several different compounds. The type of plastic used to attach biofilms may also influence the total quantity or relative abundance of bacteria types and the performance of microconstituent removal.

Table Of Contents

Chapter 1 Introduction

Introduction

Excess nutrients discharged into natural water systems by human activity are of global concern, in part because they result in eutrophication of receiving waters (Vitousek et al., 1997). To reduce the potential for eutrophication, nitrogen in wastewater commonly removed by a combination of nitrification (ammonia oxidation) and denitrification (nitrite and nitrate reduction to nitrogen gas) during wastewater treatment before it is discharged back into the environment.

In conventional activated sludge (CAS) wastewater treatment, nitrifying (commonly autotrophic) and ordinary heterotrophic bacteria grow in planktonic agglomeration (flocs). Treatment performance is affected by the average amount of time that the mixed liquor is in the system, a parameter known as solids retention time (SRT). Because nitrifiers are generally slow growing, that can require higher SRTs than non-nitrifying systems, which can increase requirements for aeration and loading to secondary clarifiers. Moving bed biofilm reactors (MBBR) and integrated fixed film activated sludge (IFAS) systems include biofilms grown on plastic media, either in separate reactors (MBBRs), or by adding plastic media to activated sludge systems (IFAS). A primary driver for these systems is that they have been shown to be highly effective at increasing nitrification rates (Hem et al., 1994, Randall et al., 1996), as the long SRTs inherent in biofilms is conducive to nitrifier growth (Siripong et al., 2007).

Increasing SRT in CAS is well known for improving nitrification and has been suggested to improve the removal of synthetic organic trace organics as well (Nakada et al., 2006). For this reason, MBBR and IFAS treatment may be a low cost method of upgrading treatment plants to achieve better nitrification.

Objectives

1) The first objective of this study was to evaluate the effect of mixing on nitrification fluxes using two contrasting commercial available media geometry (R1 and R2) and the effect of mass transfer resulting from a closed media (R2) vs. an open media (R1).

2) The second objective of this study was to evaluate differences in removal of targeted trace organics in moving bed bioreactors with and without inhibition of nitrification.

3) The third objective was to compare two different MBBR plastic materials for nitrification performance, organic microconstituent removal performance, and determine the effects of plastic type on biofilm quantity.

Hypothesis

The first hypothesis is that the performance of floating media that support biofilms in MBBR and IFAS systems may be enhanced by geometric design. The internal fluid dynamics of different commercially available floating media may be influenced by contrasting designs of channel dimensions and sidewalls. Internal fluid

flow may affect mass transfer from the bulk liquid to the biofilm by influencing boundary layer thickness and therefor reaction rates. Internal fluid velocity may also affect biofilm sloughing due to mixing induced shear. For these reasons, the physical characteristics of MBBR plastic media may determine the influence that mixing intensity, dissolved oxygen (DO) and temperature have on nitrification performance, biofilm thickness, biofilm community structure, and chemical inhibition.

The second hypothesis is that nitrification can increase the removal rates of trace organics other than the estrogens that have been previously suggested to be removed by nitrification in activated sludge. Analyzing a broad array of trace organics in mixed heterotrophic/nitrifying and purely heterotrophic systems will gives us a better understanding of the benefits to nitrification in the removal of all other synthetic organic contaminants found in wastewater.

The last hypothesis for this study is that nutrient and trace organics removal from wastewater can be improved by altering the chemistry of the biofilm attachment surfaces. Surface chemistry of plastic biofilm carriers used in IFAS and MBBR systems determines adhesion, attachment strength, and detachment of microbial populations that effect system functionality. Attachment surface chemistry may be exploited to engineer biofilms for the removal of synthetic organic contaminants through biodegradation and/or adsorption.

Chapter 2 The Effect of Geometric Design and Temperature on Moving Bed Bioreactor Media Performance and Resulting Biofilm Populations

Introduction

The research described in this chapter evaluated the effect of mixing, temperature and dissolved oxygen on nitrification fluxes. Two different commercially available media with contrasting geometries were used in lab scale reactors to grow nitrifying biofilms and evaluate how these variables affect nitrification performance and attached microbial populations.

Background

Nitrification

Nitrification is a 2 step biological process shown in equations 2.1 and 2.2.

$$2NH_4^+ + 3O_2 \rightarrow 2NO_2 + 4H^+ + 2H_2O \quad (2.1)$$

$$2NO_2^- + O_2 \rightarrow 2NO_3^- \quad (2.2)$$

The first step is the oxidation of ammonia to nitrite by the ammonia oxidizing bacteria (AOB) such as *Nitrosomonas* under aerobic conditions (Kowalchuk et al., 2001) The second step of nitrification is the aerobic oxidation of nitrite to nitrate by nitrite oxidizing bacteria (NOB), including the genus *Nitrobacter* (Kowalchuk et al., 2001). AOB and NOB obtain energy from by coupling oxygen reduction with ammonia and nitrite oxidation, respectively. Autotrophic nitrifiers use this energy to convert CO_2 to cellular carbon (Metcalf and Eddy 2003). Recently, several other groups of bacteria,

such as xanthamondacia, springamonadacia, pseudomonas stutzeri yzn-001, and Alcaligenes faecalis have been reported to oxidize ammonia by an unknown heterotrophic pathway (Fitzgerald et al., 2015, Jo et al., 2005, Zhang et al., 2011) to nitrite and nitrate.

Ammonia Inhibition

Many compounds are known to inhibit nitrification, including heavy metals such as zinc, copper, cadmium (Chandran and Love, 2008; Juliastuti et al., 2003), and a variety of organic compounds. Bacterial growth in biofilms found in integrated fixed-film activated sludge (IFAS) may provide protection to nitrifiers for some inhibitors (Kim et al., 2010).

Disruptions of performance in these highly loaded nitrifying reactors resulted in high ammonia effluent concentrations. Nitrite oxidizing bacteria (NOB) inhibition by free ammonia (FA) was possible in the follow experiment, and may account for the high nitrite concentrations through out most of the study (Figures 2.5B and 2.6B).

Based on relationships reported by Anthonisen et al., 1976, the minimum levels of ammonia and nitrite inhibition for the pH ranges and temperatures used in our study (pH = 7.15 to 7.5 and T = 10.5 or 21 degrees Celsius) were calculated and compared to measured values to determine the possibility of AOB and/or NOB inhibition (Schuler and Melcer 2014**)**. The ranges of ammonia species (NH_4^+ + FA) and nitrite (NO_2^- + Free nitrous acid (FNA)) concentrations at which inhibition may begin were calculated using pKa relationships (Table 2.1).

Table 2.1. Concentrations of nitrogen species at which inhibition may begin for AOB and NOB calculated from data in Anthonisen et al., 1976 (from Schuler and Melcer 2014).

		T = 21°C		T = 10.5°C	
		pH = 7.15	pH = 7.5	pH = 7.15	pH = 7.5
AOB inhibition by ammonia					
	FA, mg N/L	total ammonia, mg N/L		total ammonia, mg N/L	
Low estimate	8	1,400	**620**	3,100	**1,400**
High estimate	120	20,700	9,300	46,000	21,000
NOB inhibition by ammonia					
	FA, mg N/L	total ammonia, mg N/L		total ammonia, mg N/L	
Low estimate	0.1	14	**6.2**	31	**14**
High estimate	1	140	62	310	140
AOB or NOB inhibition by nitrite					
	FNA, mg N/L	total nitrite, mg N/L		total nitrite, mg N/L	
Low estimate	0.07	370	830	**280**	620
High estimate	0.8	4,700	11,000	3,500	7,900

Biofilm Mass Transfer

Mass transfer into a biofilm can be modeled as transport of a constituent from a bulk solution, with diffusion through a laminar boundary layer, and then with diffusion through a biofilm (Figure 2.1). (De Beer et al., 1996)

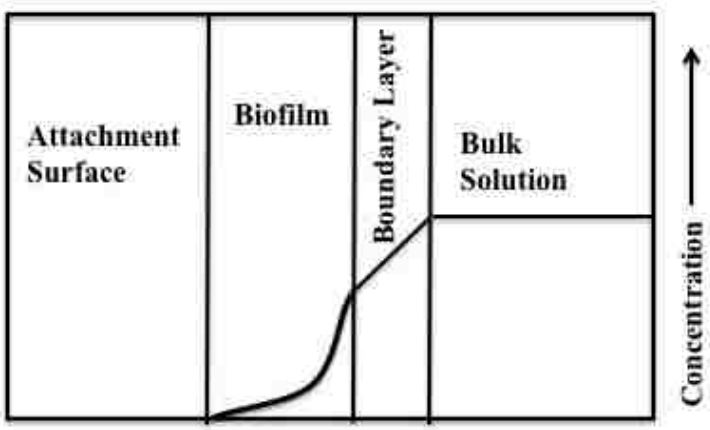

According to this model, increased mixing rates will decrease the boundary layer thickness, thereby increasing the rate of mass transport into and out of a biofilm (De Beer et al., 1996). For nitrification, key transported constituents are oxygen and ammonia into the biofilm, and nitrite, nitrate, and protons out of the biofilm (Eq. 2.1 and 2.2).

Hypothesis

It was hypothesized that the performance of suspended media that carry biofilms in MBBR and IFAS systems may be enhanced by geometric design. It was also hypothesized that while increasing mixing rates will tend to increase nitrification rates, the extent of this affect will depend on media geometry, with a less pronounced affect in

media with more “open” design. The internal fluid dynamics of different media may be influenced by media geometry. Internal fluid flow may affect mass transfer from the bulk liquid to the occupying biofilm by influencing boundary layer thickness and therefor reaction rates. Internal fluid flow may also influence the susceptibility of the biofilm to sloughing due to mixing induced shear. For these reasons, the physical characteristics of MBBR plastic media may determine the influence that mixing intensity, dissolved oxygen (DO) and temperature have on nitrification performance, biofilm thickness, biofilm community structure, and chemical inhibition.

Objectives

The objectives of the research described in this Chapter were to 1) evaluate the effect of mixing on ammonia flux in two types of commercially available MBBR media with contrasting geometries. 2) Compare the biofilm populations on each media type after reaching equilibrium at the maximum ammonia uptake. 3) Evaluate the effect that temperature has on moving bed biofilm populations at high and low temperatures.

The experimental approach to address these objectives was to grow nitrifying biofilms on each media type in continuously flowing, well-mixed reactors. Once nitrifying biofilms were well established, batch testing with mixing as an experimental variable was conducted to determine the effect of mixing on ammonia flux.

Methods

Reactor Operation

Specifications of the continuous systems are listed in Table 2.2, and a schematic is shown in Figure 2.2.

Table 2.2 Reactor Specifications

Parameter	R1	R2
Reactors		
Total volume (including headspace) (L)	17.4	17.4
Working volume (liquid + media) (L)	9.36	9.42
Liquid volume (L)	8.15	7.96
Dimensions including head space		(W x D x H)
(inches)		8.0 x 8.0 x 16.6
(cm)		20.3 x 20.3 x 42.2
Flow rate (L/d)	10.1	10.1
HRT based on working volume (hour)	22.3	22.4
HRT based on liquid volume (hour)	19.4	19
Media		
Media specific surface area (m^2/m^3)	650	630
Media fill volume (percent)	32.1	31.9
Media area in reactor (m^2)	1.95	1.89
Media area/working volume (m^2/m^3)	208	201
Controls		
Aeration and mixing method		Coarse bubble
Target mixing rate (G) (-/sec)		240–327 (variation discussed below)
Dissolved oxygen concentration (mg/L)		>6.5 mg/L (measured but not controlled)

Table 2.2 Reactor Specifications

Parameter	R1	R2
pH control range	7.15–7.50	
Temperature (°C)	21.0 or 10.5 in temperature-controlled water bath	

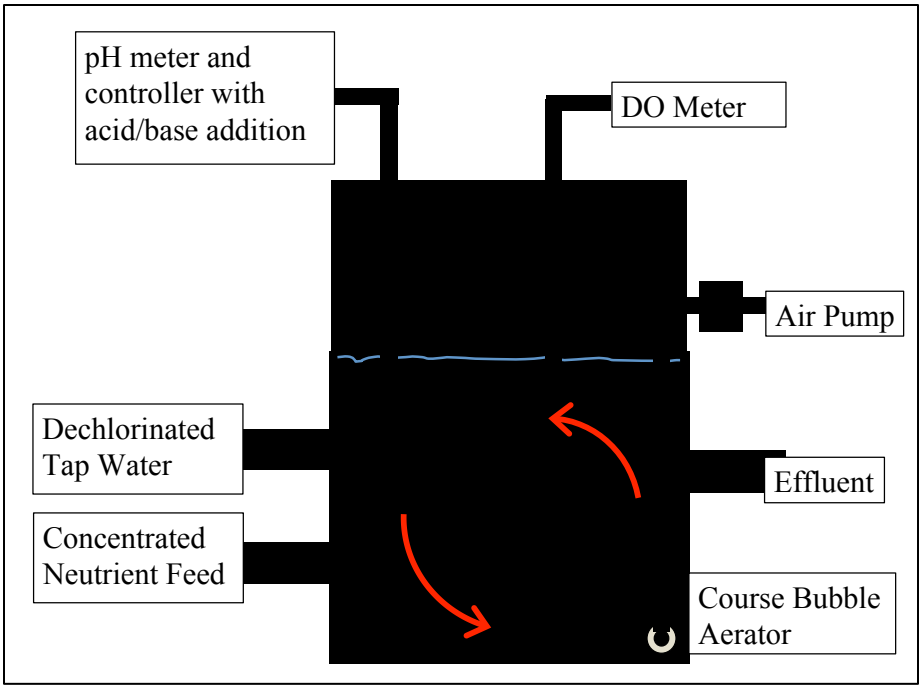

Two commercially available media were tested. The Reactor 1 (R1) and 2 (R2) media had similar specific surface areas (Table 2), but R1 media were smaller (14 mm long, 12 mm diameter) with a more open design (with openings on all sides), while R2 media were larger (15 mm long, 20 mm diameter) and had a more protected interior (with openings on 2 sides). (Figure 2.3)

[redacted]

Reactor Feed

The reactors were continuously fed a synthetic wastewater that was high in ammonia, but low in organic carbon in order to produce a highly active nitrifying biofilm for batch testing. Table 2.3 shows the composition of the synthetic feed. An asterisk denotes net concentrations after combining nutrient and water feeds.

Table 2.3: Synthetic Feed (based on Hem et al., 1994)

Chemical	Concentration (mg/L)*
NH_4Cl	Variable
KH_2PO_4	100
$NaHCO_3$	350
$FeSO_4$-$7H_2O$	5
$CaCl_2$	16
$MgSO_4$-$7H_2O$	40
$CuSO_4$-$5H_2O$	0.12
$NaMoO_4$	0.0019
EDTA	6.6

Synthetic feed was continuously fed to the reactors using peristaltic pumps as two separate streams of dechlorinated tap water and autoclaved, concentrated nutrient feed. The feed was added in this manner to reduce the volume of nutrient feed preparation. Tap water was used to provide a source of trace elements. The tap water residual chlorine was removed by bubble aeration for 24 hours (h) following the addition of 1.5 mg/L sodium bisulfite ($NaHSO_3$) (Bill et al., 2010). Net concentrations of the synthetic feed (as added to the reactor after mixing with water) are shown in Table

2.3. Treated effluent overflowed each reactor via the effluent port, the location of which determined the reactor volume No organic carbon was included in the feed to reduce the heterotroph component of the biofilms as much as possible. Ammonium chloride was the sole source of nitrogen in the feed, and its concentration was adjusted with the goal of maintaining a target effluent ammonia concentration between 10 and 50 mg N/L. This ammonia residual aimed to prevent limiting biofilm activity with out creating an excess of ammonia to inhibit nitrification. Influent ammonia feed concentrations varied from initial concentrations of 30 to 40 mg N/L early in reactor biofilm development to 400 to 600 mg N/L once the biofilm was fully matured.

Mixing

Mixing of the reactors was done by coarse bubble aeration through a horizontal section of polyvinyl chloride pipe spanning the bottom width of the reactor. Coarse bubble air was delivered at a steady flow rate to provide constant mixing intensity in the reactors. Mixing intensity can be described by the velocity gradient (G, 1/s), which can be calculated using Equation 2.3 (Parker 1970).

$$G = \sqrt{\frac{Q * \gamma * H_L}{\mu V}} \qquad \text{(eq. 2.3)}$$

where:

G = velocity gradient (1/s)

Q= airflow rate (m^3/s)

γ = water specific weight (N/m^3)

H_L = head loss (m) (distance from aerators to water surface)

μ = water dynamic viscosity ($N*s/m^2$)

V= volume (m^3) (working volume used for all calculations)

Mixing rates in the continuous reactors and in the batch experiments were selected based upon a review of typical G values used in full-scale MBBR installations (Melcer et al., 2014). Table 2.4 presents data from 16 full-scale reactors, some of which comprised several basins, along with calculated G values. Figure 2.4 is a histogram of this distribution.

Table 2.4. Full-Scale MBBR Plant Calculated Values of G (SI Units) (from Schuler and Melcer 2014)

Plant	Volume	Depth	Air Rates per Basin (m^3/min)				G (1/s)			
	m^3	m	Basin No.				Basin No.			
			1	2	3	4	1	2	3	4
A	623	4.1	92	61			315	257		
B	1,133	4.9	88	74			249	228		
C	696	6.1	27	27	27	27	198	198	198	198
D1	1,631	4.9	139	139			261	261		
D2	2,276	4.9	96	96			183	183		
E	580	6.1	42	35			270	247		
F	58	3	9	6	6		274	228	221	
G1	306	3.7	9	9			134	134		
H	505	6.1	66	23			360	212		
I	1,133	5.5	119	60			306	218		
J1	1,298	5.3	107				267			
J2	882	4.4	43				189			
G2	842	6.2	54	54	54		255	255	255	
SJ	1,245	4.9	46				171			
M	169	4.1	11				210			
P	187	3	33	27			296	270		

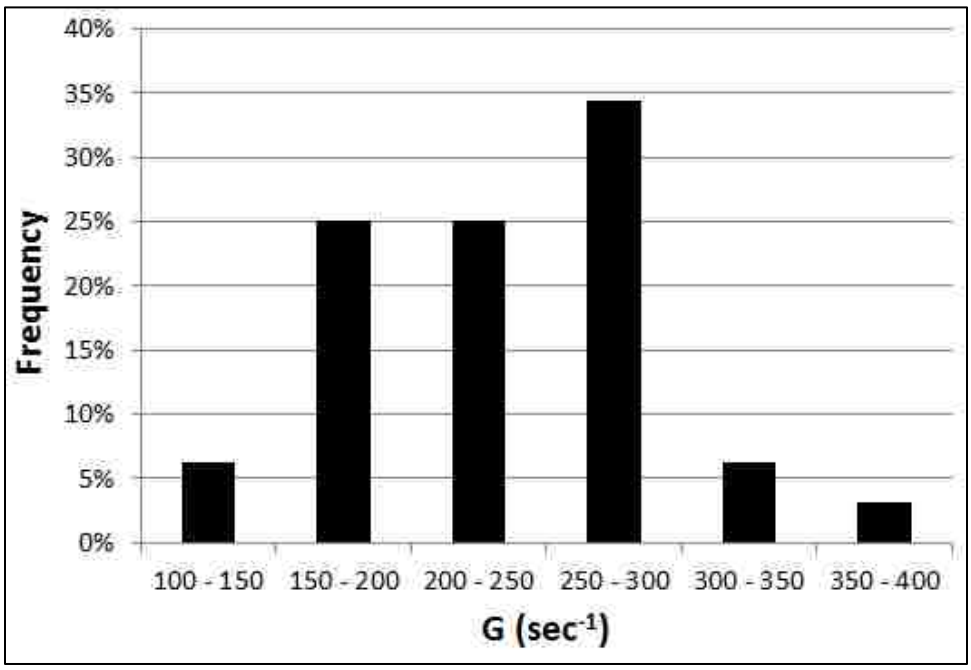

[redacted]

The range of G values calculated for these systems was 134/s to 360/s. The average across all plants was 233/s. Most of the high G values are associated with plant operating at high oxygen uptake rates.

The high end of the G value range (380/s) used in batch experiments was based on the range shown in Table 2.4. The minimum batch experiment G value of 158/s was based on the minimum G value that provided enough movement of the media in order to keep the media well mixed. The initial mixing rate used in each continuous system was 240/s but was increased to 298/s after approximately one month of operation in order to reduce sloughing observed in initial batch tests.

Startup and Routine Operation of Continuous System

Both reactors were inoculated in March of 2013. 3 L of each media were incubated at room temperature for 3 days in a bucket containing 10 L of fresh activated sludge, with coarse-bubble mixing. The activated sludge was obtained from the Albuquerque, New Mexico, Southside Water Reclamation Facility (SWRF) activated sludge system, which has a Modified Ludzack-Ettinger configuration. After inoculation with sludge, the media were transferred to the continuous flow reactor that initially contained approximately 5 L of activated sludge and 5 L of primary effluent obtained from the SWRF. Thereafter the systems were operated with continuous synthetic feed.

The reactors were run in three phases, which differed in temperature (Table 2.5).

Table 2.5. Reactor Operation Phases

	R1 **Begin–end**	**R2** **Begin–end**
Phase 1: T = 21°C	3/19/2013–9/2/2013 Day 0-169	4/25/2013–9/2/2013 Day 0-169
Phase 2: T = 10.5°C	9/3/2013–1/13/2014 Day 169-302	9/2/2013–1/22/2014 Day 169-309
Phase 3: T = 21°C	1/13/2014–4/21/2014 Day 302-718	1/23/2014–4/21/2014 Day 309-718

In Phase 1, the reactors were run at 21°C in a temperature-controlled water bath. After an apparent steady state was reached in each phase several batch tests were run (described below). Steady state was assumed as the system consumed a consistent amount of ammonia given a constant ammonia loading rate.

In Phase 2, the temperature was decreased to 10.5°C in both reactors and the target G value in Reactor 2 remained at 298/s. Due to an operational error the G value in R1 ranged from 305/s to 327/s from day 168, to day 282 after which it was returned to

298/s. In Phase 3, the temperature was returned to 21°C in both reactors. This was done to test whether the reactors could utilize ammonia at the ammonia loading rate values applied during Phase 1, and to conduct additional batch experiments to evaluate the effects of bulk liquid phase DO concentration on mass transfer characteristics in both reactors.

Batch Testing

Batch nitrification tests were conducted on the media grown in the continuous systems in which mixing (aeration) rates were varied from G = 160/s to 390/s.. Additional tests were conducted with varied dissolved oxygen concentrations from 3 to 21 mg/L. Batch tests were conducted by stopping the continuous feed, rinsing the media, and adding fresh feed. Measurements of NH_3, NO_2^-, and NO_3^- were then taken over time.

The batch testing data consisted of ammonia, nitrate, and nitrite concentrations measured at specific time intervals. During each test the average temperature, airflow rate, and DO concentration were recorded. The average rate of ammonia oxidation was estimated by a best-fit linear regression over the course of the batch experiment. Flux rates were calculated according the Equation 2.4.

$$J = \frac{dC}{dt} \times \frac{1}{SSA} \times \frac{1}{F} \qquad (2.4)$$

Where

J = mass flux relative to media surface area (g/m2/d)

SSA = media specific surface area (m^2/m^3)

F = media fill percentage (unitless)

C = ammonia concentration (g/m^3)

t = time (day)

Biomass

Prior to batch testing, 5 to 10 media pieces were taken from a given reactor, and each piece was thoroughly cleaned by brushing using Proxabrush "Go-Betweens" (Sunstar Americas Inc. Schaumburg, IL.) which were developed for dental cleaning. The removed biofilm was collected by rinsing with DI water, the total attached solids (TAS) and volatile attached solids (VAS) in the rinse water was measured according to the total and volatile suspended solids Standard Methods 2540B and 2540E, respectively (American Public Health Association et al., 2012). The biofilm mass concentration in the reactor was calculated using Equation 2.5:

$$\text{Total biofilm solids, TBS } \left(\frac{\text{mg}}{\text{L}}\right) = \frac{\text{dry mass removed from media (mg)}}{\text{reactor working volume (L)}} \times \frac{\text{total media pieces}}{\text{pieces of media tested}} \quad \text{(eq. 2.5)}$$

Nitrogen Species

Samples taken for nitrogen species analysis were immediately filtered through a 0.45 μm nylon membrane syringe filter, stored at 4°C, and measured within 24 hours. All measurements of nitrogen species were performed using Hach kits with a Hach

DR2700 spectrophotometer (Hach Company, Loveland, Colorado, USA) as follows: NH4-N: Nitrogen-Ammonia Reagent Set, TNT, AmVer (Salicylate), High Range, Product 2606945, NO2-N: NitriVer 3 TNT Reagent Set, Nitrogen-Nitrite, Low Range, Product 2608345, NO3-N: NitraVer X Nitrogen-Nitrate Reagent Set, High Range, Product 2605345. All kits were used in accordance with the manufacturer's instructions, except a correction for potential nitrite interference with the nitrate measurement was started on January 6, 2014. The manufacturer's instructions note that nitrite interference could occur at nitrite concentrations greater than 12 mg/L. Per the manufacturer's instructions, this interference was removed by adding 400 mg urea to 10 mL of sample. Nitrate concentrations measured prior to January 6, 2014, may therefore overestimate the actual values.

pH Control

pH was measured and controlled in the range of 7.15 to 7.5 in each reactor with a pH controller (Chemcadet Model 5652-00, Cole-Parmer, Vernon Hills, Illinois, USA) with a combination, double-junction, gel-filled pH electrode (Model EW-59001-70, Cole-Parmer, Vernon Hills, Illinois, USA). Acid and base solutions were 0.1 M hydrogen chloride (HCl) and 0.7 M sodium carbonate (Na2CO3), respectively.

Dissolved Oxygen

DO was measured using a Hach IntelliCAL LDO101 standard luminescent/optical DO probe with a Hach HQ440d multi-parameter meter (Hach Company, Loveland, Colorado, USA).

Illumina Next Gen DNA Sequencing

MBBR media was thoroughly cleaned by brushing using Proxabrush "Go-Betweens" dental brushes (Sunstar Americas Inc. Schaumburg, IL.) The removed biofilm was collected by rinsing with DI water, and excess liquid was centrifuged off to form a pellet. The pellet was frozen and shipped to RTL Genomics, Research and Testing Laboratory (Lubbock, TX) for DNA extraction and Illumina Next Generation sequencing using the 357wF-785R assay and 784F [5′ -RGGATTAGATACCC-3′] and 1064R [5′ -CGACRRCCATGCANCACCT-3′]) bacterial DNA primers.

Results and Discussion

R1 performance in terms of ammonia removal, nitrite and nitrate production, and biofilm biomass (VBS) over the 4 experimental phases is shown in Figures 2.5A, 2.5B, and 2.5C. Similarly, R2 performance is shown in Figures 2.6A, 2.6B and 2.6C

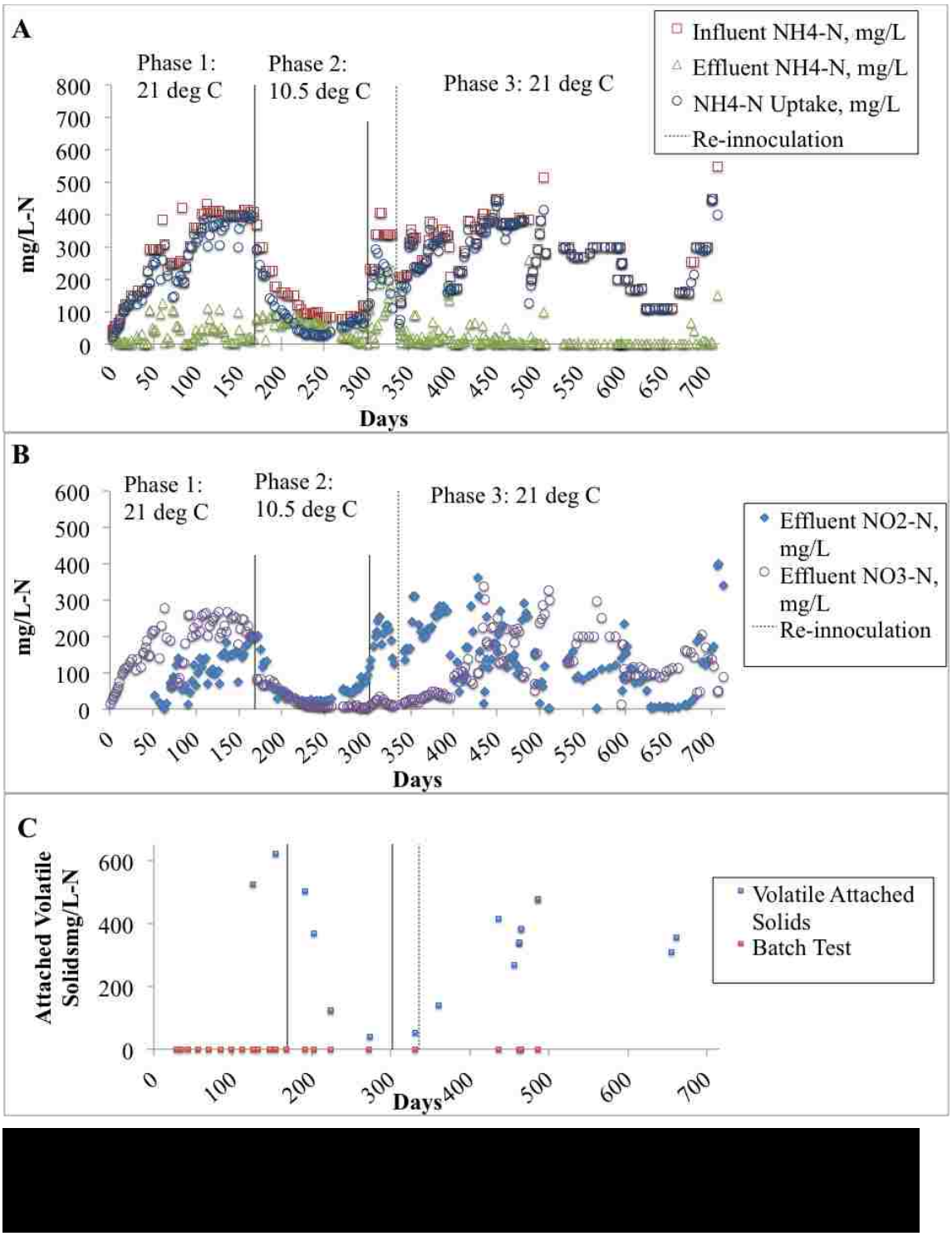

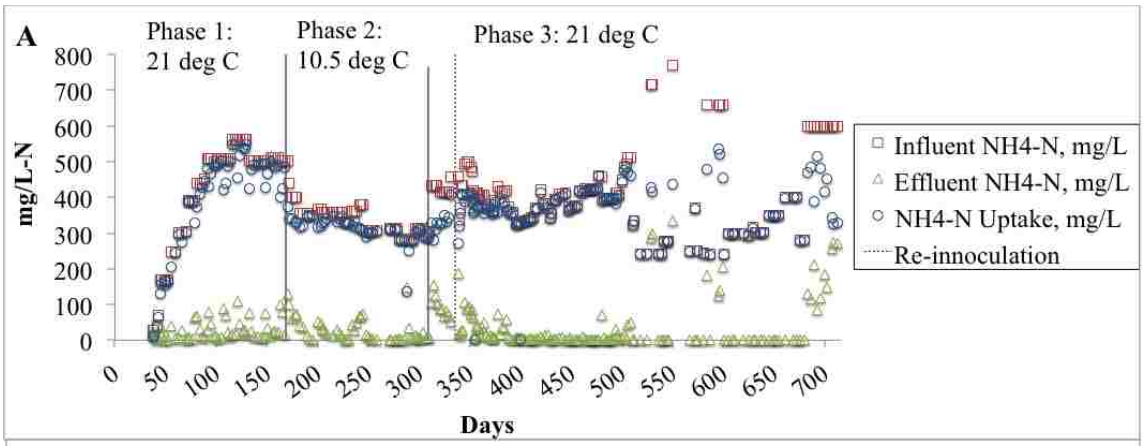

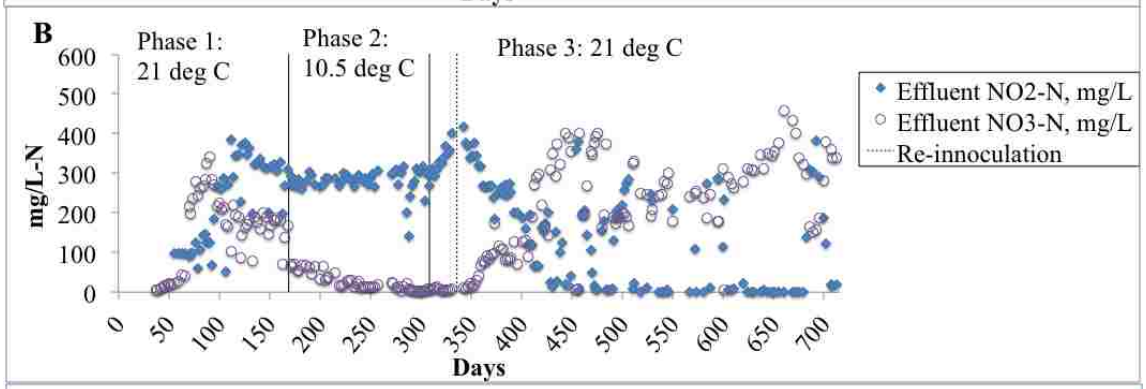

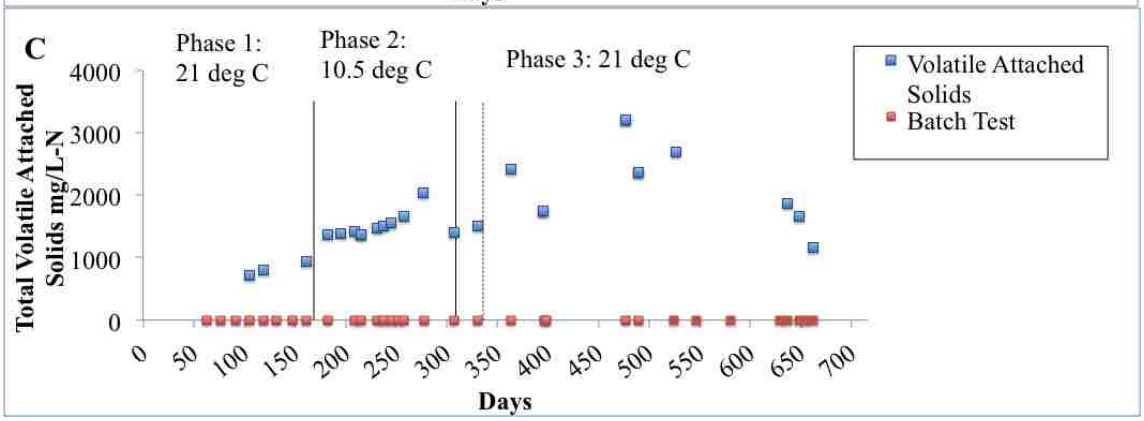

Phase 1 Reactor Performance

As noted, the objective of experimental Phase 1 was to grow biofilms in both reactors at room temperature in order to conduct batch tests at variable mixing rates.

After inoculation, ammonia uptake increased in both reactors (Figures 2.5A and Figure 2.6A), as well as nitrite and nitrate concentrations (Figures 2.5B and Figure 2.6B). The ammonia feed concentration was gradually increased after startup in both reactors an attempt to neither limit nitrifier growth because of low reactor NH3 concentrations or to inhibit nitrifier growth because of high reactor NH3 concentrations.

In R1, the ammonia feed concentration was gradually increased from 40 mg N/L to 400 mgN/L, with the goal of maintaining effluent ammonia concentration between 10 and 50 mg N/L (Figure 2.5A). Nitrification was initially complete in R1, as nitrate concentrations nearly matched ammonia uptake. Toward the end of Phase 1, concentrations of nitrite increased steadily relative to nitrate concentrations (Figure 2.5B), indicating decreasing NOB activity relative to AOB activity . The reason for nitrite accumulation in this phase and later phases is not known, but NOB inhibition by free ammonia (NH_3) was possible during much of the study, as discussed in Background section of the chapter. Higher influent ammonia concentrations were used in this study (up to 433 mg NH3-N/L in R1, Phase 1) than normally found in domestic wastewater to provide highly active biofilms. One consequence of this was that disruptions in reactor performance could greatly increase effluent ammonia concentrations, and this may have inhibited NOB activity (thereby increasing nitrite concentrations as seen at the end Phase 1 in reactor 1). High nitrite concentrations may have also contributed to NOB inhibition as well. AOB inhibition by FA was estimated to begin under the "worst-case"

condition of pH = 7.50 at total ammonia concentration of 620 to 9,300 mg N/L at T = 21.5°C and 1,400 to 21,000 mg N/L at T = 10°C (Table 2.1). As AOB never experienced concentrations of FA to this order of magnitude in Reactor 1 or 2 throughout the study (Figure 2.5A and Figure 2.6A), AOB inhibition by FA was unlikely in either reactor.

NOB inhibition by FA was estimated to occur under the "worst case" condition of pH = 7.50 at total ammonia concentration of 6.2 to 62 mg N/L at T = 21.5°C and 14 to 140 mg N/L at T = 10°C (Table 2.1). These inhibitory levels were within the range of effluent ammonia concentrations observed in this study (Figures 2.5A and Figure 2.6A), and may account for the high nitrite concentrations observed in both reactors throughout the study.

The most likely form of inhibition was high ammonia concentrations decreasing NOB activity, although it is also possible that high nitrite concentrations decreased NOB activity as well. A decrease in NOB activity is apparent by accumulating nitrite and low nitrate concentrations in both reactors (Figure 2.5B and Figure 2.6B).

Occasional small decreases in apparent ammonia uptake and effluent nitrate and nitrite effluent concentrations were observed, followed by periods of recovery over several days. These events occurred immediately after batch tests due to the refilling of the reactor after each batch test with fresh feed solution. The replacement feed consisted of a high ammonia concentration relative to the effluent solution removed from the reactors before the batch tests, with zero nitrate and nitrite concentrations. This practice applied a pulse ammonia load to the reactors, while removing all accumulated nitrate and nitrite. It typically took the reactor several days to equilibrate back to a steady state. For this reason, the increases in effluent ammonia and decreases in ammonia uptake and

nitrite and nitrate concentrations during Phase 1 was likely the result of the batch testing procedure, rather than a decrease in performance. The batch test procedure was modified after Phase 1 in both reactors such that the reactor liquid phase was removed before batch testing, saved, and returned after the batch test was complete, before restarting the continuous system.

R2 was inoculated approximately one month after R1 (Figure 2.6A). Initial ammonia loadings were increased more rapidly in R2 than in R1, to prevent ammonia limiting conditions that were experienced during startup of R1, as indicated by low effluent ammonia concentrations. For example, after 30 days of operation, the R2 feed ammonia concentration had been increased to 304 mg N/L, with nearly complete uptake, while after 30 days R1 influent had been increased to 166 mg N/L (Figure 2.5). Two months after startup, R2 activity reached an approximate steady state at approximately 500 mg N/L ammonia uptake, with influent ammonia concentration equal to 415 mgN/L.

Similar to R1, nitrate concentrations in R2 initially matched the ammonia uptake rate, followed by a gradual increase in nitrite concentration. Nitrite levels in R2 were nearly double the nitrate concentrations (300 and 160 mg N/L, respectively) by the end of Phase 1.

Phase 1 Microbial Biomass and Populations

R1 produced a biofilm with less total biomass than R2, with a value of 619 mg/L (0.30 mg/cm^2) in R1 and 2000 mg/L (1.00 mg/cm^2) in R2 at the end of Phase 1. It is hypothesized that the open design of the R1 media resulted in higher internal fluid

velocities and induced shear, when compared to the more protected R2 media. Higher shear associated with the R1 media may explain the difference in attached biomass that accumulated by the end of Phase 1.

Figure 2.7 shows the relative abundance of bacteria family present in the R1 and R2 biofilm at the end of Phase as determined by Illumina DNA sequencing analysis.

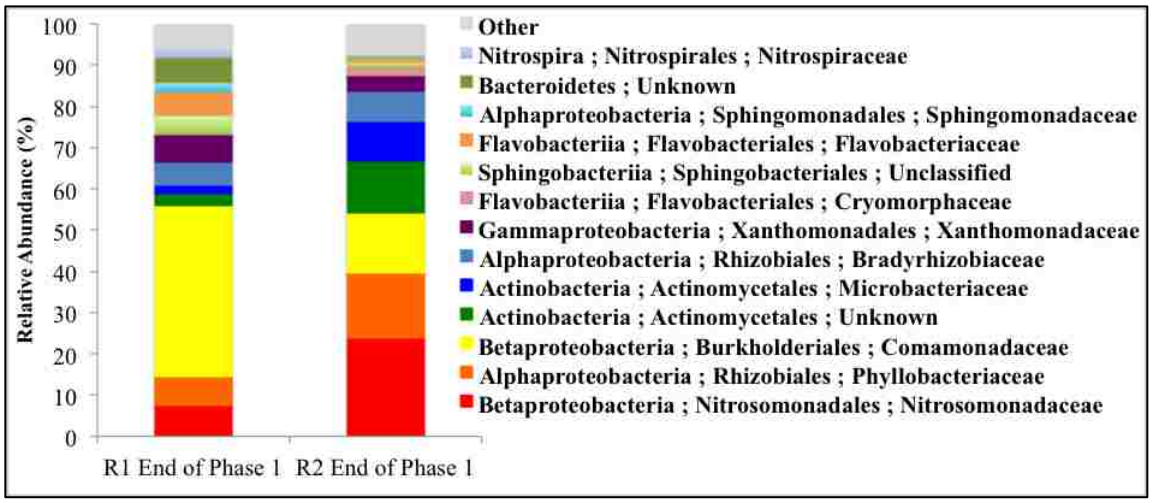

The bacteria family *Comamonadaceae* made up the majority of the R1 biomass (41.5%) but was less abundant on the R2 media (14.5%). Xin et al., 2016 reported that *Comamonadaceae* (also measured by Illumina) dominated a sequencing batch kettle reactor (SBKR) for wastewater nutrient removal operated at varying aeration pressures As aeration pressure increased from 0.2 to 0.6MPa in the SBKR, the relative abundance of *Comamonadaceae* increased from 22% to 40% as a result of increased dissolved oxygen in the higher pressure aeration systems, suggesting that *Comamonadaceae* may thrive in oxygen-rich environments. These results may have been consistent with those obtained for Phase 1 of this study, as the reactor with higher *Comamonadaceae* population (R1) may have had higher dissolved oxygen concentrations in the biofilm, as

indicated by (1) less biofilm per surface area on R1 compared to the R2 media, which likely indicated a thinner biofilm with less resistance to oxygen mass transfer, and (2) the more open structure of the R1 media relative to the R2 media (Figure 2.3) may have resulted in less resistance to liquid flow through the media and consequently higher local fluid velocities, which would decrease the laminar boundary layer (Figure 2.2) and increase rates of oxygen mass transfer into the biofilm. The higher internal fluid velocities are also consistent with thinner biofilms, as the higher shear forces would tend to lead to thinner biofilms.

In addition, R2 exhibited a higher relative abundance of the AOB family Nitrosomonadaceae (24%) than did R1 (8%) and may explain greater ammonia uptake observed in R2 during this time. A lower relative abundance of the AOB family *Nitrosomonadaceae* in R1 compared to R2 may also be attributed to competition with the most abundant bacteria *Comamonadaceae* found in on R1 media. A higher relative abundance of the NOB *Nitrospiraceae* in R1 (2.5%) and the absence of this family in R2 (0.04%) may be attributed to inhibition of NOB by the higher ammonia concentrations in R2 throughout much of Phase 1 (Figure 2.5A and Figure 2.6A) These results were also consistent with the observed higher nitrite concentrations in R2 than in R1 during Phase 1 (Figure 2.5 and Figure 2.6), as nitrite accumulation is evidence of decreased NOB activity relative to AOB activity.

During Phase 2, both reactors were operated at a lower temperature to evaluate how different media geometries respond to stressful conditions. The temperature was decreased in both reactors after sampling on September 2, 2013 (day 168) from 21 degrees Celsius to 10 degrees Celsius.

Phase 2 Reactor Performance

The effluent ammonia concentration in Reactor 1 increased to approximately 85 mg N/L shortly after the decrease in temperature at the start of Phase 2 (Figure 2.5A). In order to achieve the target ammonia effluent range of 10–50 mg N/L mg N/L the feed ammonia concentration was decreased. Despite this effort, the effluent ammonia concentration remained higher than the target range at approximately 75 mg N/L. During this time, effluent nitrate and nitrite concentrations decreased to less than 20 mg N/L. Toward the end of Phase 2 ammonia influent was reduced to 90 mg/L in order to achieve an effluent ammonia concentration of 20 mg N/L at equilibrium. The nitrite concentration increased to approximately 60 mg N/L at the end of Phase 2, with nitrate concentrations less than 10 mg N/L.

The biomass in R1 decreased from 540 mg/L (0.26 mg/cm^2) in late September (day 195), to 41 mg/L (0.02mg/cm^2) by mid-December (day 272) in Phase 2 (Figure 2.6C) . The role of the unintentional increase in mixing rate in R1 Phase 2 from 298/s to 327/s described earlier is not known, but it is possible that this contributed to deterioration of AOB and NOB activity by increasing shear and sloughing of the biofilm. As noted, the R1 mixing rates was decreased to 298/s on day 283, however performance did not improve.

The decreased temperature in R2 Phase 2 also resulted in decreased AOB and NOB activity, as indicated by reduction in R2 ammonia uptake and nitrate production (Figures 2.5A and Figure 2.5B). NOB activity was particularly affected, with a decrease in nitrate concentrations from approximately 200 mg N/L at the end of Phase 1 to 13 mg N/L in mid November (day 241). In response to the reduction in ammonia uptake, the

influent ammonia was decreased from 379 mg N/L to 307 mg N/L in order to reduce the possibility of NOB inhibition by higher ammonia effluent. Ammonia effluent decreased from 72 mg N/L in mid (day 241) November, to 1.8 mg N/L in early December (day 258), but reactor nitrate concentrations continued to decrease to nearly zero by the end of Phase 2. Despite ammonia uptake decreasing in this phase, the amount of biofilm in the reactor increased from approximately 1500 mg/L (0.74 mg/cm^2) to 2000 mg/L (1.00 mg/m^2) VAS (Figure 2.5C)

Phase 2 Microbial Biomass and Populations

Figure 2.8 shows the results from Illumina DNA sequencing analysis performed on a R2 biomass sample at the end of Phase 2, Phase 3. Illumina analyses were not conducted on R1 in Phase 2 due to the large loss in R1 biomass during this time.

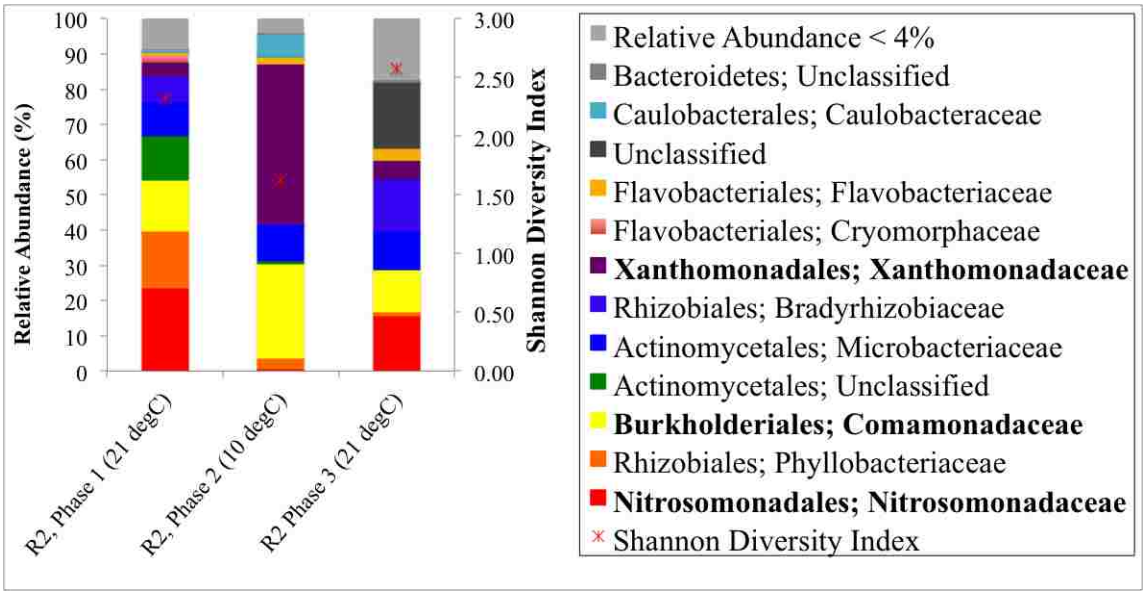

[redacted]

In R2, moving from Phase 1 21 degrees C to Phase 2 10 degrees C dramatically affected the relative abundance of bacteria families present on the biofilm. By the end of Phase 2, the family Nitrosomonadaceae decreased in relative abundance from 23.7% (end of phase 1) to 0.6% percent. This reduction in Nitrosomonadaceae was consistent with the reduction in ammonia uptake during Phase 2, shown in Figure 2.6A. Despite ammonia uptake decreasing in this phase, the amount of biofilm in the reactor increased from approximately 1500 mg/L (0.74 mg/cm^2) to 2000 mg/L (1.00 mg/m^2) VAS (Figure 2.5C) suggesting that colder temperatures facilitated growth or organisms that nitrify less efficiently or not at all, or possibly decreased detachment rates. Illumina sequencing results shown in Figure 2.8 show the family Xanthomonadaceae increased from 4.0% at the end of Phase 1 to 45.3% at the end of Phase 2. Xanthomonadaceae is reported to by Allen et al., 2004 and Cydzik-Kwiatkowska 2015 to be crucial contributors to extra cellular polysaccharide (EPS) production in biofilm communities, possibly explaining

the continuous increase of biomass on R2 media during this phase. In studies conducted by Fitzgerald et al., 2015, the family Xanthomonadaceae was found to be involved with heterotrophic ammonia oxidation under low dissolved oxygen conditions (<0.3mg.L) In R2, where the biofilm is dominated by Xanthomonadaceae, the biofilm thickness increased and dissolved oxygen may have decreased deep inside the biofilm. Relative abundance of the family *Comamonadaceae* also increased from 14.5% at the end of Phase 1 to 26.9% at the end of Phase 2. This may be explained by the preference of *Comamonadaceae* for oxygen rich environments, and the increase in dissolved oxygen saturation from temperature decrease. Extremely low levels of nitrate in Phase 2 (Figure 2.6B) were consistent with the complete absence of the only detected NOB family Nitrospiraceae in R2. Figure 2.8 also shows that the overall family diversity expressed by Shannon Diversity Index (SDI) greatly decreased from Phase 1 to Phase 2.

Phase 3 Reactor Performance

During Phase 3, the reactors were returned to 21°C in order to supplement high-temperature batch testing (described below) conducted during Phase 1. Ammonia uptake increased in R1 after the Phase 3 temperature increase (Figure 2.5A), but did not return to the levels of uptake observed during Phase 1. Biomass measurements in R1 demonstrated only a small increase in solids in Phase 3, from 41 mg/L (0.02 mg/cm^2) in mid December (day 272), to 56 (0.03 mg/cm^2) mg/L in mid February (334) (Figure 2.5C). In an effort to accelerate recovery from the Phase 2 crash, R1 was reinoculated using the same protocol employed at the start of the experiment. Following reinoculation (day 336, Figure 2.5C), R1 biomass concentration increased to 140 mg /L (0.07 mg/cm^2)

on March 13, 2014 (day 360) however this concentration was well below levels observed in Phase 1 (645 mg/L). Reactor activity increased following reinoculation, but ammonia uptake did not return to Phase 1 levels.

In order to accommodate for increasing ammonia uptake that resulted from temperature increase at the start of Phase 3, the feed ammonia concentration to R2 was increased from 300 to 435 mg N/L. Although ammonia uptake increased, the effluent ammonia concentration also increased, averaging 70 mg N/L in the first month of Phase 3.

Visual inspection of the media determined that approximately 40 percent of the R2 media contained little to no biomass in early Phase 3. It was hypothesized that these were media that had been removed and cleaned for biomass measurements, and that biomass had not re-grown on them over the course of the study. It may have been that the inoculation procedure (incubating the media in activated sludge for several days) at the beginning of the study was critical for priming of the media for biofilm growth, while use of the zero organic carbon synthetic feed contributed to a poor environment for biofilm regrowth on the media. For this reason, the media with no attached biofilm were removed from R2 and they were reinoculated on February 17, 2014 (day 336) with activated sludge according the same protocol used at the beginning of the study. Plastic media in R2 with significant visible biomass were not reinoculated.

The media with little visible biomass that were reinoculated increased from 1.60 mg/media to 54.3 mg/media 30 days after reinoculation. Ten media without visible biomass were marked and returned to the reactors without reinoculation. There was comparably little increase in biomass on these media (from 1.60 mg/media to 5.8

mg/media after 30 days). These results confirmed the hypothesis that biofilm regrowth was very slow on cleaned media returned directly to the reactor after biomass measurement, and it is therefore confirms the importance of the initial inoculation.

After reinoculation, R2 ammonia uptake quickly increased, although it did not return to the Phase 1 levels. After remaining at 0 mg/L through much of Phase 3, nitrate concentrations steadily increased after reinoculation with a simultaneous decrease in nitrite concentrations.

Phase 3 Microbial Biomass and Populations

As shown in Figure 2.12, after increasing the temperature in Phase 3, the relative abundance of the families Xanthomonadaceae and Comamonadaceae decreased to levels similar to that at the end of Phase 1 (5.1% and 11.6%, respectively). This may suggest that the colder temperatures facilitated the increase of Xanthomonadaceae and modest decrease of Comamonadaceae. At the same time, the relative abundance of Nitrosomonas at the end of Phase 3 recovered to similar levels to the end of Phase 1. This recovery may be attributed to increasing temperature to a more preferred environment of Nitrosomonas. Figure 2.8 also shows that the overall bacterial diversity expressed by SDI recovered in Phase 3 to levels similar to conditions at the end of Phase 1.

Batch Testing

Batch testing of the R1 and R2 media was conducted in all phases of the study (Figure 7), in which mixing rates were varied to determine effects in nitrification rates. In Phase 1, batch tests were conducted at various mixing rates with out controlling dissolved oxygen. As shown in Figure 2.9 increasing the mixing had a more dramatic effect on ammonia flux on the R2 media than the R1 media.

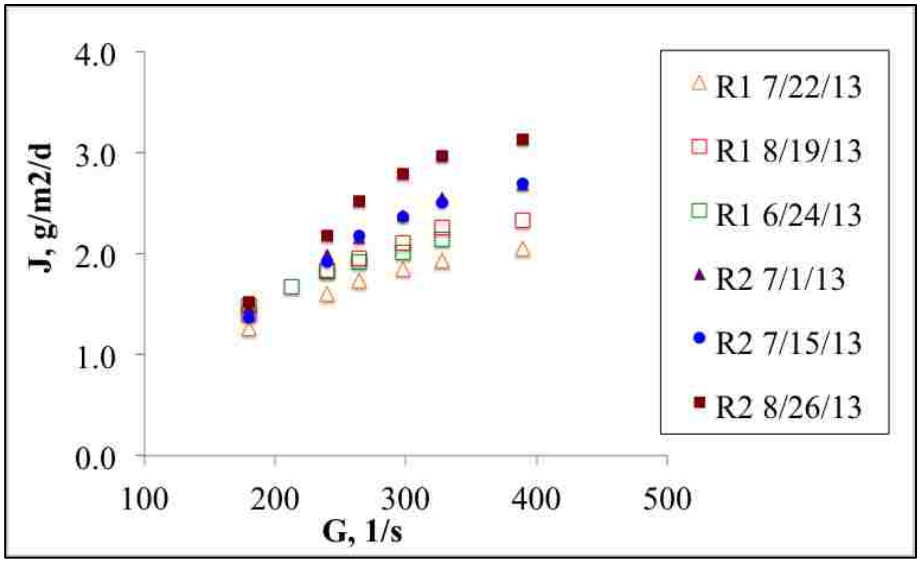

As shown in Figure 2.9, both biofilm carrier media produced a similar flux values at the lower mixing values during Phase 1. At higher mixing rates, the fluxes in R2 tended to increase to a greater degree than they did in R1. It was hypothesized that this was because the R2 media had a more protected interior than the R1 media, and so fluid velocities in the R2 media may have been lower than those in the R1 media. The result would be a greater differential between the bulk fluid concentrations and the those at the biofilm surface in R2 than in R1, and this would be most pronounced at lower mixing rates. As mixing rates were increased, these differentials were expected to decrease in both systems, resulting in increased flux rates in both cases. The greater

effect of increasing mixing on flux rates in R2 relative to R1 was consistent with a greater protection by the R2 media design.

Increasing mixing rates entrained more oxygen into the bulk liquid, and therefor raised the dissolved oxygen of the system. Variable dissolved oxygen batch tests were conducted to show that increasing dissolved oxygen, also increased flux, and needed to be controlled in future batch tests so that mixing is the only variable.

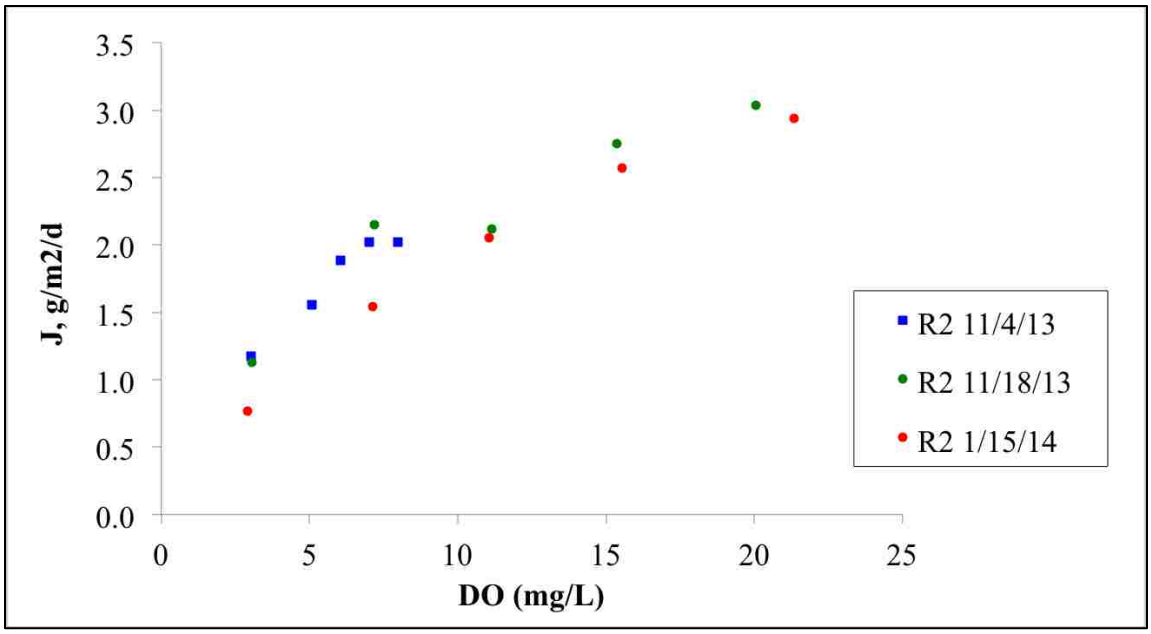

Figure 2.10 shows the result for variable dissolved oxygen batch testing at a G value of 298/s in Phase 2 in R2. The notable increases in dissolved oxygen that occurred by varying G may have had a profound effect on ammonia flux. The observed effect of increased mixing in Phase 1 tests may therefore have been amplified by higher dissolved oxygen concentrations at high mixing rates. In Phase 2 and Phase 3 dissolved oxygen was controlled in each batch test by varying the amount of N_2 gas in the aeration stream for each mixing value.

Figure 2.11 shows similar results to Phase 1 batch testing in batch testing during Phase 2 however; R1 produces a lower flux at the low end G values when compared to R2.

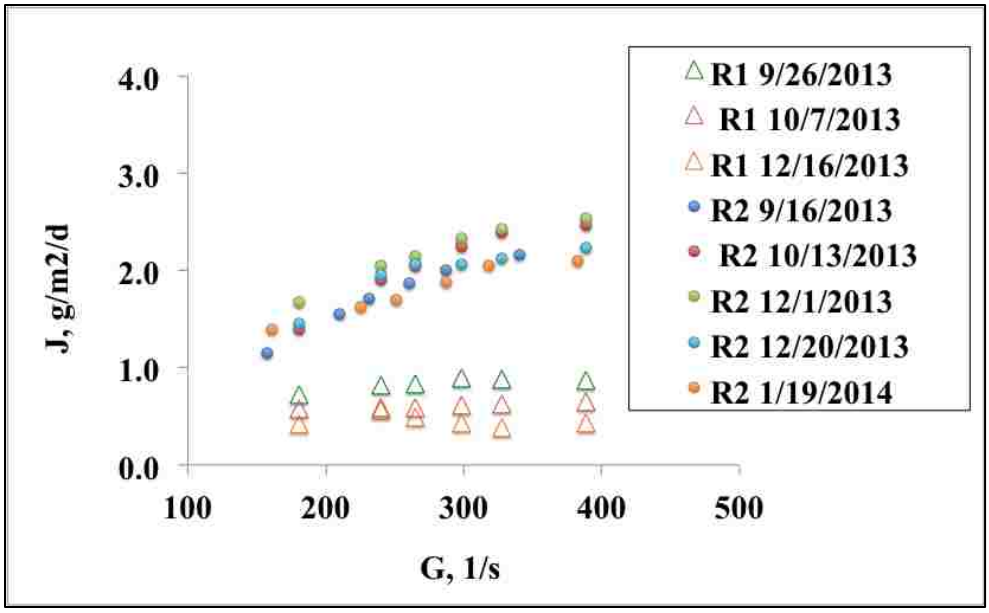

This is most likely due to a large decrease in the attached biomass and the ammonia uptake in the continuous system (Figure 2.5A and Figure 2.5C) in R1 after decreasing the temperature. Similar to Phase 1 batch testing, increasing mixing has very little effect on flux on the R1 media. As shown in Figure 2.11, increasing mixing to a higher G value in R2 also increased flux in a similar fashion to phase 1 batch testing. Dissolved oxygen was controlled during these batch tests from 6.5mg/L to 7mg/L, and may account for the slightly reduced effect of mixing on flux compared to Phase 1 testing for both R1 and R2.

Additional tests were conducted in Phase 3, to confirm the effect of mixing on ammonia flux at the 21 degree temperature phase, with controlled dissolved oxygen. The results of these additional batch tests are shown in Figure 2.12.

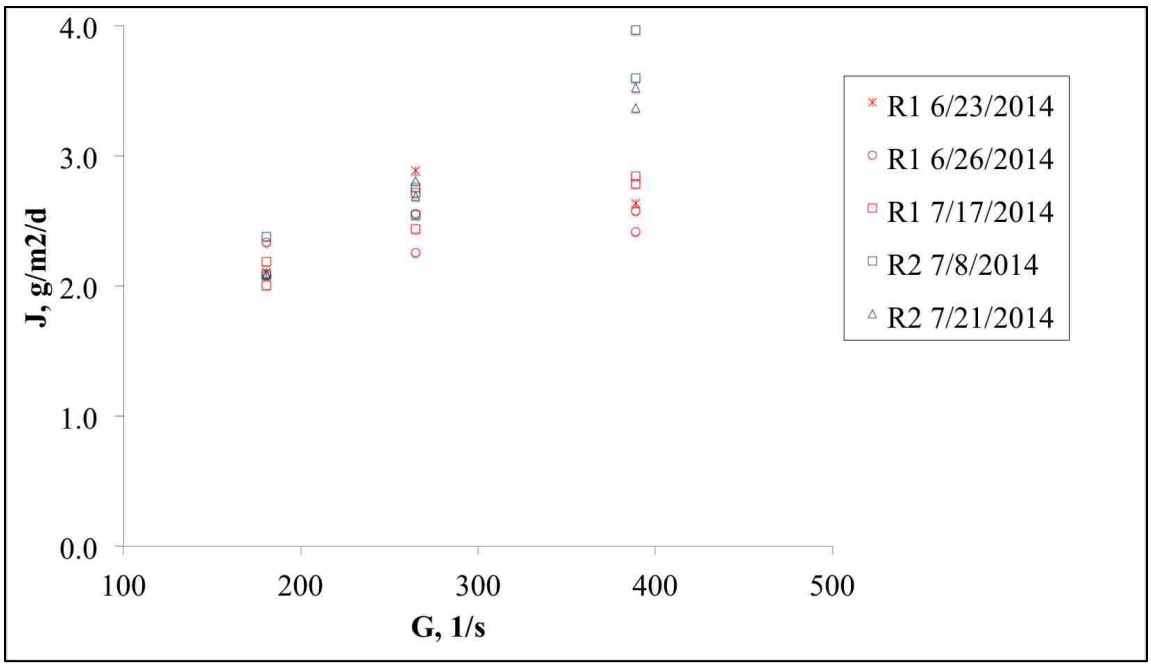

Figure 2.12 confirms the results from the Phase 1 batch testing, by showing similar trends observed in Figure 2.11 for both the R1 and R2 media while controlling dissolved oxygen between 6.5mg/L to 7mg/L.

Conclusions

Following nitrification reactor startup of commercially available MBBR/IFAS media designed with contrasting geometries, system performance and microbial communities varied greatly in the resulting biofilms.

Media geometry likely influenced internal fluid dynamics within each type of plastic biofilm carrier. The open media produced a thinner biofilm with a low abundance of the known AOB Nitrosomonas, while the sheltered design produced a thicker biofilm rich in Nitrosomonas.

Batch testing each media type at various mixing rates indicates that nitrification performance in the more protected media benefits from increasing mixing, where the open R1 media does not.

Decreasing temperature from 21 to 10.5 degrees Celsius in R1 resulted in the eventual failure of the media to retain its biomass. Although nitrification performance was decreased, sloughing was not observed in the sheltered R2 media design and may suggest that decreasing temperature makes a biofilm more susceptible to mixing induced shear.

Following the drop in temperature the R2 media decreased in overall diversity, all but eliminating the AOB Nitrosomonas while largely favoring the family Xanthomonadaceae. Xanthomonadaceae is known for heterotrophic nitrification by an unknown pathway and its occurrence explain the disappearance of the known AOBs with only a modest decrease in nitrification performance.

After increasing the temperature back to 21 degrees, the R2 biofilm diversity and microbial family relative abundance returned to similar level to before the temperature decrease.

Media geometry likely influenced internal fluid dynamics within the plastic biofilm carrier.

Chapter 3: An Assessment of Moving Bed Bioreactors and the Importance of Nitrification on the Removal of Trace Organics.

Introduction

The research described in this chapter was to evaluate the contribution of nitrification activity to trace organic removal in MBBRs systems. The experimental approach was to test the removal of trace organics in batch experiments where nitrification is occurring, and where nitrification was inhibited by allylthiourea.

Background

Nitrification is a 2 step biological process shown in equations 3.1 and 3.2.

$$2NH_4^+ + 3O_2 \rightarrow 2NO_2 + 4H^+ + 2H_2O \qquad (3.1)$$

$$2NO_2^- + O_2 \rightarrow 2NO_3^- \qquad (3.2)$$

The first step is the oxidation of ammonia to nitrite by the ammonia oxidizing bacteria (AOB) such as *Nitrosomonas* under aerobic conditions (Kowalchuk et al., 2001) The second step of nitrification is the aerobic oxidation of nitrite to nitrate by nitrite oxidizing bacteria (NOB), including the genus *Nitrobacter* (Kowalchuk et al., 2001). AOB and NOB obtain energy from by coupling oxygen reduction with ammonia and nitrite oxidation, respectively. Autotrophic nitrifiers use this energy to convert CO_2 to cellular carbon (Metcalf and Eddy 2003). Recently, several other groups of bacteria, such as xanthamondacia, springamonadacia, pseudomonas stutzeri yzn-001, and Alcaligenes faecalis have been reported to oxidize ammonia by an unknown

heterotrophic pathway (Fitzgerald et al., 2015, Jo et al., 2005, Zhang et al., 2011) to nitrite and nitrate.

Trace organics

Microconstituents in wastewater effluent include pharmaceuticals, personal care products, industrial chemicals, and synthetic hormones present at low concentrations (Ternes et al., 1998; Paxeus et al., 2004). This class of contaminants is receiving increasing attention due their persistence in the environment, and potential to impact the ecosystem (Kolpin et al., 2002). By mimicking and disrupting natural endocrine systems, trace organics may impair immune systems, lead to feminization of aquatic organisms, and interfere with reproduction. Removing trace organics is particularly important in arid regions where water scarcity and direct/indirect reuse is becoming more prevalent. Advanced physiochemical processes are effective at removing trace organics, however costly due to excessive energy consumption. With constraints on energy usage and carbon footprint, biological treatment of trace organics is of interest due to cost effectiveness and benefits to downstream physiochemical processes. Engineering biofilms to enhance microconstituent removal may be achieved by designing surfaces where chemical and physical properties of the attachment surface enrich a biofilm that is more capable of removing such compounds. Targeting specific biofilm populations for attachment to a system, and altering biofilm morphology will be examined in this study to possibly improve microconstituent removal with out increase space or energy requirements.

Cometabolism of Trace Organics

Microconstituents are found at very low concentrations in wastewater, but may pose a risk for aquatic ecosystems and human health if they are not eliminated during wastewater treatment (Fischer et al., 2014). Toxicity at high concentrations under lab conditions makes some microconstituents insufficient to support bacterial growth as the sole carbon source. Concentrations of emerging organic pollutants in wastewater are so low (ng/L) that they cannot support metabolic activity even if they are biodegradable. For these reasons, cometabolism is theorized to be the dominating biodegradation process for many microconstituents found in wastewater. (Fischer et al., 2014, Ngoc et al., 2013). Cometabolism in wastewater treatment and bioremediation refers to the inadvertent breakdown of synthetic organic compounds by enzymes created when microorganisms metabolize simple and essential nutrients for growth (Ngoc et al., 2013). While metabolizing simple sugars, bacteria strain S. maltophilia KB2 has been shown to breakdown the synthetic organic compound naproxen more efficiently when compared to a system where naproxen is the only substrate for growth (Wojcieszynska et al., 2014). As KB2 breaks down those simple sugars, specific enzymes are created that will inadvertently aid in the degradation of naproxen.

In pure cultures of the nitrifying bacteria N. europaea, an enzyme suspected to be ammonia mono oxygenase (AMO) easily breaks down microconstituents such as triclosan and bisphenol A (Roh et al., 2009). AMO is produced during oxidation of ammonia to nitrite. As AMO production is inhibited by allylthiourea (ATU), these micro constituents are unable to be metabolized by a pure culture of N. europaea. This indicates that BPA and Triclosan are removed cometabolically by the oxidation of

ammonia. Similar tests by Roh et al., 2009 also show that triclosan and BPA can be metabolized in mixed cultures found in wastewater treatment plant nitrifying sludge both in the presences and absence of the ammonia mono oxygenase inhibitor. This suggests that in addition to cometabolic processes during nitrification, heterotrophic processes may be involved in breaking down micro contaminants co-metabolically. Further research is warranted to match heterotrophic and autotrophic metabolic processes to newly emerging contaminants that may be degraded by the cometabolic pathway. Following the biological transformation of micropollutants in wastewater, micro-constituents such as estrogen may appear to be removed, however they may only be converted to daughter products that may also have adverse effects on the environment and require further investigation (e.g. estradiol discussed below). (Yi et al., 2007)

Khunjar et al., 2011 reported that AOBs transformed ethinyl estradiol (EE2) five times faster than heterotrophs, but not remove trimethoprim. In this same study, heterotrophs mineralized EE2 and AOB formed EE2 metabolites, and bio transformed trimethoprim. EE2 removal was significantly slowed as an inhibitor to nitrification was added. This would suggest that AOB inhibition has an effect on EE2 removal, but not the removal of trimethoprim.

Conjugation

The majority of natural and synthetic hormones are excreted from humans or animas in a conjugated form, where the addition of a sulfate or glucuronide group increases solubility to facilitate excretion (Kovalova et al., 2006). The fate of synthetic organic compounds at a wastewater treatment plant can be divided into three main

pathways. Mineralization to CO2 and water, retention onto solids found in sludge, and release into receiving waters in the deconjugated parent form (Halling-Sorensen et al., 1998). As conjugated synthetics enter the treatment plant and are deconjugated, the apparent concentration of the parent compound may appear to increase in the effluent of the wastewater treatment plant. An example of this is the tendency for 17b-estradiol-17glucuronide and 17b-estradiol-3glucuronide to deconjugated and form 17b-estradiol when in contact with activated sludge. (Ternes et al., 1999) Although the conjugated form is not detected, the occurrence of the deconjugated form deceptively suggests production in the wastewater treatment process.

Hypothesis

Our hypothesis is that nitrification can increase the removal rates of trace organics other than the estrogens that have been previously suggested to be removed by nitrification in activated sludge.

Analyzing a broad array of trace organics in mixed heterotrophic/nitrifying and purely heterotrophic systems gives a better understanding of the benefits to nitrification in the removal of all synthetic organic contaminants found in wastewater.

Objectives

The objective of this study was to evaluate differences in removal of targeted trace organics in moving bed bioreactors with and without inhibition of nitrification. This was tested by measuring trace organics in batch tests where 1) nitrification was

occurring with heterotrophic activity, and 2) nitrification was inhibited by allylthiourea but heterotrophic metabolisms were allowed to occur.

Methods

Specifications of the continuous systems are listed in Table 3.1, and a schematic is shown in Figure 3.1.

Table 3.1: Reactor Specifications

Parameter	Reactor
Reactors	
Total volume (including headspace) (L)	17.4
Working volume (liquid + media) (L)	9.42
Liquid volume (L)	7.96
Dimensions including head space	(W x D x H)
(inches)	8.0 x 8.0 x 16.6
(cm)	20.3 x 20.3 x 42.2
Flow rate (L/d)	10.1
HRT based on working volume (hour)	22.4
HRT based on liquid volume (hour)	19
Media	
Media specific surface area (m^2/m^3)	630
Media fill volume (percent)	31.9
Media area in reactor (m^2)	1.89
Media area/working volume (m^2/m^3)	201
Controls	
Aeration and mixing method	Coarse bubble
Target mixing rate (G) (-/sec)	300

Table 3.1: Reactor Specifications

Parameter	Reactor
Dissolved oxygen concentration (mg/L)	>6.5 mg/L (measured but not controlled)
pH control range	7.15–7.50
Temperature (°C)	21

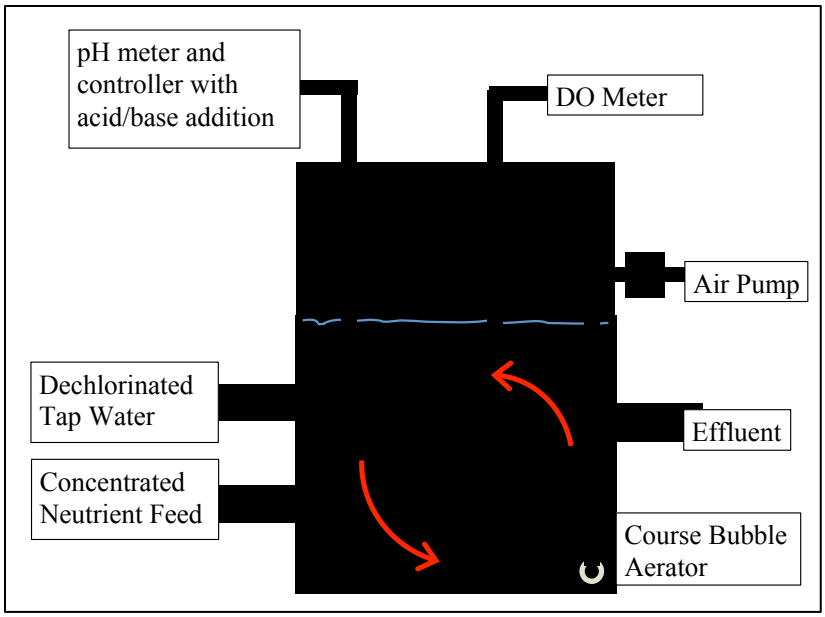

The Reactor media had specific surface areas shown in (Table 3.1) and geometry shown in Figure 3.2, (15 mm long, 20 mm diameter)

Reactor Feed

The MBBR was fed primary effluent from the Albuquerque WWTP for the duration of this study. The reactor was originally inoculated with activated sludge to accelerate the formation of biofilm on the media. 3 L of media were incubated at room temperature for 3 days in a bucket containing 10 L of fresh activated sludge, with coarse-bubble mixing. The activated sludge was obtained from the Albuquerque, New Mexico, Southside Water Reclamation Facility (SWRF) activated sludge system, which has a Modified Ludzack-Ettinger configuration and operated with synthetic feed for approximately two years as part of a previous study (Schuler and Melcer. 2014). The reactor feed was switched to primary effluent and operated an additional month to insure

acclimation before the start of this study. Primary effluent (PE) was used to provide a source of carbon for heterotrophic growth, ammonia nitrogen for autotrophic growth, and trace amounts of synthetic organic contaminants. PE was collected weekly and stored at 4 °C for supplying continuous feed. All PE batch test feed samples were collected fresh from the WWTP, and used that day.

Reactor Mixing

Mixing of the reactors was done by coarse bubble aeration through a horizontal section of pvc pipe spanning the bottom width of the reactor. Coarse bubble air was delivered at a steady flow rate to provide constant mixing intensity in the reactors. Mixing intensity was expressed as G (1/s), which can be calculated using Equation 3.3 (Parker 1970).

$$G = \sqrt{\frac{Q * \gamma * H_L}{\mu V}} \qquad \text{(eq. 3.3)}$$

where:

G = velocity gradient (1/s)

Q= airflow rate (m^3/s)

γ = water specific weight (N/m^3)

H_L = head loss (m) (distance from aerators to water surface)

μ = water dynamic viscosity ($N*s/m^2$)

V= volume (m^3) (working volume used for all calculations)

Mixing rates in the continuous reactors and in the batch experiments were selected based upon a review of typical G values used in full-scale MBBR installations found in Schuler and Melcer 2014.

Batch Testing

Batch tests were conducted with (aeration) rates were at G = 300/s. Batch tests were conducted by stopping the continuous feed, rinsing the media, and adding fresh primary effluent feed. Measurements of NH_3, NO_2^-, and NO_3^- were then taken over time. Samples to be analyzed by the trace organics and hormone methods described below were taken at t=0 and t=6 hours. 20 mL Samples were collected in 40 mL silanized, amber glass vials for trace organic analysis. Samples were preserved with 1 g/L sodium azide to prevent microbial degradation. Samples were stored on ice and shipped to the University of Arizona where within 24h of collection where they were stored at 4°C. 1 Liter samples for hormone analysis were spiked with 100 ng of isotopically labeled surrogate standards before extraction. Analytes were extracted in using Oasis HLB cartridges (6 mL, 500 mg) (Waters Corporation, Milford, MA) manually at UNM.

Solid Phase Extraction

The SPE cartridges were sequentially preconditioned with 5 mL of methyl tertiary butyl ether MTBE, 5 mL of methanol, and 5 mL of reagent water. The samples were then loaded onto the cartridges at 10 mL/min, after which the cartridges were rinsed with 5 mL of HPLC water and then dried with a light vacuum. Next, the analytes were eluted with 5 mL of methanol followed by 5 mL of 10/90 (v/v) methanol/MTBE.

The extracts were dried and redissolved in 0.2 mL of ethyl acetate and 1.8 mL of hexane at the University of Arizona, and the following cleanup methods. The mixed solutions were applied to silica cartridges (6 mL, 500 mg, Waters) which had been preconditioned with 4 mL water-saturated ethyl acetate and 4 mL hexane/ethyl acetate (90:10, v/v). After the cartridges were rinsed with 3 mL of hexane/ethyl acetate (90:10, v/v), the analytes were eluted with 5 mL of water-saturated ethyl acetate. The elutes were dried and reconstituted with 1.0 mL of methanol for LC-MS/MS analysis

Biomass measurement

Prior to batch testing, 5 to 10 media pieces were taken from a given reactor, and each piece was thoroughly cleaned by brushing using Proxabrush "Go-Betweens" (Sunstar Americas Inc. Schaumburg, IL) which were developed for dental cleaning and is available in U.S. drug stores. The removed biofilm was collected by rinsing with DI water, the total suspended solids (TSS) and volatile suspended solids (VSS) in the rinse water was measured according to Standard Methods 2540B and 2540E, respectively (American Public Health Association et al., 2012).

The biofilm mass concentration in the reactor was calculated using Equation 3.4:

$$\text{Total biofilm solids, TBS } \left(\frac{\text{mg}}{\text{L}}\right) = \frac{\text{dry mass removed from media (mg)}}{\text{reactor working volume (L)}} \times \frac{\text{total media pieces}}{\text{pieces of media tested}} \quad \text{(eq. 3.4)}$$

Nitrogen

All samples for nitrogen species analysis were immediately filtered through a 0.45 µm nylon membrane syringe filter, stored at 4°C, and measured within 24 hours. All measurements of nitrogen species were performed using Hach kits with a Hach DR2700 spectrophotometer (Hach Company, Loveland, Colorado, USA) as follows: NH4-N: Nitrogen-Ammonia Reagent Set, TNT, AmVer (Salicylate), High Range, Product 2606945, NO2-N: NitriVer 3 TNT Reagent Set, Nitrogen-Nitrite, Low Range, Product 2608345, NO3-N: NitraVer X Nitrogen-Nitrate Reagent Set, High Range, Product 2605345. All kits were used in accordance with the manufacturer's instructions, except a correction for potential nitrite interference with the nitrate measurement was started on January 6, 2014. The manufacturer's instructions note that nitrite interference could occur at nitrite concentrations greater than 12 mg/L. Per the manufacturer's instructions, this interference was removed by adding 400 mg urea to 10 mL of sample. Nitrate concentrations measured prior to January 6, 2014, may therefore overestimate the actual values.

pH Control

pH was measured and controlled in the range of 7.15 to 7.5 in each reactor with a pH controller (Chemcadet Model 5652-00, Cole-Parmer, Vernon Hills, Illinois, USA) with a combination, double-junction, gel-filled pH electrode (Model EW-59001-70, Cole-Parmer, Vernon Hills, Illinois, USA). Acid and base solutions were 0.1 M hydrogen chloride (HCl) and 0.7 M sodium carbonate (Na2CO3), respectively.

Dissolved Oxygen

DO was measured using a Hach IntelliCAL LDO101 standard luminescent/optical DO probe with a Hach HQ440d multi-parameter meter (Hach Company, Loveland, Colorado, USA).

Illumina Next Gen DNA Sequencing

MBBR media was thoroughly cleaned by brushing using Proxabrush "Go-Betweens" dental brushes (Sunstar Americas Inc. Schaumburg, IL). The removed biofilm was collected by rinsing with DI water, and excess liquid was centrifuged off to form a pellet. The pellet was frozen and shipped to RTL Genomics, Research and Testing Laboratory (Lubbock, TX) for DNA extraction and Illumina Next Generation sequencing using the 357wF-785R assay and 784F [5′ -RGGATTAGATACCC-3′] and 1064R [5′ -CGACRRCCATGCANCACCT-3′]) bacterial DNA primers.

Liquid Chromatography Mass Spectrometer (LC-MS) Analysis

All samples were analyzed using an automated online SPE unit coupled to a liquid chromagraph-tandem mass spectrometer from Agilent Technologies. An Agilent Poroshell 120 EC C-18 (2.1x50 mm, 2.7 µm) column was used for chromatographic separation of all analytes. The column was maintained at 30˚C throughout the run. A dual eluent mobile phase comprising of water with 0.1% acetic acid (A) and ACN with 0.1% acetic acid (B) at 350 µL/min was used for separation. For the first 4 min, the gradient was held at 5% B while the sample was loaded onto the online SPE cartridge and the binary pump was conditioning cartridge 2. At 4 min, the switching valve turned

to the ELUTE position (position 2) and solvent B was linearly increased to 100% at 11 min. This gradient was held till 12 min before returning to the initial condition at 12.5 min. A post-time of 2 min was added to allow the column to re-equilibrate before the next analysis. This resulted in a total cycle time (extraction + analysis) of 14.5 min per sample.

Mass spectrometry was performed on an Agilent 6460 triple quadrupole mass spectrometer. The optimization of the mass spectrometer was divided into two: (i) compound-specific optimization and (ii) source-dependent optimization. Details of the optimization process have been published previously (Anumol, Merel et al., 2013). The optimized compound parameters and retention times (RT) are shown in appendix Table 3.2 while source-dependent parameters for both ESI positive and negative modes (run simultaneously) are shown in appendix Table 3.3.

The mass spectrometer was run in dynamic multiple reaction monitoring (DMRM) mode with a delta RT of 0.7 minutes for each compound. Fast polarity switching with the dielectric capillary allowed for simultaneous analysis in ESI positive and negative in the same run. Two transitions: a quantifier (most-abundant product) and qualifier were used for most of the compounds to increase specificity of the method. Data acquisition and analysis was performed using Agilent MassHunter software (version Rev B.06.00). Isotope dilution was used for quantification of all analytes (Vanderford and Snyder 2006). RT locking and product ion ratio monitoring reduced the possibility of false positives in the method. The method detection limits calculated in ultra-pure water are shown in appendix Table 3.4 The limit of detection (LOD) and method detection limits for all TORCs are provided in appendix Table 3.4. Data analysis

and processing was carried out using the Agilent MassHunter (v 6.00) software and all quantification was done using the isotope dilution method (Vanderford and Snyder 2006).

Ultra-High Performance Liquid Chromatography Mass Spectrometer Analysis (UHPLC-MS/MS)

Analysis was performed using an Agilent (Palo Alto, CA) 1290 binary pump coupled to an Agilent 6460 Triple Quadrupole mass spectrometer. All analytes were monitored in dynamic multiple reaction monitoring (DMRM) mode using electrospray ionization (ESI) source. The MRM transitions and MS source parameters are provided in appendix Table 3.2 and appendix Table 3.3

An Agilent ZORBAX Eclipse Plus C8 Rapid Resolution HD column (1200 bar, 50 × 2.1 mm, 1.8 µm particle size) was used for ER agonists (estrone, 17α-estradiol, 17β-estradiol, 17α-ethinylestradiol and bisphenol A) in ESI negative mode, while an Agilent ZORBAX Eclipse Plus C18 Rapid Resolution HD column (1200 bar, 100 × 2.1 mm, 1.8 µm particle size) was used for analysis of other hormones in ESI positive mode. The column was maintained at 30 °C at a flow rate of 0.4 mL/min for the entirety of the run in both ionization modes. For ER agonists, water (A) and methanol (B) were used as mobile phases. The gradient was as follows: 10% B increased to 40% in 0.5 min, increased linearly to 70% in the next 6.0 min, then to 100% in 0.1 min and held for 1.0 min. A 2.5-min equilibration step at 10% B was used at the beginning of each run. For the other hormones, water containing 0.1% (v/v) formic acid (A) and acetonitrile (B) were used as mobile phases. The gradient was as follows: 5% B held for 1.5 min, increased linearly to 20% in 1.5 min, to 45% in the next 1.0 min, to 65 % in the next 3.0

min, to 100% in the next 1.0 min and held for 1.0 min. A 1.5-min equilibration step at 5% B was used at the beginning of each run. An injection volume of 5 µl was used for analysis of all samples.

Quantitation and Quality Control

The instrument detection limits (IDLs) were determined by the lowest standard in calibration curve with signal to noise ratio of at least 3 (S/N > 3) and 80% accuracy. Due to the varying IDLs from this study, a conservative lowest calibration point of 0.1 µg/L was chosen for all compounds. The remaining calibration points were at 0.2, 0.5, 1.0, 2.0, 5.0, 10, 20, 50, 100, and 200 µg/L. All concentrations that were above the highest point in the calibration curve were diluted and re-analyzed. The method reporting limits (MRLs) were calculated by multiplying the reciprocal of the concentration factor (CF) of the SPE process by the concentration of the second calibration point. The MDLs of analytes were shown in appendix Table 3.4 All analytes were calibrated externally using linear or power regression with 1/*x* weighting. Correlation coefficients were required to be at least 0.990 and typically exceeded 0.995. Quality control samples at low, medium and high (random) concentrations as well as were included every 10 samples to ensure the integrity of mass spectrometric analysis. The data was then processed with MassHunter Quantitative Analysis B.04.00. At least one lab blank and one lab fortified blank sample were carried out for every 10 samples.

Results and Discussion

Reactor Performance

Continuing the reactor operation from a previous study, the MBBR reactor switched from the synthetic feed to primary clarifier effluent (PE) from the Albuquerque SWRF on 03/06/15 to provide a source of carbon for heterotrophic growth, nitrogen for autotrophic growth, and synthetic organic microconstituents shown in Figure 3.4 and Figure 3.5.

The following figures (Figure 3.3A – Figure 3.3C) show nitrification performance history (ammonia loading, effluent nitrate, and nitrite) and biomass for the reactor used in this study approximately one year before it was switched to primary effluent feed.

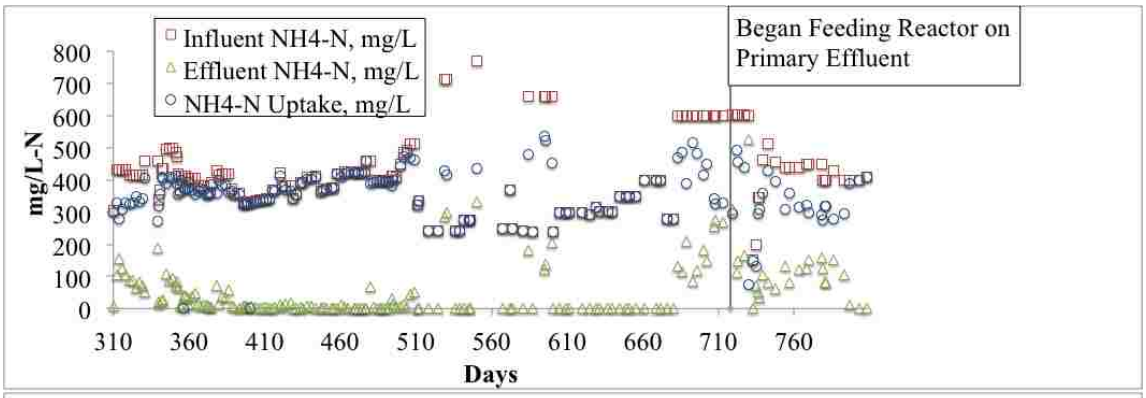

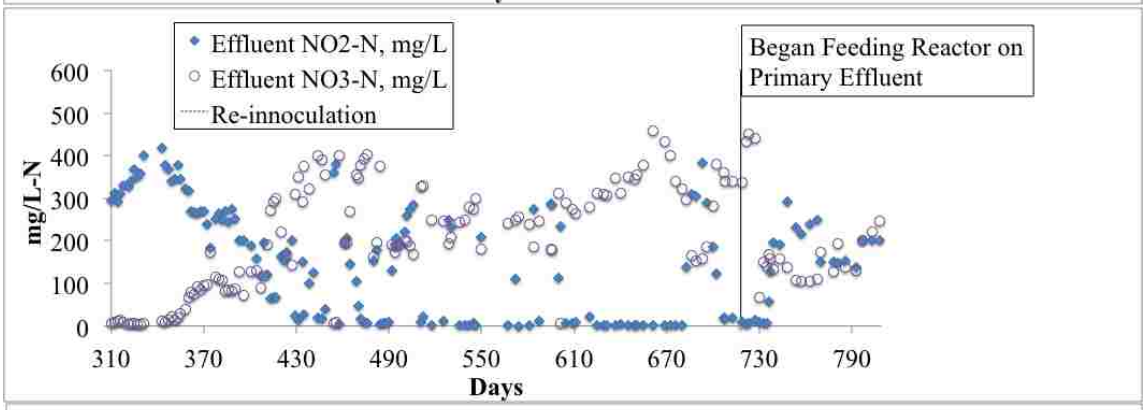

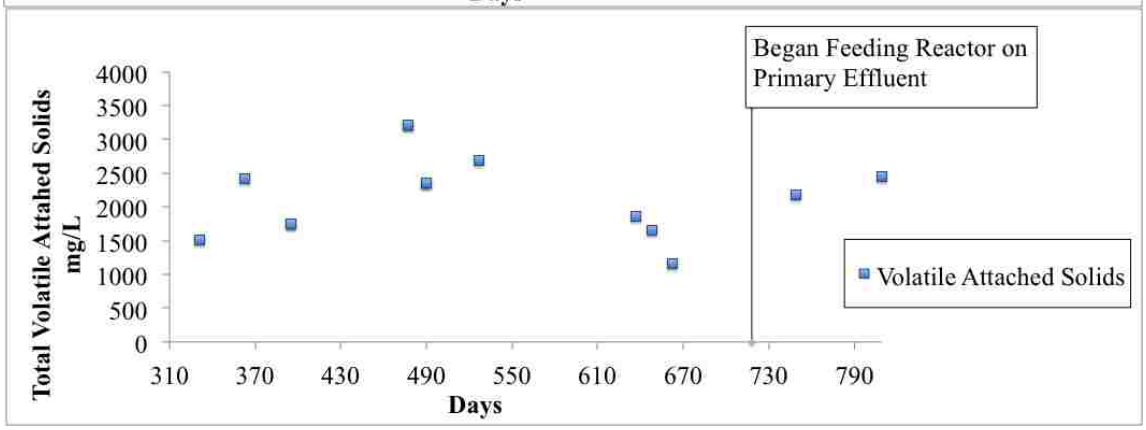

Ammonia and DOC concentrations in the primary effluent were approximately 40-50 mg NH4-N/L and 50-55 mg/L respectively. PE was supplemented with ammonia in the continuous feed to match similar influent levels as seen at the end of the previous experiment shown in Figure 3.3.

Influent Characteristics

Figure 3.4 shows the results of several trace organics detected in the primary effluent on three different days spanning three months, at concentrations of 100 ng/L or parts per trillion (PPT) to 80 ug/L or parts per billion (PPB) (this LC-MS data was provided by the Snyder Lab at the University of Arizona).

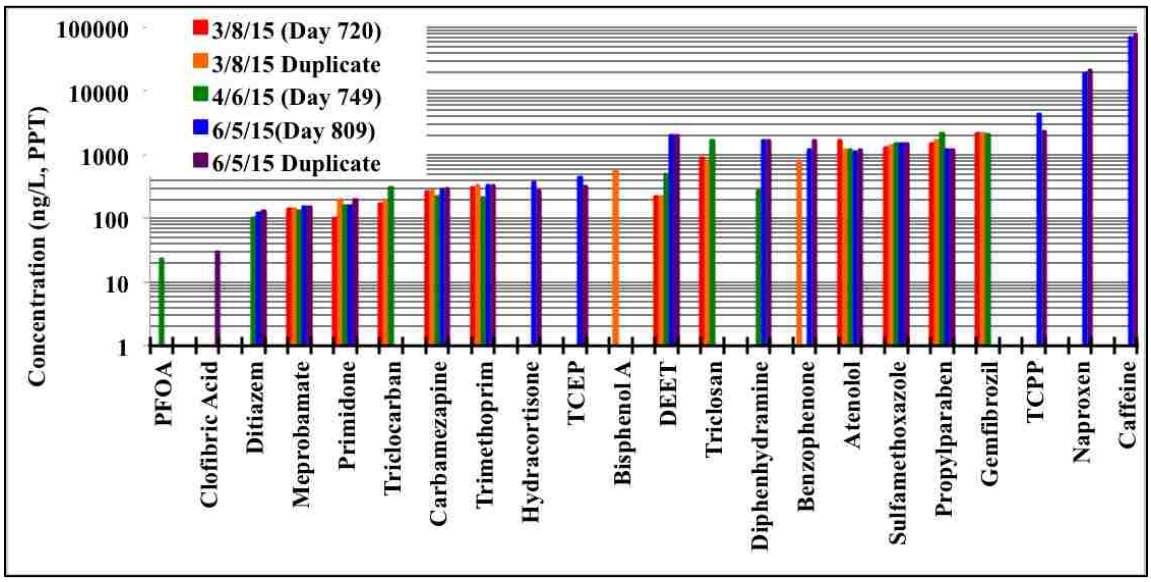

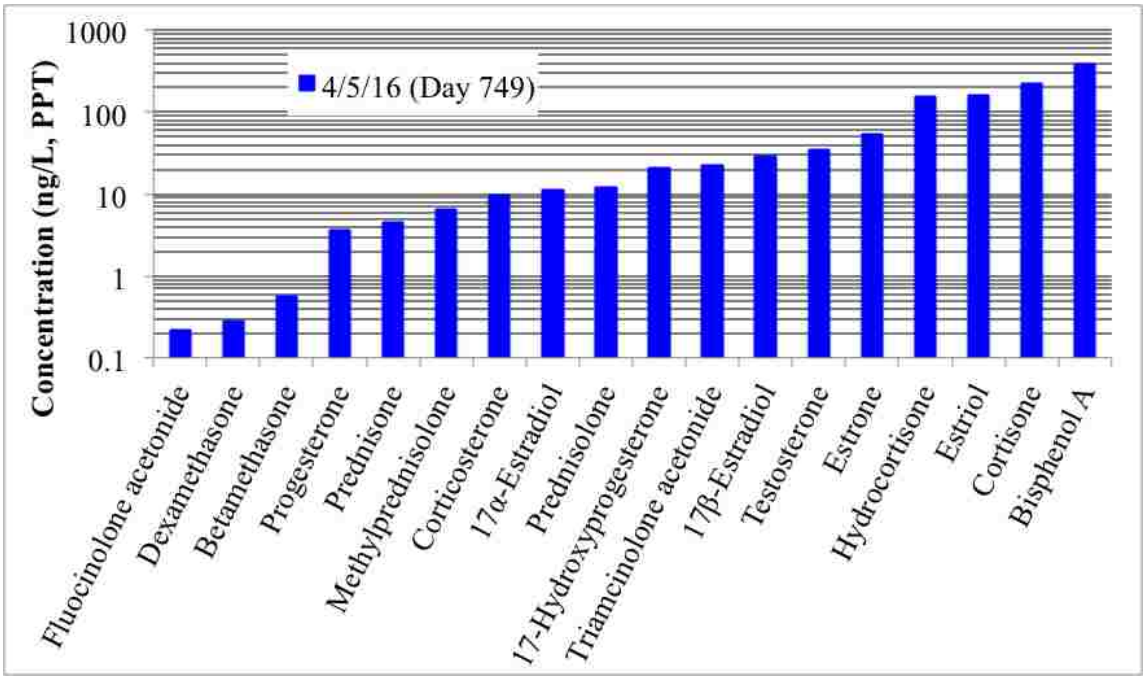

Figure 3.5 shows the concentration of trace organics for primary effluent samples collected and analyzed by UHPLC-MS/MS on 04/05/15 by the Snyder Research Group, which ranged from 0.2 ng/L to ng/L 400. Concentrations of triclosan, carbamazepine, bisphenol a, estradiol, and estriol measured in the Albuquerque SWRP primary effluent were very similar to those reported by Nakada et al., 2006, who surveyed 5 different waste water treatment plant influents in Tokyo, Japan for several synthetic organic compounds. One significant difference in synthetic organic composition between this study and Nakada et al., 2006 is the presence of naproxen in concentrations of up to 100 times greater at the Albuquerque wastewater treatment plant. The compound Ethinylestradiol (EE2) that is persistent in ecosystems, and widely accepted as being eliminated by cometabolic processes (Fischer 2014) was not detected in our samples.

Microbial Populations

In order to better understand the microbial communities that are associated with the removal of synthetic compounds, biomass samples were analyzed by Illumina next generation sequencing before and after the switch to primary effluent feed. Figure 3.6 shows the results of Illumina next generation DNA for these samples.

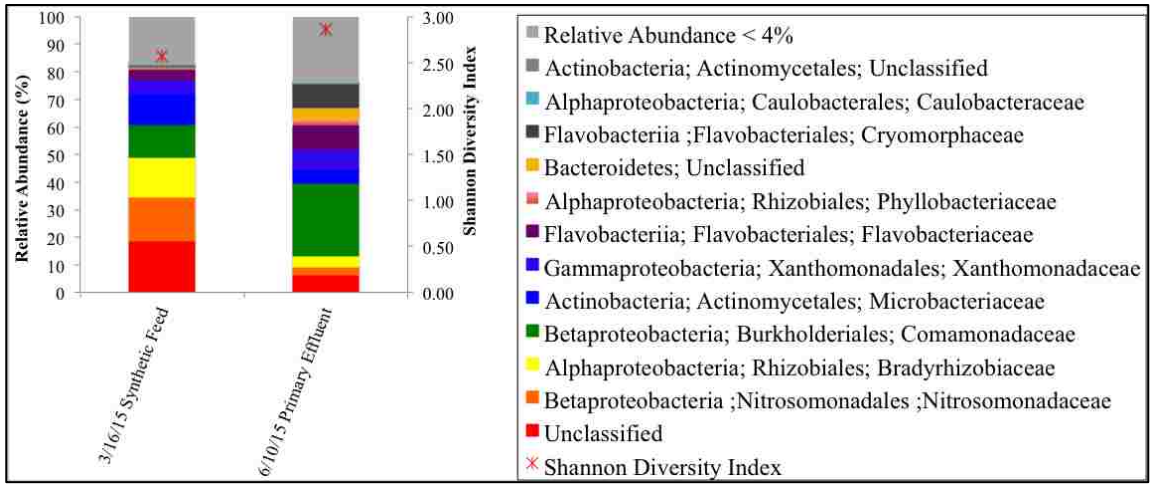

The relative abundance of bacteria populations found in the biofilm changes in several ways after being switched to primary effluent feed. Nitrosomonas decreases from 15.8% at before the feed switch, to 2.7% after acclimation to primary effluent. The reduction in Nitrosomonas is also accompanied by an increase in Comamonadaceae from 11.9% to 26.6%. For the first time in this study, a significant abundance the family Cryomophaceae is detected at 8.9%. Cryomophaceae has been reported by Bowman 2014 to be found in environments with rich organic carbon, making the most likely explanation for its occurrence to be the introduction of DOC rich PE. As determine by SDI (Figure 3.6), the overall diversity of microbial populations on the R2 media increased by the end of phase 4 from 2.58 to 2.87.

Batch Testing AMO Inhibition

To evaluate the possible role of heterotrophic or autotrophic cometabolism of the trace organics in primary effluent, batch tests were performed on MBBR media in AMO inhibited conditions (heterotrophic) and in the absence of AMO (mixed heterotrophic/autotrophic) using the AMO inhibitor allylthiourea. On 04/06/15 MBBR media was split into 4 separate reactors containing 766 mgTSS/L and 686 mgVSS/L, and initial concentrations of 50 mgNH4-N/L and approximately 50 mgDOC/L. $R2_A$,$R2_B$,$R2_C$, and $R2_D$ contained 0, 0.1, 0.4, and 3 mg/L ATU. Batch tests were run at the continuous system mixing rate (G=298/s) for 6 hours to allow for the slow degradation of recalcitrant contaminants. All four reactors were analyzed for NH4 (Figure 3.7) and NO_x measurements (Data not shown, see appendix) at half hour intervals. Reactors $R2_A$ and $R2_D$ were analyzed for trace organics and hormones at hour 1 and hour 6 (Figure 3.9 and Figure 3.10), and dissolved organic carbon at 1-hour intervals (Figure 3.8).

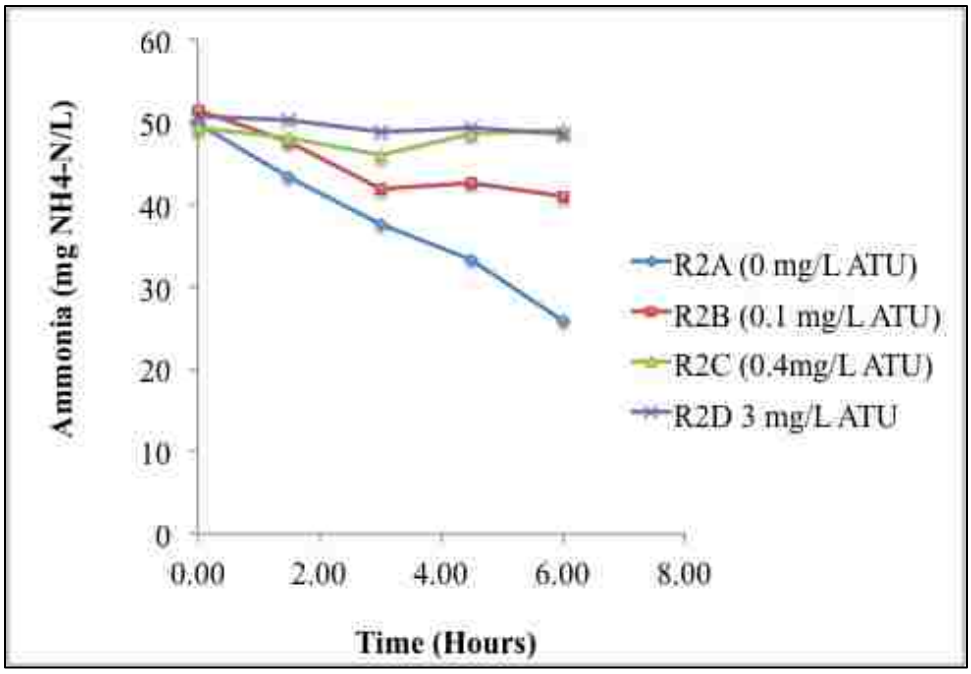

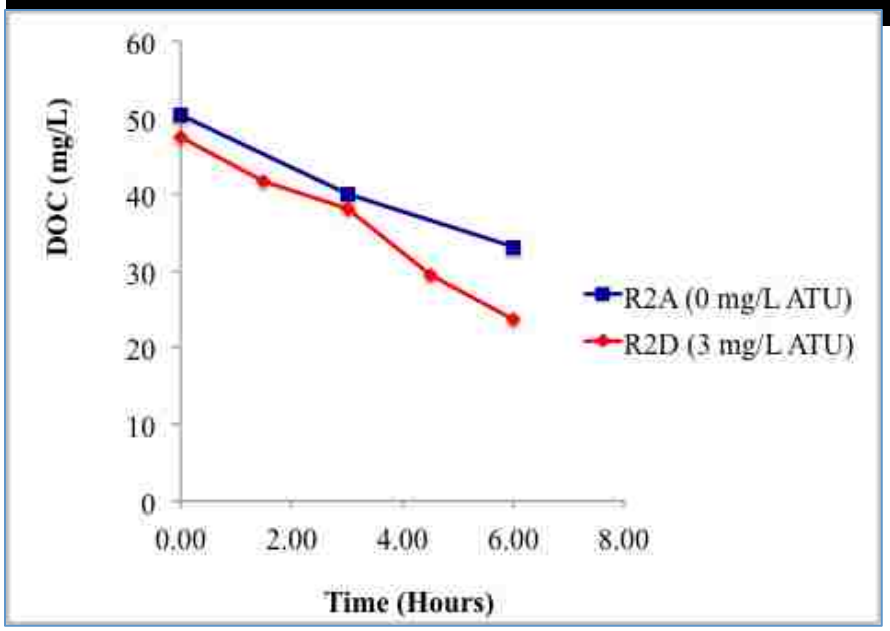

Figure 3.7 shows that in $R2_A$ ammonia is readily being oxidized to Nitrite in the absence of ATU and in $R2_D$, ammonia oxidation to nitrite is completely inhibited by the 3mg/L dose of ATU. Interestingly, Figure 3.8 shows that ATU may have had a small positive effect on the uptake of DOC. It is possible that the uptake of DOC was enhanced by the inhibition of AOBs, eliminating competition for available oxygen use to metabolize DOC. These results show R2A is a system mixed with heterotrophic (DOC uptake) and autotrophic (Ammonia Oxidation) metabolisms and only heterotrophs are active in R2D.

Of the 48 target compounds analyzed, 16 were below the detection limit, and 3 were the detection limit (Caffeine, Naproxen, Ibuprofen, >2500 ppt).

Trace Organics Removal

Figure 3.9 shows results for the removal of compounds analyzed by LC-MS in the 04/06/15 batch experiments with and without inhibition. Compounds at concentrations below the detection limit at t=0 are not included.

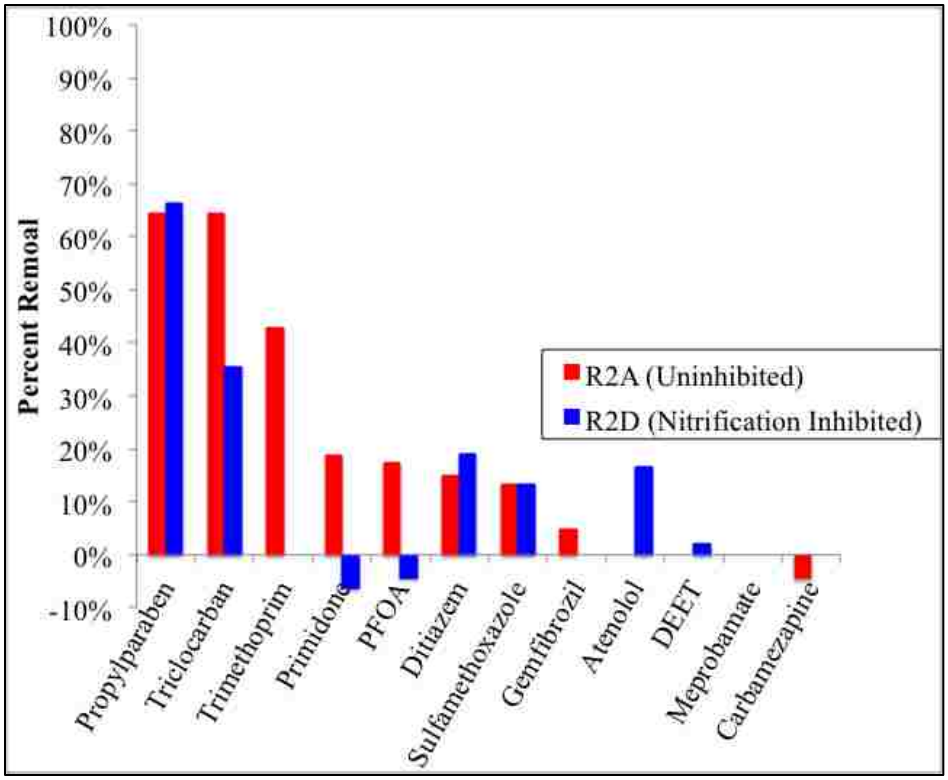

Figure 3.4

Of the 12 compounds successfully analyzed, 4 of the compounds (triclocarban, trimethoprim, primidone, PFOA) were more efficiently removed by the control reactor containing no allylthiourea (Removal in R2A was at least 10% greater than in R2B) shown in Figure 3.9. Trimethoprim and Primidone were the only compounds shown in this analysis to have significant removal in R2A (43%) and no removal in the reactor where nitrification was completely inhibited. This observation is similar to Batt et al.,

2006 who observed enhanced biotransformation of trimethoprim in nitrifying activated sludge (70% removal) when compared to AMO inhibited activated sludge (25% removal). Interestingly, our results and Batt et al., 2006 suggest a trend in the removal of trimethoprim during batch testing (Figure 3.9) that is contrary to what was reported by Khunjar et al., 2011 who found that the removal of trimethoprim was not effected by AOB inhibition in flow through AOB culture and activated sludge reactors.

Primidone has been reported by Kovalova et al., 2006 to increase in concentration in membrane bioreactor (MBR) systems used to treat concentrated hospital wastes.

Results from this experiment suggest that nitrification may enhance the removal of Primidone (19% removal in R2A) and overtake the rate that deconjugation occurs resulting in apparent Primidone production as seen in the AMO inhibited system (-6% removal in R2D).

Triclocarban is a relatively hydrophobic compound ($\log k_{ow}$=4.9) and is well known to readily sorb and accumulate in biosolids. The results from this experiment may indicate that significantly more triclocarban is being removed in the uninhibited reactor (64.5%) than in the nitrification inhibited reactor (35.5%) as in both cases triclocarban is being absorbed to biomass in both reactors, however this suggests that cometabolism is adding additional removal by the biodegradation of triclocarban.

Figure 3.10 shows results for the removal of compounds analyzed by LC-MS/MS. Compounds with concentrations less than the detection limit at t=0 have been omitted.

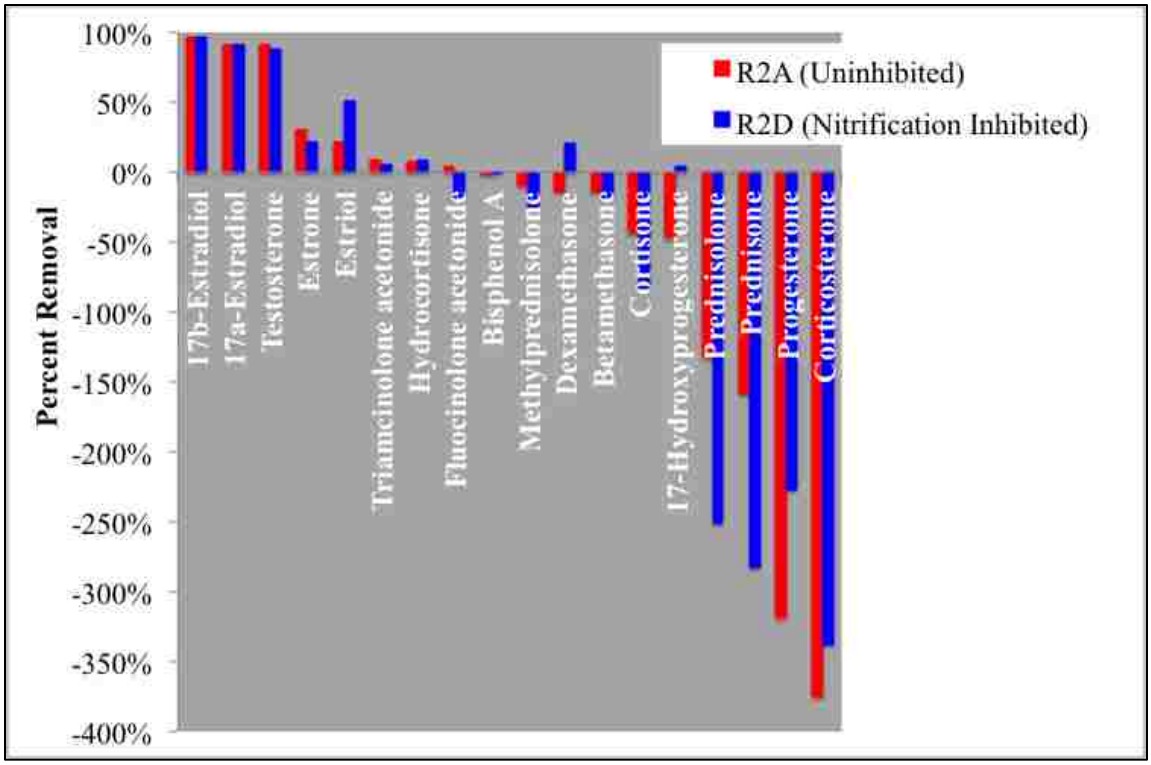

Figure 3.5

As shown in Figure 3.10, of the compounds analyzed by the LC-MS/MS, nearly as many compounds showed negative removal as positive removal. A likely cause of this is the occurrence of contaminants in a conjugated form, where the compound is brought back to the unconjugated form after a biotransformation takes place. Yi et al., 2007 reported various mechanisms for the conjugation (sulfate addition) and hydroxylation of different forms of estrogen in wastewater. Another example of a contaminant that is well documented to be found in a conjugated form in wastewater is Sulfamethoxazole (Kovalova et al., 2012). Kovalova et al., measured both the

conjugated form N4-acetylsulfamethoxazole before treatment with MBR, and increases in Sulfamethoxazole after treatment resulting in negative removal. For this study, we observed an overall removal efficiency of Sulfamethoxazole in R2A and R2B at 13.3%. This may underestimate the actual removal efficiency of Sulfamethoxazole as it may be produced from existing N4-acetylsulfamethoxazole at a slightly slower rate than it is removed.

The sex hormone progesterone has been well documented by Clemens et al., 1982 to form several glucuronide conjugates in animals during metabolism in the liver. The results of this study are the first to suggest de-conjugation of progesterone in wastewater treatment, by the apparent increase of progesterone after coming into contact with both nitrifying and heterotrophic biofilms.

The results of this study shown in Figure 3.10 support previous studies done by Shi et al., 2004, who showed that both nitrifying activated sludge, and nitrifying inhibited systems were able to degrade esterone, 17B-estradiol, estriol, and 17a-ethynlestradiol. This study also showed that 17B-estradiol was the most easily degraded out of the estrogens tested, as it is readily transformed to esterone. This finding is also consistent with our results that show nearly 100 percent degradation of 17B-estradiol in both R2A and R2D, and may indicated that the removal of esterone is under estimated due to this transformation.

To evaluate the MBBR effectiveness of removing recalcitrant trace organics during continuous operations, a sample from the continuous feed reactor was taken on 04/06/15 before interrupting operations for batch testing.

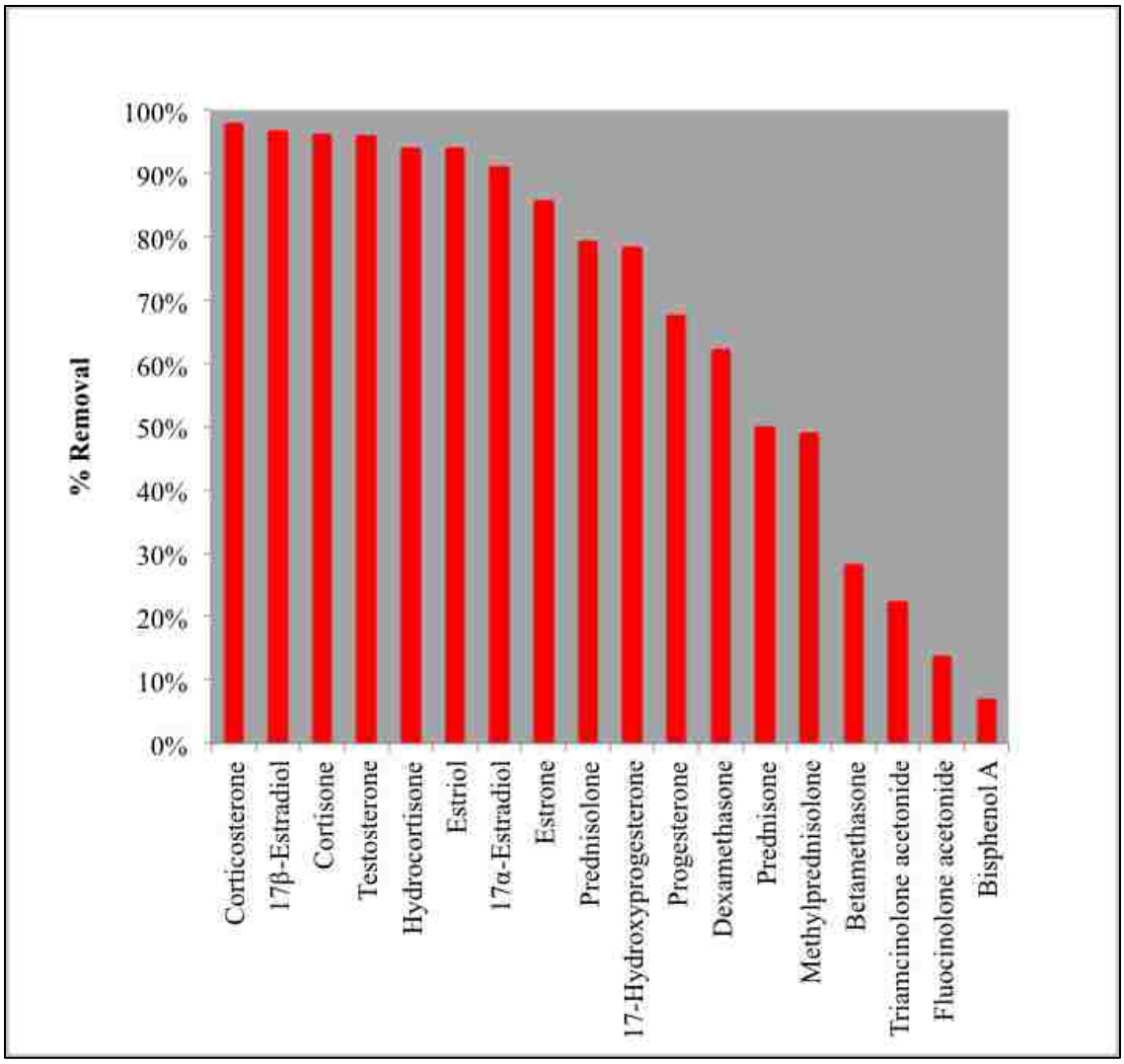

As shown in Figures 3.10 and 3.11, compounds such as prednisolone, prednisone, progesterone and corticosterone that were produced in the batch testing

experiments, were effectively removed in the continuous feed. A likely cause of this is that slow processes remove these compounds over many steps. One difference between batch testing and the continuous feed is the 6 hour batch testing time starting with reactor liquid being replaced with fresh feed, compared to the 22.4 hour hydraulic residence time of the continuous feed (Table 3.1). Batch testing was also conducted by splitting up the parent reactor into individual reactors with approximately 25% of the biomass. Enhanced removal in the continuous system may therefore be due to increased adsorption and biodegradation from to higher solids concentrations, and more nitrification continuous system operations. This data suggests that moving bed bioreactors are very effective at removing the array of compounds tested in the continuous system, however long HRTs maybe be necessary to remove more recalcitrant organic compounds that require multiple steps to degrade.

Conclusions

The analysis of Albuquerque's primary effluent revealed consistent concentrations of synthetic organic compounds found in other studies of treatment plants around the world. Several of these compounds are present but not detected in a conjugate form. When coming into contact with biofilms, it is possible that these compounds deconjugated to underestimate removal, or produce the parent compound in reactor effluents. Of the compounds analyzed, triclocarban, trimethoprim, primidone, and PFOA were more efficiently removed by the control reactor containing no allylthiourea (Figure 3.9). This finding supports other studies that suggest trimethoprim and Primidone degradation are cometabolic processes. Our observation of enhanced removal for triclocarban and PFOA in nitrifying MBBR reactors is the first to suggest a

cometabolic degradation pathway for these compounds under these conditions.

Chapter 4: A Comparison of Nylon and High Density Polyethylene Plastic Biofilm Carriers In Moving Bed Bioreactors.

Introduction

The research described in this chapter examines how biofilm attachment surface material affects nitrification and trace organics removal from wastewater, with the longer term goal of improving MBBR and IFAS system performance. Specifically, the performance of biofilms grown on two plastics (nylon and high-density polyethylene, or HPDE) were compared. Typically, moving bed bioreactor (MBBR) attachment media are made from HDPE, which is relatively hydrophobic, while nylon is relatively hydrophilic. Nylon also contains amine groups in its chemical structure where HPDE does not, which may encourage attachment of desired bacterial groups.

Background

Nitrification

Nitrification is a 2 step biological process shown in equations 4.1 and 4.2.

$$2NH_4^+ + 3O_2 \rightarrow 2NO_2 + 4H^+ + 2H_2O \qquad \text{(eq. 4.1)}$$

$$2NO_2^- + O_2 \rightarrow 2NO_3^- \qquad \text{(eq. 4.2)}$$

The first step is the oxidation of ammonia to nitrite by the ammonia oxidizing bacteria (AOB) such as *Nitrosomonas* under aerobic conditions (Kowalchuk et al., 2001) The second step of nitrification is the aerobic oxidation of nitrite to nitrate by nitrite oxidizing bacteria (NOB), including the genus *Nitrobacter* (Kowalchuk et al., 2001). AOB and NOB obtain energy from by coupling oxygen reduction with ammonia and nitrite oxidation, respectively. Autotrophic nitrifiers use this energy to convert CO_2 to

cellular carbon (Metcalf and Eddy 2003). Recently, several other groups of bacteria, such as xanthamondacia, springamonadacia, pseudomonas stutzeri yzn-001, and Alcaligenes faecalis have been reported to oxidize ammonia by an unknown heterotrophic pathway (Fitzgerald et al., 2015, Jo et al., 2005, Zhang et al., 2011) to

Trace organics

Microconstituents in wastewater effluents consist of pharmaceuticals, personal care products, industrial chemicals, and synthetic hormones found in very small concentrations (Ternes et al., 1998; Paxeus et al., 2004). This class of contaminants is receiving increasing attention due the ability to persist in the environment, disrupt ecosystem health (Kolpin et al., 2002). By mimicking and disrupting natural endocrine systems, trace organics may impair immune systems, lead to feminization of aquatic organisms, and interfere with reproduction. Removing trace organics is particularly important in arid regions where water scarcity and direct/indirect reuse is becoming more prevalent. Advanced physiochemical processes are effective at removing trace organics, however costly due to excessive energy consumption. With constraints on energy usage and carbon footprint, biological treatment of trace organics is of interest due to cost effectiveness and benefits to downstream physiochemical processes. Engineering biofilms to enhance microconstituent removal may be achieved by designing surfaces where chemical and physical properties of the attachment surface enrich a biofilm that is more capable of removing such compounds. Targeting specific biofilm populations for attachment to a system, and altering biofilm morphology will be

examined in this study to possibly improve microconstituent removal with out increase space or energy requirements.

Surface Chemistry

Attachment surface energy is well known to effect bacterial attachment and adhesion (Van Loosdrecht et al., 1990). Some microorganisms have been shown to have attachment preferences to surfaces of different chemistries in studies utilizing self assembling monolayers (SAMs) (Ista et al., 2004, 2010; Khan et al., 2011). These studies used self assembling monolayers (SAM) to vary the surface energy and functional groups of an attachment surface. The driving force for cell attachment to a surface has been suggested by Ista et al., 2004 to be the surface tension between the cell and a surface, making selection of material for a attachment surface important for engineering biofilm functionality. Kahn et al., 2011 found that ammonia oxidizing pure cultures of Nitrosomonas europaea and Nitrospira multiformis had higher rates of adhesion on SAMs with higher surface energies than did the heterotroph Escherichia coli. Khan et al., 2013 found a positive correlation between attached biomass and attachment to plastics with a range of surface energy values incubated in a full scale activated sludge system. These authors also found a general positive correlation between surface energy, ammonia uptake, and estrogen removal expressed as a rate specific to the amount of biomass. This may indicate that AOB populations preferred and occurred in greater relative abundance on the higher surface energy plastics that may be used to produce biofilms with improved estrogen removal capabilities. Nylon, the alternative plastic used in this study contains amine groups in its chemical structure where HPDE

does not. Lackner et al., 2009 showed that self assembled monolayers modified with amine groups effectively increased biofilm attachment to the surface.

Hypothesis

The hypothesis for this study is that nutrient and trace organics removal from wastewater can be improved by altering the chemistry of the biofilm attachment surfaces. Surface chemistry of plastic biofilm carriers used in IFAS and MBBR systems determines adhesion, attachment strength, and detachment of microbial populations that effect system functionality. Attachment surface chemistry may be exploited to engineer biofilms for the removal of synthetic organic contaminants through biodegradation and/or adsorption.

Objectives

The objective of this study was to compare two different MBBR plastic materials for nitrification performance, organic microconstituent removal performance, and determine the effects of plastic type on biofilm quantity.

Methods

Reactor Design

Specifications of the continuous systems are listed in Table 4.1, and a schematic is shown in Figure 4.1. Conical shaped reactors (Imhoff cones) were used to facilitate keeping nylon media in suspension, as described below.

Table 4.1 Reactor Specifications

Parameter	Nylon	HDPE
Reactors		
Total volume (including headspace) (L)	1.6	1.6
Working volume (liquid + media) (L)	1.15	1.15
Liquid volume (L)	0.93	0.95
Flow rate (L/d)	0.7	0.7
HRT based on working volume (hour)	27.4	27.4
HRT based on liquid volume (hour)	22.14	22.62
Media		
Media specific surface area (m^2/m^3)	472	472
Media fill volume (percent)	15	15
Media area in reactor (m^2)	0.0404	0.0404
Media area/working volume (m^2/m^3)	35.1	35.1
Water Contact Angel (Degrees) (Kahn et al., 2013)	51 - 55	89-91
Surface Energy γ_{total} (mj/m^2) (Kahn et al., 2013)	47.9 - 49.9	29.6 - 31.2
Controls		
Aeration and mixing method	Coarse bubble	
Target mixing rate (G) (-/sec)	700	
Dissolved oxygen concentration (mg/L)	>6.5 mg/L (measured but not controlled)	
pH control range	7.15–7.50	
Temperature (°C)	21	

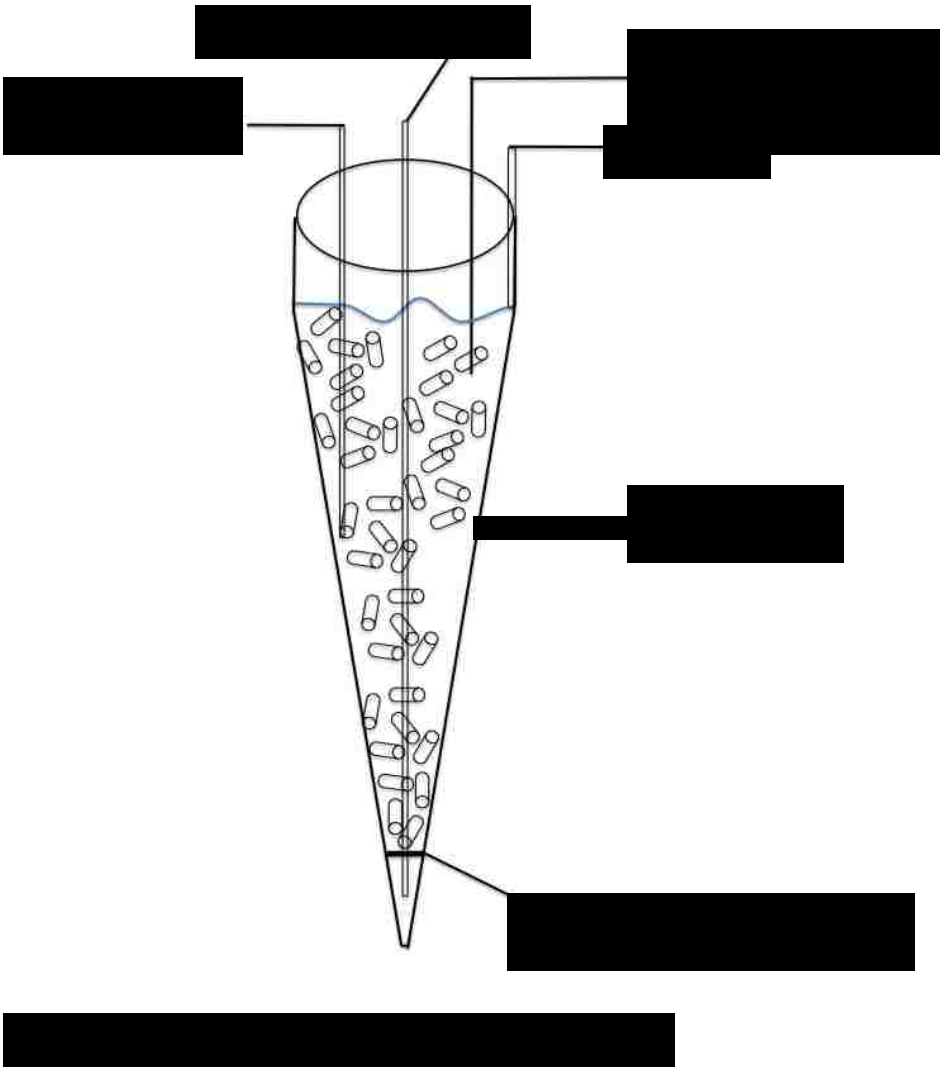

Reactor Feed

The reactors were continuously fed a synthetic wastewater containing ammonia, and zero organic carbon with the goal of producing a highly active nitrifying biofilm for batch testing. Table 4.2 shows the composition of the synthetic feed.

Table 4.2. Synthetic Feed (based on Hem et al., 1994)

Chemical	Concentration (mg/L)
NH_4Cl	Variable
KH_2PO_4	100
$NaHCO_3$	350
$FeSO_4$-$7H_2O$	5
$CaCl_2$	16
$MgSO_4$-$7H_2O$	40
$CuSO_4$-$5H_2O$	0.12
$NaMoO_4$	0.0019
EDTA	6.6

Ammonium chloride was the sole source of nitrogen in the feed, and its concentration was periodically adjusted with the goal of maintaining a target effluent ammonia concentration between 5 and 5 and 20 mg N/L (actual effluent ammonia varied considerably with reactor performance). This ammonia residual aimed to prevent limiting biofilm activity without creating an excess of ammonia that could inhibit nitrification. Influent ammonia feed concentrations varied from initial concentrations of 10 mg N/L early in reactor biofilm development to approximately 50 mg N/L once the biofilm was fully matured.

Reactor Mixing

Unlike HDPE, the nylon media was denser than water so it required a strong upward flow to stay in suspension. In order to address this, reactor geometry was changed from the rectangular prism type reactor used in previous experiments, to an inverted cone design using a glass Imhoff cone (Figure 4.1) where aeration was delivered from the narrow bottom of the reactor, providing strong upward flow and preventing Nylon media from settling. Mixing of the reactors was done by coarse bubble aeration, delivered by the glass tube shown in Figure 4.1. A screen was placed at the bottom of the cone shaped reactor to prevent any media from settling below the aerator. Coarse bubble air was delivered at a steady flow rate to provide constant mixing intensity in the reactors. Mixing intensity can be expressed as the velocity gradient G (1/s), which can be calculated using Equation 4.3 (Parker 1970).

$$G = \sqrt{\frac{Q * \gamma * H_L}{\mu V}} \qquad \text{(eq. 4.3)}$$

Where:

G = velocity gradient (1/s)

Q= airflow rate (m^3/s)

γ = Water specific weight (N/m^3)

H_L = head loss (m) (distance from aerators to water surface)

μ = water dynamic viscosity ($N*s/m^2$)

V= volume (m^3) (working volume used for all calculations)

The mixing rate was set to G = 700/s in this study. This was higher than typical in full-scale systems G = 180/s to 389/s; (Melcer and Schuler 2014), as this was found to be necessary to keep the nylon media in suspension.

Batch Testing

Batch tests to determine removal of trace organics were conducted as follows. Reactor continuous feed was stopped and the liquid phase was removed, and filtered through a 1um glass filter. The plastic media was set aside and the glass cone container was scrubbed with a brush to remove any biofilm and rinsed with DI. The filtered liquid phase was dosed with ammonia, and triclosan or caffeine to be used in the batch test. Caffeine was tested at concentrations of 80-200 mg/L and triclosan was tested at concentrations of 100 ug/L. For some experiments, 100 mL samples were taken of the liquid before adding back the biofilm, and in all experiments samples were taken at 1 minute and at 60 minutes after adding the media. These samples were used for measurements of trace organics. 5 mL samples were filtered for measurements of NH_3, NO_2^-, and NO_3^- at the 1 minute and 60 minute sampling times.

Nitrogen

Ammonia

All samples for nitrogen species analysis were immediately filtered through a 0.45 µm nylon membrane syringe filter, and stored at -20°C. All measurements of ammonia as nitrogen were performed using Hach kits with a Hach DR2700 spectrophotometer (Hach Company, Loveland, Colorado, USA) as follows: NH4-N: Nitrogen-Ammonia Reagent Set, TNT, AmVer (Salicylate), High Range, Product 2606945. All kits were used in accordance with the manufacturer's instructions.

NO_x

All samples for nitrogen species analysis were immediately filtered through a 0.45 µm nylon membrane syringe filter, and stored at -20°C. All measurements of ammonia as nitrogen were performed using Hach kits with a Hach DR2700 spectrophotometer (Hach Company, Loveland, Colorado, USA) as follows: NH4-N: Nitrogen-Ammonia Reagent Set, TNT, AmVer (Salicylate), High Range, Product 2606945. All kits were used in accordance with the manufacturer's instructions.

All samples for nitrogen species analysis were immediately filtered through a 0.45 µm nylon membrane syringe filter, and stored at -20°C. All measurements of ammonia as nitrogen were performed using a Thermo Scientific Ion Chromatography System (ICS-1100) with an auto sampler. The column was a Thermo Scientific Dionex IonPa AS9-HC, with a Dionex AERS 500 4 mm suppressor set at current of 45 uS. The eluent was 9mM Sodium Carbonate set at flow rate through the column at 1ml/min.

pH Control

pH was measured and controlled in the range of 7.15 to 7.5 in each reactor with a pH controller (Chemcadet Model 5652-00, Cole-Parmer, Vernon Hills, Illinois, USA) with a combination, double-junction, gel-filled pH electrode (Model EW-59001-70, Cole-Parmer, Vernon Hills, Illinois, USA). Acid and base solutions were 0.1 M hydrogen chloride (HCl) and 0.7 M sodium carbonate (Na2CO3), respectively.

Biomass

10 media pieces were taken from a given reactor, and each piece was thoroughly cleaned by brushing using Proxabrush "Go-Betweens" dental brushes (Sunstar Americas Inc. Schaumburg, IL). The removed biofilm was collected by rinsing with DI water, the total suspended solids (TSS) and volatile suspended solids (VSS) in the rinse water was measured according to Standard Methods 2540B and 2540E, respectively (American Public Health Association et al., 2012).

The biofilm mass concentration in the reactor was calculated using Equation 4:

$$\text{Total biofilm solids, TBS } \left(\frac{\text{mg}}{\text{L}}\right) = \frac{\text{dry mass removed from media (mg)}}{\text{reactor working volume (L)}} \times \frac{\text{total media pieces}}{\text{pieces of media tested}} \quad \text{(eq. 4.4)}$$

Illumina DNA Sequencing

20 media pieces were taken from a given reactor, and each piece was thoroughly cleaned by brushing using Proxabrush "Go-Betweens" dental brushes (Sunstar Americas Inc. Schaumburg, IL). The removed biofilm was collected by rinsing with DI water, and excess liquid was centrifuged off to form a pellet. The pellet was frozen and shipped to RTL Genomics, Research and Testing Laboratory (Lubbock, TX) for DNA extraction and Illumina Next Generation sequencing using the 357wF-785R assay and 784F [5′ -RGGATTAGATACCC-3′] and 1064R [5′ -CGACRRCCATGCANCACCT-3′]) bacterial DNA primers.

Trace organics

Triclosan, ibuprofen, and caffeine were measured by solid phase extraction (SPE) followed by analysis on high performance liquid chromatography (HPLC) at UNM. SPE was done using Oasis HLB cartridges, 3 mL, 40 mg; Waters Corporation, Millford, MA) according to the manufacturers instructions. They were sequentially preconditioned with 6 mL of methanol, and 6mL of reagent water acidified to pH 2 with HCL. The samples were acidified to pH 2, and were then loaded onto the cartridges at a max flow rate of 10 mL/min. After loading the 100mL samples, cartridges were rinsed with 5 mL of water acidified to pH 2 and then dried with a light vacuum. Next, the analytes were eluted from the cartridge with 5 mL of methanol, and reconstituted with 5mL of reagent water.

Hewlett-Packard, HP 1100 was used for measurement triclosan, ibuprofen, and caffeine. The system consisted of a degasser, a quaternary pump, an ALS auto-sampler,

thermostat, and a variable wavelength UV-vis detector. A Waters Xterra C18 15mm column with vanguard guard cartridge was used for separation.

Caffeine, ibuprofen, and caffeine were purchased from Sigma Aldrich. Naproxen catalog number: M1275-5G, ibuprofen Catalog Number: I110-1G triclosan, Catalog Number: PHR1338-1G and dissolved into stock solutions of HPLC grade 1:1 methanol:water.

For triclosan and ibuprofen, the HPLC carrier eluent was a 20:80 A:B mixture of A) 1% trifluoroacetic acid, 99% HPLC grade water and B) 50:50: methanol:water. For caffeine the eluent mixture was 60:40 A:B A) methanol, B) HPLC grade water. Flow through the column was 0.2 mL/min at a run time of 30 minutes. The UV detector was set to 210nm.

Solid Phase Extraction

The SPE cartridges (Oasis HLB cartridges (3 mL, 40 mg) (Waters Corporation, Milford, MA) were sequentially preconditioned with 6 mL of methanol, and 6mL of reagent water acidified to pH two with HCL. The samples were acidified to pH two, and were then loaded onto the cartridges at a max flow rate of 10 mL/min. After loading the 100mL samples, cartridges were rinsed with 5 mL of water acidified to pH 2 and then dried with a light vacuum. Next, the analytes were eluted from the cartridge with 5 mL of methanol, and reconstituted with 5mL of reagent water.

Results and Discussion

Startup and Operations, Experiment 1

Figure 4.2 shows the HDPE and nylon reactor startup performance over a two-month period.

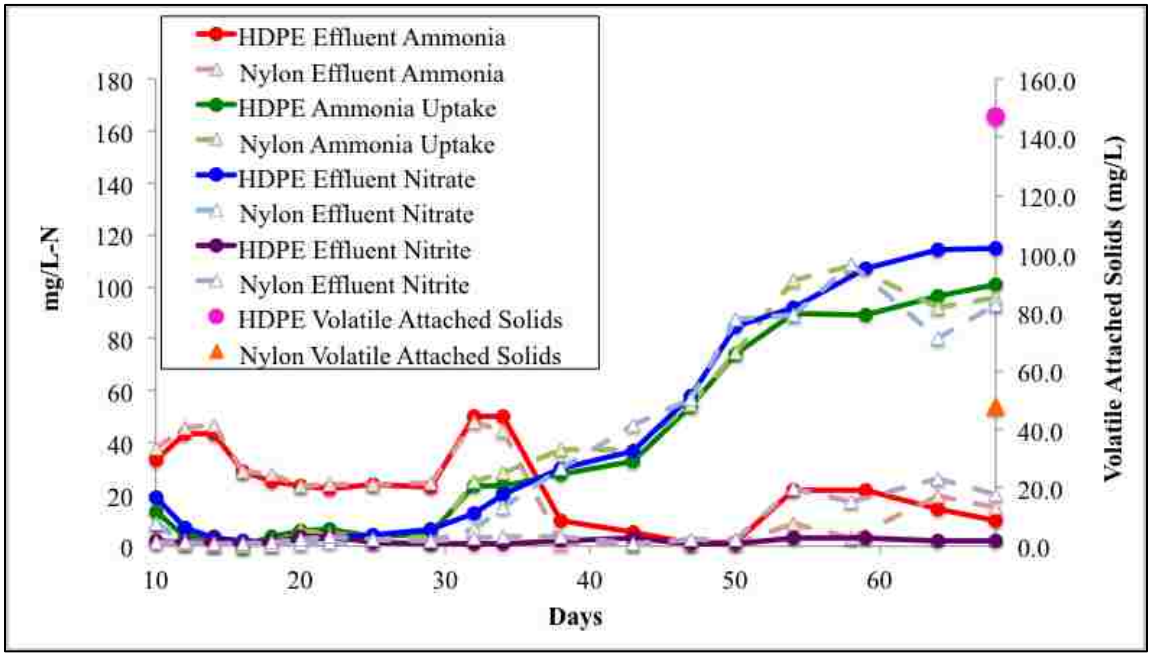

Both reactors exhibited similar performance over a two month period in terms of ammonia uptake and NO_x production (Figure 4.2). However, by the end of this study the nylon media had much less attached biomass (48 mgVBS/L) than did the HDPE reactor ((147mgVBS/L). This indicated that that the nylon reactor had a higher rate maximum specific to the amount of biofilm present (2000mgN/gVBS*d) than did the HDPE reactor (687mgN/gVBS*d). These rates are greater than those reported by Melcer and Schuler 2014, who found maximum specific rates of nitrifying biofilms at 247

mgN/gVBS*d in lab scale reactors using commercially available MBBR media. Towards the end of the two month period, nitrite concentrations were higher than in the HDPE reactor, indicating less NOB activity relative to AOB activity in the nylon reactor in the nylon reactor as compared to the HDPE reactor.

Biofilm Microbial Populations

After nearly 2 months of reactor operation, the biofilm samples were analyzed by Illumina next generation sequencing to characterize the microbial communities associated with each plastic type. Figure 4.3 shows Illumina DNA sequencing at the family taxonomic level, expresses relative abundance (percent of total operational taxonomic units, or OTUs, detected).

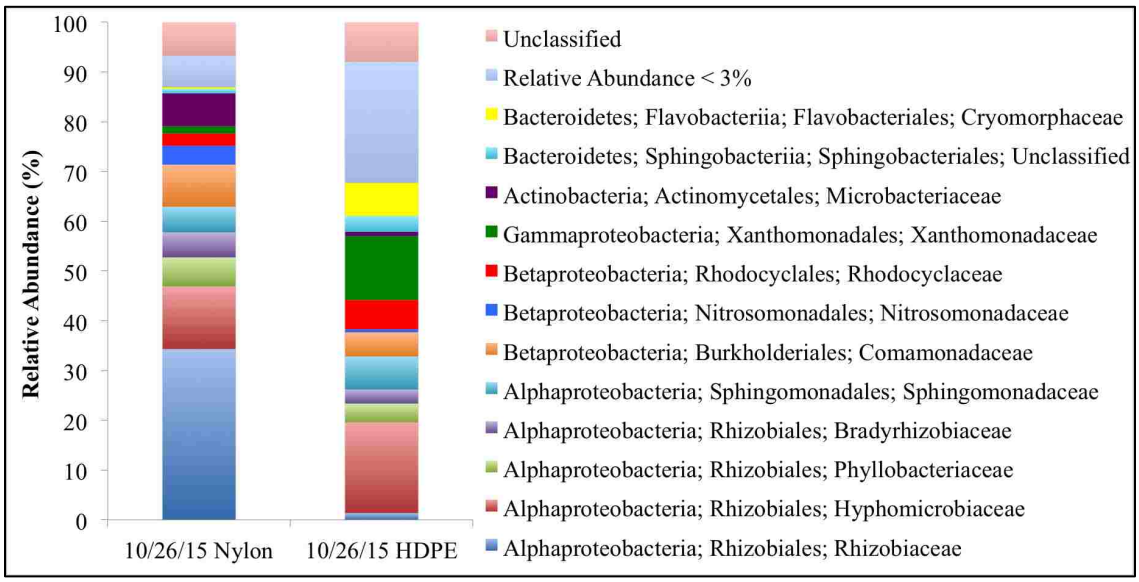

These results indicate large differences in community structures of the two biofilms. The calculated Shannon Diversity Index for the nylon biofilm population was

slightly lower than the HDPE biofilm (SDI = 2.38, 3.08 respectively), indicating a somewhat less diverse population on the nylon media. The dominant family on the nylon biofilm *Rhizobiacae*, (34.3%), while this group was much lower on the HDPE (1.37%). Bacteria from the family Rhizobiacae were reported by Sasaki et al., 2007 as an ammonia assimilating microorganism isolated from biological ammonia removal systems receiving livestock wastewater. The family *Nitrosomonadaceae*, which are well-known AOB (Kowalchuk et al., 2001), was also found in greater abundance on the nylon carrier (3.77%) than on HDPE (0.56%). Although the total amount of biofilm was less on the nylon plastic, a difference in performance is not observed because the nylon biofilm is more concentrated in AOB type organisms. In studies conducted by Fitzgerald et al., 2015, the family Xanthomonadaceae was found to be involved with heterotrophic ammonia oxidation under low dissolved oxygen conditions (<0.3mg.L) On the HDPE media, where the biofilm by has a higher relative abundance of Xanthomonadaceae compared to Nylon (12.9% and 1.4% respectively), the thicker HDPE biofilm may have decreased dissolved oxygen deep inside the biofilm, facilitating the growth of this heterotrophic AOB organism.

At a higher taxonomic level, the order *Rhizobiales* comprised the majority of the nylon attached biomass accounting for 57.7%, and was only 26.2% on the HDPE attached biofilm. In addition to this the nylon reactor biofilm also has a higher concentration of *s* (8.5%) than found on HDPE (4.9%) This is important to note, as it has been determined by Esplugas et al., 2013 that Rhizobiales along with burkholderiales are important organisms associated with the removal sulfamethoxazole, as the sole carbon source in sequencing batch biofilm reactors. Sulfamethoxazole is a

synthetic organic chemical that functions as an antibiotic to treat bacterial infection, and is also commonly found in trace amounts in influents to wastewater treatment plants. The organisms belonging to proteobacteria that are more abundant on nylon media and able to metabolize Sulfamethoxazole, may also have the potential to remove a wider variety of other common synthetic organics found in wastewater.

Startup and Operations, Experiment 2

After the experiment described above, fresh media were reinoculated in both reactors. This was done in part because approximately 30 percent of the media in each reactor had been sacrificed for biomass and Illumina sequencing measurements. A new set of reactors were again inoculated, and started up in with the same operating parameters listed Table 4.1 and configuration listed in Figure 4.1. The primary objective of this second experimental run was to evaluate the ability of nitrifying biofilms grown on different plastics to remove organic microconstituents commonly found in wastewater. Figure 4.4 shows the startup nitrification performance of these reactors.

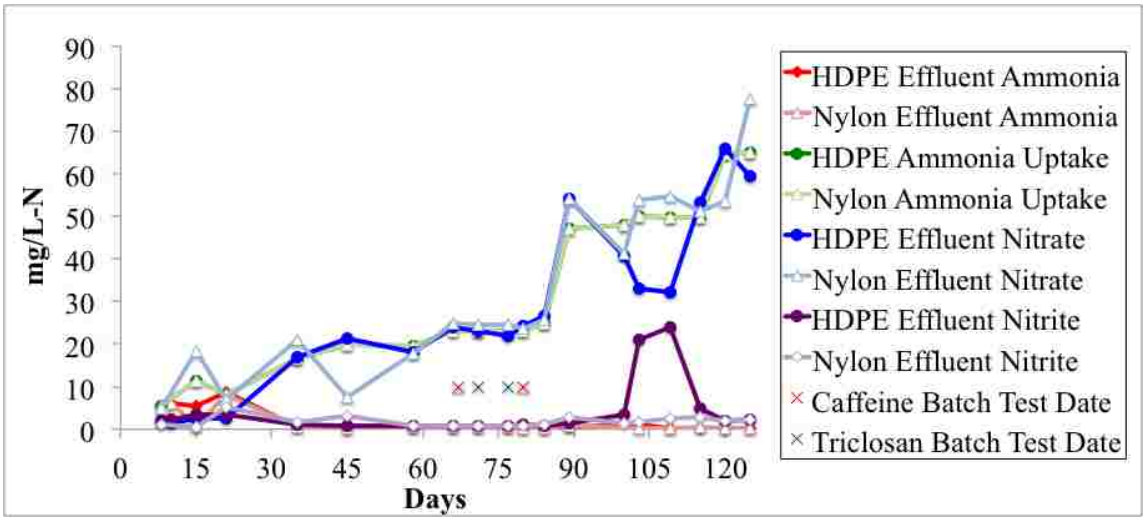

Influent ammonia to the continuous system was held at a concentration of 25mg/L during for batch test dates shown in Figure 4.4 in order to ensure complete and equal conversion of ammonia to nitrate in both reactors.

Triclosan and Caffeine Batch Tests

In all batch test experiments conducted, sampled were extracted and measured for organic microconstituents 1 minute after dosing and 61 minutes after dosing. This information allows us to calculate an hourly removal rate for each chemical following the rapid initial removal due to adsorption. Figure 4.5 shows the results of this test.

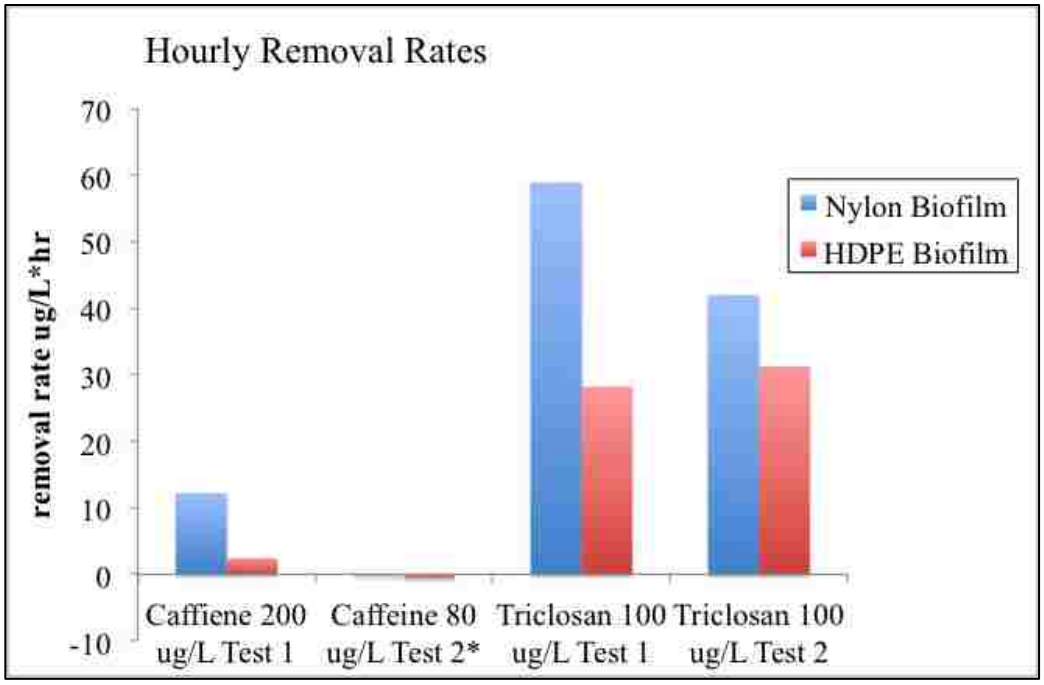

As shown in Figure 4.5 when compared to HDPE, the nylon biofilm was able to remove more caffeine in the 200ug/L dose and triclosan in both 100ug/L dose batch tests. In the less concentrated 80ug/L caffeine test, and the 500ug/L ibuprofen test both the nylon and HDPE attached biofilms did not remove significant amounts of caffeine in the one hour following the rapid initial removal.

Figure 4.6 shows the nylon and HDPE biofilm reactor batch test concentrations and removal efficiency of triclosan in both short and long term time periods by measuring concentration before the biofilm is added (t=0), immediately after the addition of the biofilm to the liquid (t=1 min) and at 61 minutes following the dose.

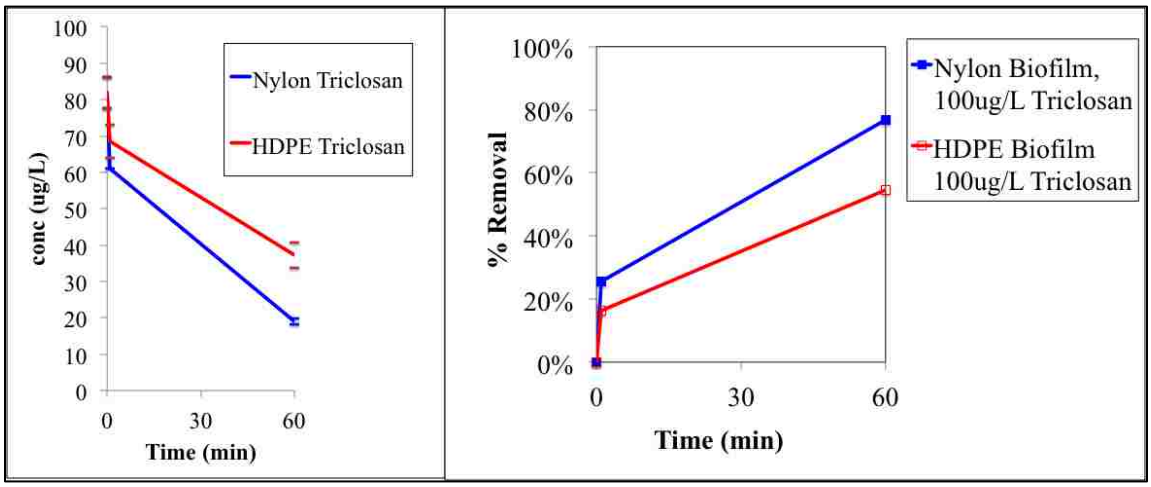

As shown in Figure 4.6, the nylon reactor removed a greater percentage of triclosan than did the HDPE reactor both at 1 minute (6% and 16%, respectively) and at 61 minutes (77% and 55%, respectively). The rate of removal was more rapid during the first minute (Nylon average 1252 mg/L*min, HDPE average 800 mg/L*min) than it was during minutes 1 to 61 (Nylon average 41 mg/L*hr, HDPE average 31.3 mg/L*hr) a decreasing rate of removal is consistent with first order kinetics.

In order to discern between adsorption/biotransformation of the organic microconstituent to the biofilm, and adsorption to the plastic, a batch tests containing a similar triclosan dose were conducted on the nylon and HDPE media with and without biofilms attached. Figure 4.7 shows the results this batch test in terms of concentration and percent removal following a 100ug/L dose of triclosan before the biofilm is added (t=0), immediately after the addition of the biofilm to the liquid (t=1 min) and at 61 minutes following the dose.

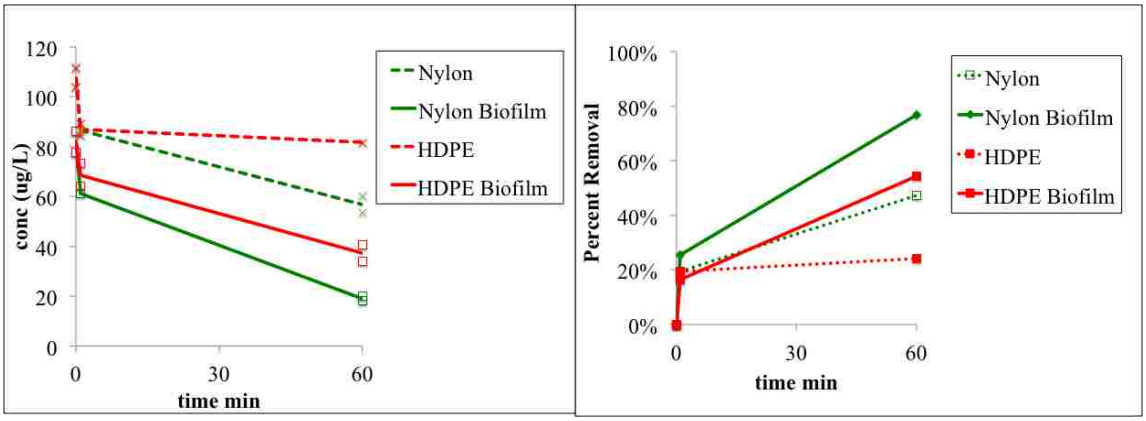

The results of this experiment show that the choice of plastic has little effect on the amount of triclosan adsorbed in the first minute of the experiment. Over 61 minutes, additional triclosan adsorbed to the nylon plastic (47%) but not the HDPE. In all batch tests conducted with biofilm attached to the nylon and HDPE, more removal was observed from 1 to 61 minutes than compared to tests conducted without the biofilm. Adding a biofilm to the nylon media seems to have increased this initial adsorption, whereas the biofilm attached to the HDPE did not. More removal was observed in the biofilms attached to nylon when compared to HDPE in both the 1 minute and 1 hour test intervals.

Alternatively, the results shown in Figure 4.7 could be consistent with initial adsorption combined with biodegradation later in the experiment. Interestingly, the biofilm grown on the nylon surface removed 26% of the 100ug/L triclosan dose where the HDPE grown biofilm only removed 16% during the initial and rapid 1-minute uptake. In the following 60 minutes, the nylon biofilm also removed more triclosan than

the HDPE media (78%, 54% removal respectively), which may indicate enhanced biotransformation occurring on the nylon grown biofilm.

Figure 4.8 shows the nylon and HDPE biofilm reactor batch test concentrations and removal efficiency of caffeine in both short and long term time periods by measuring concentration before the biofilm is added (t=0), immediately after the addition of the biofilm to the liquid (t=1 min) and at 121 minutes following the 80 ug/L caffeine dose.

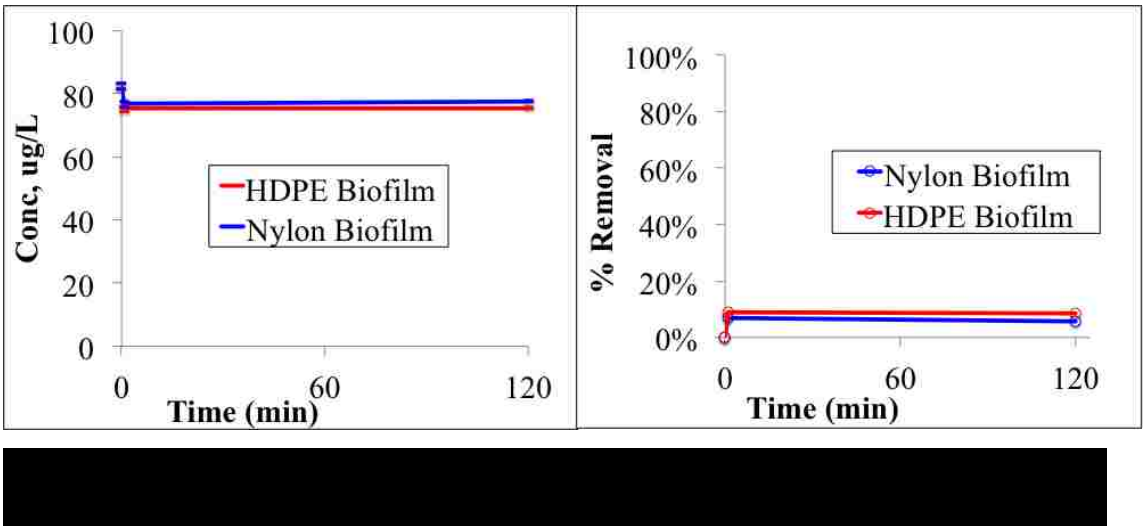

Following the 80ug/L dose of caffeine the Nylon and HDPE grown biofilms removed 8.7% and 7% respectively in the first minute, but in either case did not further remove any measurable caffeine over the next 60 minutes. This most likely indicates that adsorption to the biofilm is the main removal mechanism in both systems, and biotransformation does not occur. Differences in initial adsorption between the two biofilms may indicate that varying the hydrophobicity and surface energy of the plastic (Table 4.1) influenced the hydrophobicity of the biofilm formed. The relative removal of each chemical in the first minute may be explained by contrasting hydrophobicity where

triclosan is more hydrophobic (log K_{ow} 4.76) and caffeine is more hydrophilic (log K_{ow} 0.091).

This data supports the idea that using nylon plastic as an attachment surface may facilitate and enhances the removal of organic microconstituents. A reasonable explanation for this may be that the nylon plastic alone adsorbs more of the contaminant, making it more available to the biofilm that is growing on the surface to remove by further adsorption and biotransformation. Another explanation may be that the nylon plastic with greater surface energy selected for microorganism better suited to remove organic microconstituents through metabolism (discussed above).

Conclusions

After successfully starting up nitrifying biofilms grown on either nylon or HDPE plastic, it was determined that neither plastic benefited overall nitrification performance. Despite no differences in overall performances, when compared to the HDPE biofilm the nylon plastic media formed a thinner biofilm that was more active on a specific rate. The nylon biofilm was slightly less diverse with a higher concentration of nitrifiers and potential organic microconstituent metabolizers. A likely explanation for this is the differences in hydrophobicity between the two plastic types. Batch testing results indicated enhanced removals rates in the biofilms attached to nylon for caffeine in the larger dose (200ug/L), and all triclosan tests. No removal in either reactor was observed for caffeine in the smaller dose (80ug/L), and ibuprofen.

Chapter 5 Conclusions

1) Following nitrification reactor startup of commercially available MBBR/IFAS media designed with contrasting geometries, system performance and microbial communities varied greatly in the resulting biofilms. Media geometry likely influenced internal fluid dynamics within each type of plastic biofilm carrier. The open media produced a thinner biofilm with a low abundance of the known AOB Nitrosomonas, while the sheltered design produced a thicker biofilm rich in Nitrosomonas. Batch testing each media type at various mixing rates indicates that nitrification performance in the more protected media benefits from increasing mixing, where the open R1 media does not. Decreasing temperature from 21 to 10.5 degrees Celsius in R1 resulted in the eventual failure of the media to retain its biomass. Although nitrification performance was decreased, sloughing was not observed in the sheltered R2 media design and may suggest that decreasing temperature makes a biofilm more susceptible to mixing induced shear. Following the drop in temperature the R2 media decreased in overall diversity, all but eliminating the AOB Nitrosomonas while largely favoring the family Xanthomonadaceae. Xanthomonadaceae is known for heterotrophic nitrification by an unknown pathway and its occurrence explain the disappearance of the known AOBs with only a modest decrease in nitrification performance. After increasing the temperature back to 21 degrees, the R2 biofilm diversity and microbial family relative abundance returned to similar level to before the temperature decrease. Media geometry likely influenced internal fluid dynamics within the plastic biofilm carrier.

2) The analysis of Albuquerque's primary effluent revealed consistent concentrations of synthetic organic compounds found in other studies of treatment plants

around the world. Several of these compounds are present but not detected in a conjugate form. When coming into contact with biofilms, it is possible that these compounds deconjugated to underestimate removal, or produce the parent compound in reactor effluents. Of the compounds analyzed, triclocarban, trimethoprim, primidone, and PFOA were more efficiently removed by the control reactor containing no allylthiourea (Figure 4.11). This finding supports other studies that suggest trimethoprim and Primidone degradation are cometabolic processes. Our observation of enhanced removal for triclocarban and PFOA in nitrifying MBBR reactors is the first to suggest a cometabolic degradation pathway for these compounds under these conditions.

3) After successfully starting up nitrifying biofilms grown on either nylon or HDPE plastic, it was determined that neither plastic benefited overall nitrification performance. Despite no differences in overall performances, when compared to the HDPE biofilm the nylon plastic media formed a thinner biofilm that was more active on a specific rate. The nylon biofilm was slightly less diverse with a higher concentration of nitrifiers and potential organic microconstituent metabolizers. A likely explanation for this is the differences in hydrophobicity between the two plastic types. Batch testing results indicated enhanced removals rates in the biofilms attached to nylon for caffeine in the larger dose (200ug/L), and all triclosan tests. No removal in either reactor was observed for caffeine in the smaller dose (80ug/L), and ibuprofen.

Chapter 6 References

Allen, Welch, Prebyl, Baker, Meyers, Sayler, (2004). Analysis and glycosyl composition of the exopolysaccharide isolated from the floc-forming wastewater bacterium Thauera sp. MZ1T. Environmental. Microbiology. 6, 780–790.

Anthonisen, A.C., Loehr R.C., Prakasam T.B., Srinath, E.G., (1976). Inhibition of nitrification by ammonia and nitrous acid. Journal of the Water Pollution Control Federation 48(5):835–852

Anumol, T., Merel, S., (2013). Ultra high performance liquid chromatography tandem mass spectrometry for rapid analysis of trace organic contaminants in water. Chemistry Central Journal 7(1): 104.

Batt, A., Kim, S., Aga, D. (2006). Enhanced Biodegradation of Iopromide and Trimethoprim in Nitrifying Activated Sludge. Environ. Sci. Technol. 2006, 40, 7367-7373.

Bill, K.A., Bott, C.B. and Murthy, S.N., (2010). Evaluation of sulfide-driven autotrophic denitrification in a moving bed biofilm reactor, Water Environment Federation, Proceedings of the Water Environment Federation Annual Conference (WEFTEC), New Orleans.

Chandran, K. and Love, N.G., (2008). Physiological state, growth mode, and oxidative stress play a role in Cd(II)-mediated inhibition of Nitrosomonas europaea 19718. Applied and Environmental Microbiology 74(8), 2447-2453.

Clemens, J., Estergreen, V. (1982). Metabolism and conjugation of [4-14C]progesterone by bovine liver and adipose tissues, in vitro. Steroids 40(3) (1982) 287-306

Cydzik-Kwiatkowska, Agnieszka (2015). Bacterial structure of aerobic granules is determined by aeration mode and nitrogen load in the reactor cycle. Bioresource Technology 181, 312–320

De Beer, D., Stoodley, P., & Lewandowski, Z. (1996). Liquid flow and mass transfer in heterogeneous biofilms. Water Research, 30(11), 2761}2765.

Fischer, Majewsky (2014). Cometabolic degradation of organic wastewater micropollutants by activated sludge and sludge-inherent microorganisms. Applications in Microbiology Biotechnology 98 6583–6597

Fitzgerald, Camejo, Oshlag, Noguera (2015) Ammonia-oxidizing microbial communities in reactors with efficient nitrification at low-dissolved oxygen water research 70 38-51

Halling-Sørensen B., Nors Nielsen S., Lanzky P.F., Ingerslev F., Holten Lützøft H.C. and Jørgensen S.E. (1998). Occurrence, fate and effects of pharmaceutical substances in the environment – a review. Chemosphere., 36, 357-393

Ista, L.K., Callow, M.E., Finlay, J.A., Coleman, S.E., Nolasco, A.C., Simons, R.H., Callow, J.A., Lopez, G.P., (2004). Effect of substratum surface chemistry and surface energy on attachment of marine bacteria and algal spores. Applied and Environmental Microbiology 70 (7), 4151-4157.

Jia, A., Escher, B. I., Leusch, F. D. L., Tang, J. Y. M., Prochazka, E., Dong, B., Snyder, S. A. (2015). In vitro bioassays to evaluate complex chemical mixtures in recycled water. Water Research, 80, 1-11.

Juliastuti, S.R., Baeyens, J. and Creemers, C., (2003). Inhibition of nitrification by heavy metals and organic compounds: The ISO 9509 test. Environmental Engineering Science 20(2), 79-90.

Kim, H., Gunsch, C.K., Geller, J.L., Boltz, J.P., Freudenberg, R.G. and Schuler, A.J., (2010). Shelter from the storm: Integrated fixed film activated sludge protects nitrifiers from toxic upsets. Proceedings of Water Environment Federation Annual Conference (WEFTEC), New Orleans.

Khan M., Chapman T., Cochran K., Schuler A., (2013). Attachment surface energy effects on nitrification and estrogen removal rates by biofilms for improved

wastewater treatment. Water Research 47 2190-2198

Khan, M., Ista, L.K., Lopez, G.P., Schuler, A.J., (2011). Experimental and theoretical examination of surface energy and adhesion of nitrifying and heterotrophic bacteria using self-assembled monolayers. Environmental Science and Technology 45 (3), 1055-1060.

Khunjar, W.O., Mackintosh, S.A., Skotnicka-Pitak, J., Baik, S., Aga, D.S., Love, N.G., (2011). Elucidating the relative roles of ammonia oxidizing and heterotrophic bacteria during the biotransformation of 17 alpha-ethinylestradiol and trimethoprim. Environmental Science and Technology 45 (8), 3605-3612.

Lackner, S., Holmberg, M., Terada, A., Kingshott, P., Smets, B.F., (2009). Enhancing the formation and shear resistance of nitrifying biofilms on membranes by surface modification. Water Research 43 (14), 3469-3478.

Lozano, N., Rice, C., Ramirez, M., Torrents, A. (2013) Fate of Triclocarban, Triclosan and Methyltriclosan during wastewater and biosolids treatment processes. Water Research 47 4519-4527

Metcalf and Eddy. (2003). Wastewater Engineering Treatment and Reuse. Forth Edition.

Ngoc, Urase, Ngo, Hu, Ogn, (2013). Insight into metabolic and cometabolic activities of autotrophic and heterotrophic microorganisms in the biodegradation of emerging trace organic contaminants. Bioresource Technology 146 721-731

Norihide Nakada, Toshikatsu Tanishima, Hiroyuki Shinohara, Kentaro Kiri, Hideshige Takada. (2006). Pharmaceutical chemicals and endocrine disrupters in municipal wastewater in Tokyo and their removal during activated sludge treatment. Water Research 40 3297-3303

Parker D. S. (1970) Characteristics of biological flocs in turbulent regimes, Doctoral thesis, University of California, Berkeley, http://disexpress.umi.com/dxweb, UMI publication number 7109887.

Paxeus, N., (2004). Removal of selected non-steroidal anti-inflammatory drugs (NSAIDs), gemfibrozil, carbamazepine, b-blockers, trimethoprim and triclosan in conventional wastewater treatment plants in five EU countries and their discharge to the aquatic environment. Water Sci. Technol. 50 (5), 253–260.

Roh, Subramanya, Zhao, Ping, Sandt, Chu (2009). Biodegradation potential of wastewater micropollutants by ammonia-oxidizing bacteria. Chemosphere 77 1084-1089

Sasaki, H., Nonaka, J., Sasaki,. T. (2006) Ammonia removal from livestock wastewater by ammonia-assimilating microorganisms immobilized in polyvinyl alcohol Journal of Industrial Microbiology and Biotechnology. 34:105–110

Schuler and Melcer. (2014). Mass Transfer Characteristics of Floating Media In MBBR and IFAS Fixed-Film Systems. Project U4R11 Final Report. Water Environment Research Foundation.

Shi, J., Fujisawa, S., Nakai, S., Hosomi, M. (2004) Biodegradation Of Natural and Synthetic Estrogens By Nitrifying Activated Sludge and Ammonia Oxidizing Bacterium Nitrosomonas europaea. Water Research 38 2323-2330

Siripong Slil, Rittman Bruce (2007). Diversity study of nitrifying bacteria in full-scale municipal wastewater treatment plants. Water Research 41 (2007) 1110– 1120

Ternes T.A., Stumpf M., Mueller J, Haberer K, Wilken R-D and Servos M. (1999) Behaviour and occurence of estrogens in municipal sewage treatment plants - II. Aerobic batch experiments with activated sludge Sci. Total Environ. 225, 91-99.

Van Loosdrecht, M.C.M., Lyklema, J., Norde, W., Zehnder, A.J.B., (1990). Influence of interfaces on microbial activity. Microbiological Reviews 54 (1), 75e87.

Vanderford, B. J. and S. A. Snyder (2006). "Analysis of pharmaceuticals in water by isotope dilution liquid chromatography/tandem mass spectrometry." Environmental Science & Technology 40: 7312-7320.

Wojcieszynska, Domaradzka, Kocurek, (2014). Bacterial degradation of naproxen - Undisclosed pollutant in the environment. Journal of Environmental Management 145 157-161

Xin Xiaodong, He Junguo, Wang Yuefei, Feng Jinghan, Qiu Wei (2016) Role of aeration intensity on performance and microbial community profiles in a sequencing batch reaction kettle (SBRK) for wastewater nutrients rapid removal. Bioresource Technology 201 (2016) 140–147

Yi Taewood, Harper Willie, (2007). The Link between Nitrification and Biotransformation of 17 Alpha Ethinylestradiol. Environmental Science and Technology 41 4331-4316

Vitousek, P., Aber, J., Howarth, R., Likens, G., Matson, P., Schindler, D., Schledsinger, W., Tilman, D. (1997). Human Alteration of The Global Nitrogen Cycle: Sources and Consequences. Ecological Applications, 7(3) 737-750

Randall, C.W., Sen, D., (1996). Full-scale investigation of an integrated fixed-film activated sludge (IFAS) process for enhanced nitrogen removal. Water Science and Technology 33 (12), 155e162.

Kowalchuk, G., Stephen, J. (2001) Ammonia-Oxidizing Bacteria: A Model For Molecular Microbial Ecology. Annual Review Microbiology, 55, 485-529

Joo, H.S., Hirai, M., Shoda, M., (2005). Characteristics of ammonium removal by heterotrophic nitrification–aerobic denitrification by Alcaligenes faecalis No. 4. Journal of Bioscience and Bioengineering 100 (2), 184–191.

Zhang, J., Wu, P., Hao, B., Yu, Z. (2011) Heterotrophic nitrification and aerobic denitrification by the bacterium Pseudomonas stutzeri YZN-001. Bioresource Technology, 102, 9866-9869

Appendix

Appendix A: Chapter 2 Data

Figure 2.5

Dates	G, 1/s	R1 Influent NH4-N, mg/L	R1 Effluent NH4-N, mg/L	R1 Effluent NO3-N, mg/L	R1 Effluent NO2-N, mg/L
3/19/13	239.8	43.6	24.8	16.2	
3/21/13	239.8	43.6	16.5	25.6	
3/22/13	239.8	56.1	20.9	34.9	
3/24/13	239.8	56.1	12.3	41.8	
3/26/13	239.8	66.2	15.6	49.1	
3/27/13	239.8	66.2	6.4	56	
3/28/13	239.8	66.2	3.9	61.1	
3/29/13	239.8	76.6	0.6	74.6	
4/1/13	239.8	106.5	6.8	96	
4/2/13	239.8	106.5	2.2	102	
4/4/13	239.8	122.7	9	111	
4/6/13	239.8	122.7	5.1	112	
4/8/13	239.8	122.7	0.8	119	
4/10/13	239.8	149.1	11.2	129	
4/13/13	239.8	149.1	2.9	137	
4/17/13	239.8	149.1	26.5	108	
4/19/13	239.8	165.7	15.6	137	
4/23/13	239.8	165.7	30.9	116	
4/25/13	239.8	165.7	0.8	154	
4/26/13	298.0	165.7	0.1	156	
4/29/13	298.0	173.1	1.9	170	
4/30/13	298.0	225	1.4	189	

Dates	G, 1/s	R1 Influent NH4-N, mg/L	R1 Effluent NH4-N, mg/L	R1 Effluent NO3-N, mg/L	R1 Effluent NO2-N, mg/L
5/2/13	298.0	293	104.7	146	
5/3/13	298.0	293	104.2	149	
5/6/13	298.0	293	49.4	207	
5/7/13	298.0	293	40	216	
5/9/13	298.0	293	42.8	217	37.1
5/13/13	298.0	293			
5/15/13	298.0	293	93.5	140	19
5/17/13	298.0	386	125	229	13.9
5/20/13	298.0	310	5	277	0.5
5/23/13	298.0	231	20.8	197	15.5
5/27/13	298.0	250	9.1	189	73.7
5/29/13	298.0	250	104.6	61	62.3
5/31/13	298.0	250	102.8	68	88.8
6/3/13	298.0	250	55.4	83	122
6/5/13	298.0	250	55.7	72	139
6/7/13	298.0	256	45.5	86	136.8
6/10/13	298.0	420	220	129	52.8
6/12/13	298.0	190	1.4	127	55.7
6/14/13	298.0	238	1.7	182	65.4
6/17/13	298.0	276	1.3	260	12
6/19/13	298.0	304	2.3	259	46.5
6/21/13	298.0	304	5.5	201	78
6/24/13	298.0	359	18.7	223	120.9
6/26/13	298.0	359	44.7	206	64.8
6/28/13	298.0	359	32.7	239	98.6
7/1/13	298.0	359	12.7	213	141.1

Dates	G, 1/s	R1 Influent NH4-N, mg/L	R1 Effluent NH4-N, mg/L	R1 Effluent NO3-N, mg/L	R1 Effluent NO2-N, mg/L
7/3/13	298.0	404	47.1	258	115.8
7/5/13	298.0	404	18.1	263	135.3
7/8/13	298.0	433	43.3	265	141.1
7/10/13	298.0	412	110.5	202	70.5
7/12/13	298.0	412	76.5	229	101.2
7/15/13	298.0	412	49.7	243	111.2
7/17/13	298.0	412	46.6	250	95.6
7/19/13	298.0	412	42.9	258	97
7/22/13	298.0	412	39.4	267	106
7/24/13	298.0	412	107.1	198	69.5
7/26/13	298.0	401	48.8	210	147.5
7/29/13	298.0	401	39.1	229	156.7
7/31/13	298.0	401	23.8	212	183.5
8/2/13	298.0	401	3.7	268	141.5
8/6/13	298.0	401	3.8	251	151.5
8/9/13	298.0	401	4.1	258	149.5
8/12/13	298.0	401	3.8	251	159.5
8/14/13	298.0	401	100	179	75
8/16/13	298.0	401	44.1	221	155.5
8/19/13	298.0	398	18.2	249	142.5
8/21/13	298.0	415	14.1	246	151.5
8/23/13	298.0	415	20.5	212	176.5
8/26/13	298.0	415	19.1	229	181.5
8/28/13	298.0	410	22.9	199	198.5
8/30/13	298.0	410	11.4	201	205.5
9/2/13	298.0	410	17	197	201

Dates	G, 1/s	R1 Influent NH4-N, mg/L	R1 Effluent NH4-N, mg/L	R1 Effluent NO3-N, mg/L	R1 Effluent NO2-N, mg/L
9/5/13	327.3	370	76.6	82	201
9/6/13	327.3	370	80.6	81	201.5
9/9/13	308.0	300	56.5	82	164
9/12/13	308.0	300	81.2	67	115
9/13/13	308.0	300	89.6	67	130
9/16/13	308.0	225	14.7	68	131.5
9/20/13	308.0	225	82.8	80	66
9/24/13	327.3	225	90.9	76	58.5
9/26/13	327.3	178	60.6	71	56
9/29/13	327.3	178	90.5	58	29.5
10/4/13	327.3	161	57.5	51	49.5
10/7/13	327.3	161	65.3	47	46.5
10/9/13	327.3	161	67.7	31	34.2
10/11/13	327.3	150	69.8	39	38.5
10/13/13	327.3	150	71.2	32	36.5
10/19/13	327.3	150	84.3	22	32.5
10/23/13	327.3	121	76.8	18.3	25
10/25/13	327.3	121	81.2	20	19.5
10/28/13	327.3	109	66	19	22.5
10/31/13	327.3	95	61.2	10	20.5
11/2/13	327.3	95	66.5	9.8	20.5
11/4/13	327.3	95	62.6	10.2	22
11/7/13	327.3	95	63.6	8.5	25.5
11/9/13	327.3	95	60.6	9.1	20.2
11/11/13	327.3	95	67.5	7.4	20.5
11/14/13	327.3	100	70.3	8.5	22.35

Dates	G, 1/s	R1 Influent NH4-N, mg/L	R1 Effluent NH4-N, mg/L	R1 Effluent NO3-N, mg/L	R1 Effluent NO2-N, mg/L
11/16/13	327.3	100	71.8	8.9	20.95
11/18/13	327.3	85	58.8	5.7	23.35
11/21/13	327.3	85	57.1	6.4	22.05
11/23/13	327.3	85	55.1	7	21.95
11/25/13	327.3	85	57.1	6.5	22.95
11/27/13	327.3	85	52.6	6.7	23.78
12/1/13	327.3	85	47.3	7.2	28.2
12/14/13	304.6	77	26.9	6	55
12/15/13	304.6	77	20.8	8	52
12/19/13	304.6	77	21.3	7	50.2
12/21/13	304.6	77	22.9	6.8	44.6
12/24/13	304.6	88	19	11.7	44
12/26/13	295.9	88	19	8.2	46
12/29/13	295.9	88	15	8.7	61
12/31/13	295.9	88	26	9.3	60
1/2/14	295.9	88	8	5.8	55
1/4/14	295.9	88	5	2.3	88
1/6/14	295.9	88	9.1	5.7	76
1/8/14	295.9	121	56	5.5	74
1/10/14	295.9	121	55	4.6	75
1/12/14	295.9	121	36	5.7	95
1/14/14	298.0	121	0.5	8.3	115
1/16/14	298.0	233	107	12.3	134
1/19/14	298.0	233	52.2	16.7	171.6
1/21/14	298.0	233	18.9	23.1	201
1/22/14	298.0	233	5.9	24.6	212

Dates	G, 1/s	R1 Influent NH4-N, mg/L	R1 Effluent NH4-N, mg/L	R1 Effluent NO3-N, mg/L	R1 Effluent NO2-N, mg/L
1/24/14	298.0	340	46	25.2	244
1/26/14	298.0	340	59	33.2	254
1/28/14	298.0	407	187	21.6	179
1/30/14	298.0	407	204	25.4	207
2/2/14	298.0	339	91	19.4	229
2/4/14	298.0	339	101	15.3	233
2/6/14	298.0	339	116	12	218
2/8/14	298.0	339	142	11.5	189
2/10/14	298.0	339	181	7.9	140
2/12/14	298.0	339	229	9.5	123
2/20/14	298.0	208	147		
2/21/14	298.0	132	56		
2/22/14	298.0	132	5.4		
2/23/14	298.0	209	27.7	18.2	159
2/24/14	298.0	209	45	17.3	136
2/26/14	298.0	209	24.9	20.2	167
2/28/14	298.0	214	40	23.1	165
3/2/14	298.0	214	3.5	26.7	168
3/4/14	298.0	314	13	26.1	240
3/5/14	298.0	316	8.8		
3/6/14	298.0	353	12	17	310
3/7/14	298.0	327	8		
3/8/14	298.0	327	20.6	27.4	310
3/10/14	298.0	330	90		
3/12/14	298.0	330	90		
3/13/14	298.0	240	16.4	18.8	231

Dates	G, 1/s	R1 Influent NH4-N, mg/L	R1 Effluent NH4-N, mg/L	R1 Effluent NO3-N, mg/L	R1 Effluent NO2-N, mg/L
3/15/14	298.0	240	4.9	29.4	212
3/17/14	298.0	240	4.5	32.2	197
3/19/14	298.0	259	22.1	36.8	205
3/21/14	298.0	259	11.3	35.5	201
3/23/14	298.0	259	4.6	36	221
3/25/14	298.0	259	2.8	40.4	220
3/26/14	298.0	292	3.7		
3/27/14	298.0	320	11.3	48	226
3/28/14	298.0	379	25.9		
3/31/14	298.0	372	67	48.8	260
4/2/14	298.0	340	31	43.2	254
4/4/14	298.0	332	13.3	45.2	278
4/6/14	298.0	332	12	37.6	283
4/8/14	298.0	332	45	37.4	265
4/10/14	298.0	326	10.9	43.2	285
4/12/14	298.0	355	25.7	38.4	274
4/15/14	298.0	347	16.9	32.8	270
4/18/14	298.0	335	174	30.4	148
4/19/14	298.0	335	155		
4/20/14	298.0	300	135		
4/21/14	298.0	207	39		
4/23/14	298.0	173	3.7	90	80
4/26/14	298.0	173	2	100	129
4/29/14	298.0	173	2.2	76	48
5/1/14	298.0	225	2.4	103.6	86
5/3/14	298.0	225	3	102	80

Dates	G, 1/s	R1 Influent NH4-N, mg/L	R1 Effluent NH4-N, mg/L	R1 Effluent NO3-N, mg/L	R1 Effluent NO2-N, mg/L
5/5/14	298.0	225	3.3	115.2	95
5/7/14	298.0	288	20.1	83.7	170
5/9/14	298.0	288	7.6	137	170
5/12/14	298.0	381	26.7	78	285
5/14/14	298.0	380	61	70	213
5/20/14	298.0	363	66	100	363
5/21/14	298.0	326	13	100	310
5/23/14	298.0	313	3	144	159
5/26/14	298.0	358	3	224	115
5/27/14	298.0	358	1.8	338	16
5/28/14	298.0	387	5.7	302	47
5/30/14	298.0	403	57	182	137
5/30/14	298.0	403	29	186	254
6/2/14	298.0	359	13.5	176	113
6/5/14	298.0	382	7	224	138
6/8/14	298.0	387	5.7	226	181
6/10/14	298.0	400	10.6	174	181
6/12/14	298.0	400	22.5	250	156
6/13/14	298.0	447	0.6	128	204
6/15/14	298.0	447	18.9	126	269
6/17/14	298.0	447	3.9	164	227
6/19/14	298.0	375	10	132	229
6/22/14	298.0	375	3	222	115
6/23/14	298.0	375	2		
6/25/14	298.0	375	50.1	122	139
6/26/14	298.0	375	23		

Dates	G, 1/s	R1 Influent NH4-N, mg/L	R1 Effluent NH4-N, mg/L	R1 Effluent NO3-N, mg/L	R1 Effluent NO2-N, mg/L
6/30/14	298.0	375	3.1	220	143
7/1/14	298.0	375	12	184	152
7/3/14	298.0	375	3.2	210	127
7/5/14	298.0	375	3.3	222	98
7/7/14	298.0	375	2.1	212	113
7/11/14	298.0	390	8.6	92	246
7/13/14	298.0	384	5.4	88	293
7/15/14	389.0	384	2.5	102	264
7/17/14	389.0	384	2.7		255
7/23/14	298.0	384	259		
7/25/14	298.0	202	22.5	50	156
7/26/14	298.0	202	3.5	70	148
7/28/14	298.0	224	1.2	154	71
7/31/14	298.0	255	1.4	238	16
8/2/14	298.0	294	2.7	249	75
8/4/14	298.0	342	2	286	62
8/6/14	298.0	381	0.4	262	118
8/9/14	298.0	515	100		
8/11/14	298.0	282	1.1	326	1.1
9/1/14	298.0	300	2.2	130	135
9/8/14	298.0	300	3.7	132	160
9/11/14	298.0	279	1.2	182	85
9/14/14	298.0	270	1.6	201	91
9/19/14	298.0	270	1.1	201	80
9/26/14	298.0	270	0.3	201	91
10/2/14	298.0	280	0.2	200	99

Dates	G, 1/s	R1 Influent NH4-N, mg/L	R1 Effluent NH4-N, mg/L	R1 Effluent NO3-N, mg/L	R1 Effluent NO2-N, mg/L
10/6/14	1.9	300	1.9	296	3
10/11/14	298.0	300	1.1	250	110
10/20/14	298.0	300	1.1	200	112
10/27/14	298.0	300	1.2	201	120
11/3/14	298.0	300	0.8	12	139
11/4/14	298.0	200	0.9	177	50
11/5/14	298.0	300	1.2	178	88
11/7/14	298.0	300	0.7	110	236
11/8/14	298.0	250	0.2	82	158
11/9/14	298.0	250	0.5	92	155
11/10/14	298.0	250	1.1	90	173
11/13/14	298.0	200	0.7	94	114
11/17/14	298.0	200	1	116	110
11/19/14	298.0	170	1	92	73
11/25/14	298.0	170	0.5	115	75
11/28/14	298.0	170	1.5	110	84
12/3/14	298.0	172	0.1	92	49.4
12/7/14	298.0	110	0.7	94	8.1
12/9/14	298.0	110	0.7	99	3
12/12/14	298.0	110	0.7	98	5
12/18/14	298.0	110	0.5	89	7
12/23/14	298.0	110	0.4	91	4.5
12/26/14	298.0	110	1.2	105	6.1
12/29/14	298.0	110	0.5	108	4
1/2/15	298.0	110	0.5	114	4
1/8/15	298.0	110	0.9	112	3.5

Dates	G, 1/s	R1 Influent NH4-N, mg/L	R1 Effluent NH4-N, mg/L	R1 Effluent NO3-N, mg/L	R1 Effluent NO2-N, mg/L
1/16/15	298.0	160	0.8	163	11.6
1/19/15	298.0	160	0.8	160	10
1/23/15	298.0	162	1.2	157	19.6
1/27/15	298.0	158	0.9	143	28.7
1/30/15	298.0	255	66	45	186
2/2/15	298.0	255	41	47	197
2/5/15	298.0	300	1.1	205	130
2/9/15	298.0	300	0.6	171	120
2/12/15	298.0	300	12	141	136
2/16/15	298.0	300	11	137	164
2/18/15	298.0	300	1.1	118	172
2/23/15	298.0	448	7	47	394
2/24/15	298.0	448	1	50	400
3/2/15	298.0	550	150	89	340
3/7/15	298.0	515	90	96	328
3/10/15	298.0	515	89	95	321
3/11/15	298.0	515	98	126	354

Figure 2.6

Date	G, 1/s	R2 Influent NH4-N, mg/L	R2 Effluent NH4-N, mg/L	R2 Effluent NO3-N, mg/L	R2 Effluent NO2-N, mg/L
4/25/13	239.8	29.6	23.9	5.4	
4/26/13	239.8	29.6	16.7	7	
4/29/13	239.8	40.1	1.9	8.6	
4/30/13	239.8	71	5.8	11	

Date	G, 1/s	R2 Influent NH4-N, mg/L	R2 Effluent NH4-N, mg/L	R2 Effluent NO3-N, mg/L	R2 Effluent NO2-N, mg/L
5/2/13	239.8	169	39	13	
5/3/13	239.8	169	11.8	16	
5/6/13	239.8	169	1.9	20.4	
5/7/13	239.8	169	13.9	22.5	
5/9/13	239.8	169	2.4	20.1	
5/13/13	239.8	248	41.5	21.7	97.4
5/17/13	239.8	248	3.8	28.7	98.1
5/20/13	239.8	301	6	44.7	98
5/23/13	239.8	301	27.9	41.2	97.7
5/24/13	298.0				
5/27/13	298.0	304	2	218	90.5
5/29/13	298.0	393	5.8	198	97.7
5/31/13	298.0	393	4.8	236	97.7
6/3/13	298.0	393	4.5	280	125
6/5/13	298.0	393	64.5	245	60.6
6/7/13	298.0	440	67.2	264	106.2
6/10/13	298.0	440	30.3	268	144.9
6/12/13	298.0	440	11.5	284	147.6
6/14/13	298.0	451	6.2	326	124.2
6/17/13	298.0	510	27	341	126
6/19/13	298.0	510	79.2	286	67.5
6/21/13	298.0	510	44.7	272	183.3
6/24/13	298.0	499	10.2	218	264.9
6/26/13	298.0	499	9.9	224	266.7
6/28/13	298.0	499	5.2	208	261.6
7/1/13	298.0	510	6.9	213	286.5
7/3/13	298.0	510	88.2	172	51.6

Date	G, 1/s	R2 Influent NH4-N, mg/L	R2 Effluent NH4-N, mg/L	R2 Effluent NO3-N, mg/L	R2 Effluent NO2-N, mg/L
7/5/13	298.0	510	70.6	166	272.1
7/8/13	298.0	510	21.1	102	386
7/10/13	298.0	510	9	220	290
7/12/13	298.0	564	16.2	196	344.5
7/15/13	298.0	564	15.5	190	346.5
7/17/13	298.0	564	108.9	87	226.7
7/19/13	298.0	564	45.1	143	371
7/22/13	298.0	564	23.7	162	377.9
7/24/13	298.0	564	28.9	171	347.1
7/26/13	298.0	564	16.2	182	363.5
7/28/13	298.0				
7/29/13	298.0	502	76.8	80	198
7/31/13	298.0	502	23.8	190	321.5
8/2/13	298.0	502	10.9	177	325.5
8/6/13	298.0	502	10.7	160	337.5
8/9/13	298.0	502	8	202	316.5
8/12/13	298.0	502	6.8	191	311.5
8/14/13	298.0	502	75.8	148	201.5
8/16/13	298.0	502	35	168	317
8/19/13	298.0	512	12.2	182	321.5
8/21/13	298.0	512	22.3	180.9	311.5
8/23/13	298.0	512	26.6	186	307.5
8/26/13	298.0	512	21.4	182	327.5
8/28/13	298.0	502	101.2	70	198.5
8/30/13	298.0	502	78.2	138	269.5
9/2/13	298.0	502	16.9	169	309.5
9/5/13	296.7	502	129	71	291.5

Date	G, 1/s	R2 Influent NH4-N, mg/L	R2 Effluent NH4-N, mg/L	R2 Effluent NO3-N, mg/L	R2 Effluent NO2-N, mg/L
9/6/13	296.7	440	99	65	271.5
9/9/13	260.6	402	62.4	72	269.5
9/12/13	260.6	402	70.8	55	264.5
9/13/13	260.6	402	73.1	55	285
9/16/13	260.6	357	39.5	67	260
9/20/13	260.6	357	37.5	69	280.5
9/24/13	296.7	357	11.9	63	305
9/26/13	296.7	351	3.6	46	294.5
9/29/13	296.7	351	2	65	271
10/4/13	296.7	368	50.9	34	266.5
10/7/13	296.7	368	47.1	65	271.5
10/9/13	296.7	360	32	29.2	288
10/11/13	296.7	360	27.8	35	286.5
10/13/13	296.7	360	20.1	39	288
10/19/13	296.7	360	14.4	50	288
10/23/13	296.7	360	28.2	16.9	269
10/25/13	296.7	360	20.2	17.6	278
10/28/13	296.7	360	12.1	19.6	300.5
10/31/13	296.7	331	2.1	27.9	296.5
11/2/13	296.7	331	2.9	29.5	286.5
11/4/13	296.7	331	1.8	31.5	285.5
11/7/13	296.7	363	43.7	14.6	265
11/9/13	296.7	363	28.9	20.8	286.5
11/11/13	296.7	363	47.9	28.7	295.5
11/14/13	296.7	379	65.9	12.5	288
11/16/13	296.7	379	68.1	13.7	281
11/18/13	296.7	379	72.3	13.5	287

Date	G, 1/s	R2 Influent NH4-N, mg/L	R2 Effluent NH4-N, mg/L	R2 Effluent NO3-N, mg/L	R2 Effluent NO2-N, mg/L
11/21/13	296.7	307	16.7	13.8	271
11/23/13	296.7	307	9.1	14.1	286.5
11/25/13	296.7	307	4	13.9	299.5
11/27/13	296.7	307	5.2	14.3	266.25
12/1/13	296.7	307	1.8	18.8	307.5
12/14/13	296.7	313	1.4	24.6	298
12/15/13	296.7	313	1.9	23.2	300
12/19/13	296.7	313	2.1	11.8	309
12/21/13	296.7	313	2.5	12.7	271
12/24/13	296.7	283	2.8	3.4	300
12/26/13	296.7	283	2	12.9	316
12/29/13	296.7	283	1.2	21.6	200
12/31/13	296.7	283	148	9.7	140
1/2/14	296.7	283	33.7	6.7	242
1/4/14	296.7	283	6.5	6.8	269
1/6/14	296.7	283	4.7	3.4	280
1/8/14	297.0	314	12.6	3.2	312
1/10/14	297.0	314	11	2.1	305
1/12/14	297.0	314	3.8	2	306
1/14/14	297.0	314	3.6	3.1	318
1/16/14	297.0	314	22.9	2.8	230
1/19/14	297.0	293	6.3	7.4	299
1/21/14	297.0	293	7.8	5.6	268
1/22/14	297.0	304	6.4	7.5	295
1/24/14	297.0	434	105	9.9	313
1/26/14	297.0	434	154	10.5	293
1/28/14	297.0	434	124	13.2	309

Date	G, 1/s	R2 Influent NH4-N, mg/L	R2 Effluent NH4-N, mg/L	R2 Effluent NO3-N, mg/L	R2 Effluent NO2-N, mg/L
1/30/14	297.0	434	104	8.4	329
2/2/14	297.0	415	89	4.1	326
2/4/14	297.0	415	87.2	6.8	340
2/6/14	297.0	415	66	6.3	368
2/8/14	297.0	415	82	4.9	351
2/10/14	297.0	415	71	4.7	357
2/12/14	297.0	458	51	7.6	401
2/20/14	297.0	459	187		
2/21/14	297.0	339	20		
2/22/14	297.0	370	14		
2/23/14	297.0	435	26.1		
2/24/14	297.0	435	29	11.3	417
2/26/14	297.0	495	107	9.7	377
2/28/14	297.0	499	88	13.7	368
3/2/14	297.0	499	94	21.6	340
3/4/14	297.0	485	72	14.4	345
3/5/14	297.0	474	86		
3/6/14	297.0	420	63	18.6	377
3/7/14	297.0	370	8		
3/8/14	297.0	413	15.3	30	344
3/10/14	297.0	413	40		
3/11/14	297.0	413	39.5	40	321
3/12/14	297.0	406	33		
3/13/14	297.0	406	11.9	68.1	318
3/15/14	297.0	406	36.4	80.1	268
3/17/14	297.0	406	49	75.2	266
3/19/14	297.0	381	13.9	93.1	265

Date	G, 1/s	R2 Influent NH4-N, mg/L	R2 Effluent NH4-N, mg/L	R2 Effluent NO3-N, mg/L	R2 Effluent NO2-N, mg/L
3/21/14	297.0	381	8.6	84.9	269
3/23/14	297.0	381	11.8	94.5	269
3/25/14	297.0	364	11.5	98.4	238
3/26/14	297.0	364	6.8		
3/27/14	297.0	364	3.7	172.8	184
3/28/14	298.0	392	6		
3/31/14	298.0	431	72	115.8	252
4/2/14	298.0	415	16	109.6	263
4/4/14	298.0	419	36.7	108	248
4/6/14	298.0	419	34	81.2	270
4/8/14	298.0	419	57	83.7	244
4/10/14	298.0	373	7.8	82	275
4/12/14	298.0	358	4	86.5	251
4/15/14	298.0	358	2.6	126.5	200
4/18/14	298.0	330	7	71.2	200
4/19/14	298.0	333	8		
4/20/14	298.0	333	8		
4/21/14	298.0	333	3		
4/23/14	298.0	333	6.7	128	188
4/26/14	298.0	335	3.8	130	159
4/29/14	298.0	338	2.2	90	118.4
5/1/14	298.0	339	2.9	118.4	195
5/3/14	298.0	343	2.8	190	120
5/5/14	298.0	343	2.6	272.3	65
5/7/14	298.0	370	1	291.1	68
5/9/14	298.0	370	3.3	299	66
5/12/14	298.0	423	10.1	221	163

Date	G, 1/s	R2 Influent NH4-N, mg/L	R2 Effluent NH4-N, mg/L	R2 Effluent NO3-N, mg/L	R2 Effluent NO2-N, mg/L
5/14/14	298.0	384	3.1	165	153
5/16/14	298.0	384	14.4	166	173
5/21/14	298.0	343	2	310	24
5/23/14	298.0	356	0	350	13
5/26/14	298.0	394	3.1	292	151
5/27/14	298.0	394	1.6	375	28
5/30/14	298.0	410	8.2	322	100
6/2/14	298.0	410	6.4		126
6/5/14	298.0	413	2	400	20
6/8/14	298.0	365	2.2	390	15.7
6/10/14	298.0	374	5.9	356	40
6/12/14	298.0	374	1.4		
6/15/14	298.0	376	1.2	7	360
6/17/14	298.0	376	1.6	8	380
6/19/14	298.0	420	1.3	400	5
6/22/14	298.0	420	10.6	196	195
6/26/14	298.0	425	2.6	268	145
6/30/14	298.0	425	2	356	105
7/1/14	298.0	425	2.1	348	48
7/3/14	298.0	425	1.9	378	17
7/5/14	298.0	425	1.9	392	8
7/7/14	298.0	425	0.9	402	6
7/8/14	298.0	461	1.3		
7/11/14	298.0	459	69	164	154
7/13/14	298.0	399	6	196	179
7/15/14	389.0	399	1.2	374	5
7/23/14	389.0	397	0.01	190	131

Date	G, 1/s	R2 Influent NH4-N, mg/L	R2 Effluent NH4-N, mg/L	R2 Effluent NO3-N, mg/L	R2 Effluent NO2-N, mg/L
7/25/14	298.0	413	30.7	174	190
7/26/14	298.0	413	14	189	205
7/28/14	298.0	408	4.3	190	195
7/31/14	298.0	448	6.3	200	221
8/2/14	298.0	486	11.7	198	259
8/4/14	298.0	493	5	189	273
8/6/14	298.0	512	43	168	285
8/11/14	298.0	324	1.1	326	8.2
8/18/14	298.0	242	0.8	250	1
8/30/14	298.0	715	300	209	230
9/5/14	298.0	242	0.5	244	1.2
9/8/14	298.0	242	0.5	248	1.1
9/11/14	298.0	277	0.4	278	1
9/14/14	298.0	277	0.4	273	7
9/15/14	298.0	277	0	300	1
9/19/14	298.0	770	334	180	209
10/6/14	298.0	250	1.1	242	1
10/11/14	298.0	370	1.1	250	110
10/13/14	298.0	250	0.2	256	0
10/20/14	298.0	243	1.3	240	1.3
10/23/14	298.0	660	181	187	274
10/26/14	298.0	240	0.5	246	11
11/3/14	298.0	660	123	180	288
11/4/14	298.0	660	138	178	285
11/8/14	298.0	660	206	312	113
11/9/14	298.0	240	0.1	7	234
11/13/14	298.0	300	1.4	290	6

Date	G, 1/s	R2 Influent NH4-N, mg/L	R2 Effluent NH4-N, mg/L	R2 Effluent NO3-N, mg/L	R2 Effluent NO2-N, mg/L
11/17/14	298.0	300	1.1	274	7
11/19/14	298.0	300	0.9	264	9
11/28/14	298.0	300	1.5	280	22
12/3/14	298.0	293	0.8	312	0.8
12/7/14	298.0	316	1.3	310	0.9
12/9/14	298.0	302	0.7	306	1.2
12/15/14	298.0	302	0.6	348	0.8
12/18/14	298.0	302	1.4	312	5
12/23/14	298.0	350	1.6	350	0.7
12/29/14	298.0	350	1.3	355	0.8
1/2/15	298.0	350	0.7	378	0.8
1/8/15	298.0	400	1.5	458	0.9
1/16/15	298.0	400	0.6	434	0.8
1/19/15	298.0	400	0.6	400	0.8
1/23/15	298.0	280	1.9	340	0.53
1/27/15	298.0	280	0.8	322	0.46
1/30/15	298.0	600	131	298	139
2/2/15	298.0	600	114	165	309
2/5/15	298.0	600	210	153	305
2/9/15	298.0	600	84	157	383
2/12/15	298.0	600	117	186	290
2/16/15	298.0	600	183	281	187
2/18/15	298.0	600	149	380	122
2/23/15	298.0	600	256	360	20
2/24/15	298.0	600	275	340	17

Figure 2.7

	Relative Abundance (%)	
	8/26/13 R2 End of Phase 1	**8/19/13 R1 End of Phase 1**
Bacteria; Proteobacteria; Betaproteobacteria; Nitrosomonadales; Nitrosomonadaceae	23.7	7.5
Bacteria; Proteobacteria; Alphaproteobacteria; Rhizobiales; Phyllobacteriaceae	15.9	7.0
Bacteria; Proteobacteria; Betaproteobacteria; Burkholderiales; Comamonadaceae	14.5	41.5
Bacteria; Actinobacteria; Actinobacteria; Actinomycetales; Unknown	12.7	3.0
Bacteria; Actinobacteria; Actinobacteria; Actinomycetales; Microbacteriaceae	9.4	2.0
Bacteria; Proteobacteria; Alphaproteobacteria; Rhizobiales ; Bradyrhizobiaceae	7.3	5.5
Bacteria; Proteobacteria; Gammaproteobacteria; Xanthomonadales; Xanthomonadaceae	4.0	6.7
Bacteria; Bacteroidetes; Flavobacteriia; Flavobacteriales; Cryomorphaceae	2.0	0.1
Bacteria; Bacteroidetes; Sphingobacteriia; Sphingobacteriales; Unclassified	1.2	4.8
Bacteria; Bacteroidetes; Flavobacteriia; Flavobacteriales; Flavobacteriaceae	0.8	5.5
Bacteria; Proteobacteria; Alphaproteobacteria; Sphingomonadales; Sphingomonadaceae	0.6	2.1
Bacteria; Bacteroidetes; Unknown; Unknown; Unknown	0.3	6.2
Bacteria; Nitrospirae; Nitrospira; Nitrospirales; Nitrospiraceae	0.0	2.5
Other	7.5	5.7

Figure 2.8

	Relative Abundance (%)		
	8/26/13 R2 End of Phase 1	**11/15/13 R2 End of Phase 2**	**3/16/15 End of Phase 3**
Proteobacteria; Betaproteobacteria ;Nitrosomonadales; Nitrosomonadaceae	23.7	0.6	15.8
Proteobacteria; Alphaproteobacteria; Rhizobiales; Phyllobacteriaceae	15.9	3.0	1.0
Proteobacteria; Betaproteobacteria; Burkholderiales; Comamonadaceae	14.5	26.9	11.9
Actinobacteria; Actinobacteria; Actinomycetales; Unclassified	12.7	0.8	0.0
Actinobacteria; Actinobacteria; Actinomycetales; Microbacteriaceae	9.4	10.2	11.1
Proteobacteria; Alphaproteobacteria; Rhizobiales; Bradyrhizobiaceae	7.3	0.4	14.7
Proteobacteria; Gammaproteobacteria; Xanthomonadales; Xanthomonadaceae	4.0	45.3	5.1
Bacteroidetes; Flavobacteriia; Flavobacteriales; Cryomorphaceae	2.0	0.1	0.3
Bacteroidetes; Flavobacteriia; Flavobacteriales; Flavobacteriaceae	0.8	2.0	3.4
Unclassified; Unclassified; Unclassified; Unclassified	0.1	0.1	18.7
Proteobacteria; Alphaproteobacteria; Caulobacterales; Caulobacteraceae	0.8	6.6	0.2
Bacteroidetes; Unclassified; Unclassified; Unclassified	0.1	0.1	0.3
Relative Abundance < 4%	8.5	4.0	17.5
Shannon Diversity Index	2.3	1.6	2.6

Figure 2.9

	G (1/s)							
R1 Test Date	**180.3**	**212.2**	**239.8**	**264.6**	**298.0**	**328.0**	**389.0**	
6/24/13	1.49	1.67	1.82	1.92	2.02	2.14		
7/8/13	1.22		1.57	1.72	1.84	1.95	1.94	**J values, g/(m2*d)**
7/22/13	1.27		1.60	1.73	1.84	1.94	2.05	
8/19/13	1.41		1.83	1.96	2.11	2.26	2.33	
	G (1/s)							
R2 Test Date	**180.3**	**212.2**	**239.8**	**264.6**	**298.0**	**328.0**	**389.0**	
7/1/13	12.30		16.60	18.00	19.90	21.40	22.40	**J values, g/(m2*d)**
7/15/13	11.40		16.10	18.20	19.80	21.00	22.50	
8/26/13	12.70		18.20	21.10	23.30	24.80	26.20	

Figure 2.10

Date	**Temp, C**	**DO (mg/L)**	**G (1/s)**	**J (g/m2/d)**
11/4/13	10.5	3.0	297	1.17
11/4/13	10.5	5.1	297	1.55
11/4/13	10.5	6.1	297	1.89
11/4/13	10.5	7.0	297	2.02
11/4/13	10.5	8.0	297	2.02
11/18/13	10.5	3.0	297	0.96
11/18/13	10.5	4.9	297	1.34
11/18/13	10.5	5.9	297	1.48
11/18/13	10.5	7.1	297	1.75
11/18/13	10.5	8.0	297	1.79
1/15/14	10.5	3.0	297	1.13
1/15/14	10.5	7.2	297	2.15
1/15/14	10.5	11.1	297	2.12
1/15/14	10.5	15.4	297	2.75
1/15/14	10.5	20.1	297	3.04

Figure 2.11

	G (1/s)						
R1 Test Date	**178**	**238**	**262**	**297**	**327**	**390**	
9/26/13	0.73	0.82	0.83	0.90	0.89	0.88	**J g/(m2*d)**
10/7/13	0.58	0.59	0.59	0.61	0.62	0.66	
12/16/13	0.41	0.56	0.50	0.44	0.38	0.43	

			G (1/s)				
R2 Test Date	**158**	**210**	**231**	**261**	**287**	**340**	
9/16/13	1.15	1.55	1.71	1.87	2.00	2.16	**J g/(m2*d)**
			G (1/s)				
	178	**238**	**262**	**297**	**327**	**390**	
10/13/13	1.39	1.90	2.04	2.25	2.39	2.46	
12/1/13	1.67	2.04	2.15	2.33	2.43	2.53	**J**
12/20/13	1.46	1.95	2.06	2.06	2.13	2.24	**g/(m^2*d)**
			G (1/s)				
	161	**225**	**251**	**287**	**318**	**383**	
1/19/14	1.40	1.63	1.70	1.88	2.04	2.09	**J g/(m^2*d)**

Figure 2.12

			G (1/s)				
R1 Test Date	**180**	**240**	**265**	**298**	**328**	**389**	
5/28/14	2.27	1.92	2.02	1.98	2.10	2.29	
6/23/14			2.87			2.60	
6/23/14	2.11		2.89			2.64	
6/26/14	2.34		2.56			2.58	J g/(m^2*d)
6/26/14	2.09		2.26			2.42	
7/17/14	2.19		2.72			2.79	
7/17/14	2.00		2.44			2.85	

	G (1/s)			
R2 Test Date	**180**	**265**	**389**	
7/8/14	2.38	2.55	3.97	
7/8/14	2.09	2.76	3.60	J g/(m2*d)
7/21/14	2.09	2.69	3.53	
7/21/14	2.09	2.81	3.37	

Appendix B: Chapter 3 Data

Table 3.2

Table 3.2. Optimized Compound Parameters in OSPE method

Compound	Prec Ion (m/z)	Prod Ion (m/z)	Frag (V)	CE (V)	Cell Acc (V)	RT (min)
		ESI Positive				
Atenolol	267.1	190.1 (145)	130	15 (20)	2	5.2
Atenolol-d_7	*274*	*190.1*	*130*	*15*	*2*	*5.2*
Atrazine	218	176 (174)	140	15 (15)	2	7.6
Atrazine-d_3	*221*	*179*	*140*	*15*	*2*	*7.6*
Benzophenone	183	105.1	85	15	2	8
Benzophenone-d_{10}	*183*	*110*	*85*	*15*	*2*	*8*
Caffeine	195.1	138 (110.1)	104	16 (24)	2	5.7
Caffeine-$^{13}C_3$	*198.1*	*140*	*104*	*16*	*2*	*5.7*
Carbamazepine	237	194 (179)	120	15 (35)	2	7.2
Carbamazepine-d_{10}	*247*	*204*	*120*	*15*	*2*	*7.2*
DEET	192	119 (91)	110	15 (30)	2	7.6
DEET-d_6	*198*	*119*	*110*	*15*	*2*	*7.6*
Diphenylhydramine	256.2	167.1 (165.1)	60	4 (44)	2	7.1
Diphenylhydramine-d_5	*261.2*	*172.1*	*60*	*4*	*2*	*7.1*
Diltiazem	415.2	178 (150)	130	24 (48)	2	7
Diltiazem-d_3	*418.2*	*178*	*130*	*24*	*2*	*7*
Fluoxetine	310	148	90	5	2	7.5
Fluoxetine-d_5	*315*	*153*	*90*	*5*	*2*	*7.5*
Hydrocortisone	363.2	327 (120.9)	130	13 (24)	2	6.9
Meprobamate	219	158 (55)	70	5 (20)	2	6.5
Meprobamate-d_7	*226*	*165*	*70*	*5*	*2*	*6.5*
Norgestrel	313.2	91 (77.1)	130	60 (75)	2	6.2
Primidone	219.3	162.1 (91.1)	70	9 (25)	2	6.1
Primidone-d_5	*224*	*167*	*70*	*9*	*2*	*6.1*
Propranolol	260	116 (56)	122	13 (29)	2	6.6
Simazine	202.1	132 (68.1)	72	16 (36)	2	7
Sulfamethoxazole	254	156 (92)	80	10 (30)	2	6.5
Sulfamethoxazole-d_6	*260*	*162*	*80*	*10*	*2*	*6.5*
TCEP	285	222.8	95	10	2	7.5

Table 3.2. Optimized Compound Parameters in OSPE method

Compound	Prec Ion (m/z)	Prod Ion (m/z)	Frag (V)	CE (V)	Cell Acc (V)	RT (min)
TCEP-d_{12}	*297*	*232*	*95*	*10*	*2*	*7.5*
TCPP	327	99 (81)	72	16 (70)	2	8.4
Testosterone	289	109 (97)	115	25 (25)	2	7.8
Trimethoprim	291	261 (230)	75	25 (25)	2	5.8
Trimethoprim-d_3	*294*	*264*	*75*	*25*	*2*	*5.8*
		ESI Negative				
Benzotriazole	118	90.1 (50)	85	16 (28)	7	6.5
Benzotriazole-d_4	*122*	*94*	*85*	*16*	*7*	*6.5*
Bisphenol A	227	212 (133)	115	11 (19)	7	7.7
Bisphenol A-$^{13}C_{12}$	*239*	*224*	*115*	*11*	*7*	*7.7*
Clofibric Acid	213	127	80	10	7	7.8
Diclofenac	294	250 (214)	75	4 (16)	7	8.6
Diclofenac-$^{13}C_6$	*316*	*272.1*	*75*	*5*	*7*	*8.6*
Gemfibrozil	249.2	121	75	6	7	9.2
Gemfibrozil-d_6	*255*	*121*	*75*	*6*	*7*	*9.2*
Hydrochlorothiazide	296	268.9 (204.7)	130	10 (15)	7	5.9
Ibuprofen	205	161	50	0	7	8.8
Ibuprofen-d_3	*208*	*164*	*50*	*0*	*7*	*8.8*
Naproxen	229	170 (169)	55	4 (24)	7	8
Naproxen-$^{13}C_1d_3$	*233*	*169*	*55*	*24*	*7*	*8*
PFHxA	312.9	268.9	66	5	7	7.4
PFHxA-$^{13}C_2$	*314.9*	*269.9*	*66*	*5*	*7*	*7.4*
PFOA	412.9	368.9 (169)	86	5 (5)	7	8
PFOA-$^{13}C_4$	*416.9*	*371.9*	*86*	*5*	*7*	*8*
PFOS	498.9	99 (80)	210	50 (50)	7	9.2
PFOS-$^{13}C_4$	*502.9*	*99*	*210*	*50*	*7*	*9.2*
Propylparaben	179.1	137.1 (92)	80	7 (20)	7	7.7
Propylparaben-d_4	*183.1*	*141.1*	*80*	*7*	*7*	*7.7*
Triclocarban	313	160 (126)	110	5 (25)	7	9.4
Triclocarban-$^{13}C_6$	*318.9*	*159.9*	*110*	*5*	*7*	*9.4*
Triclosan	289 (287)	37 (35)	75	5 (5)	7	9.4
Triclosan-$^{13}C_{12}$	*299*	*35*	*75*	*5*	*7*	*9.4*

Table 3.3

Table 3.3. Optimized source dependent parameters of mass spectrometer

Parameter	ESI Positive	ESI Negative
Gas Temperature (°C)	250	250
Gas Flow Rate (L/min)	11	11
Nebulizer (psi)	45	45
Sheath Gas Temperature (°C)	375	375
Sheath Gas Flow Rate (L/min)	12	12
Capillary (V)	4000	3500
Nozzle Voltage (V)	0	1500
Delta EMV (V)	400	400

* Samples were analyzed simultaneously in ESI+ and ESI- with fast polarity switching

Table 3.4

Table 3.4. LODs, MDLs and practical MRLs in ultrapure water for all target analytes

Analyte	LOD (ng/L)	MDL (ng/L)
Acesulfame	5	10
Atenolol	1	2.5
Atrazine	0.2	0.3
Benzophenone	5	11.3
Bisphenol A	10	13.1
Caffeine	0.2	0.5
Carbamezapine	0.1#	0.1
Clofibric Acid	0.2	0.7
DEET	0.1	0.3
Dexamethasone	10	14
Diphenhydramine	0.5	0.9
Ditiazem	0.1	0.2
Fluoxetine	1	3
Gemfibrozil	0.2	0.5
Hydracortisone	5	9.3
Ibuprofen	0.5	1.9
Iohexol	25	50
Iopamidol	5	10
Iopromide	10	20
Meprobamate	0.2	0.4
Naproxen	1	2.5
Norgestrel	10	11.6
PFBA	NA	NA

Table 3.4. LODs, MDLs and practical MRLs in ultrapure water for all target analytes

Analyte	LOD (ng/L)	MDL (ng/L)
PFHxA	1	3.6
PFOA	0.5	3
PFOS	5	6.1
Primidone	0.5	2
Propylparaben	1	1.4
Simazine	0.2	0.4
Sucralose	75	100
Sulfamethoxazole	0.2	0.5
TCEP	1	2.1
Testosterone	2.5	4.4
Triclocarban	0.5	1.1
Triclosan	1	2.6
Trimethoprim	0.1#	0.1

[#] assumed as lowest calibration standard (SNR>>3 at this concentration)
[$] adjusted for the blank
LOD: Limit of Detection (SNR>3)
MDL: Method Detection Limit (SNR>10)

Table 3.5

Table 3.5. MRM Transitions of Analytes for UHPLC-MS/MS Analysis

Compounds	MRM Transition	Frag[a]/Ceb (V)	Surrogates	MRM Transition	Frag[a]/Ceb (V)
ER agonists (ESI Negative)					
Estriol	287.2 > 145.0	170/44	Estriol-$^{13}C_3$		
	287.2 > 171.2	170/40			
Bisphenol A	227.1 > 212.0	117/16	Bisphenol A-$^{13}C_{12}$	239.2 > 224.1	109/16
	227.1 > 133.0	117/24			
Estrone	269.1 > 145.0	170/40	Estrone-$^{13}C_6$	275.2 > 144.9	160/40
	269.1 > 183.1	170/35			
17β-Estradiol	271.2 > 144.8	155/40	17β-Estradiol-$^{13}C_3$	274.2 > 148.0	175/40
	271.2 > 183.0	155/42			
17α-Estradiol	271.2 > 144.8	155/40		274.2 > 148.0	175/40
	271.2 > 183.0	155/42			
17α-Ethinylestradiol	295.2 > 145.0	155/44	17α-Ethynylestradiol-$^{13}C_2$	297.2 > 144.9	140/40
	295.2 > 159.0	155/40			

Table 3.5. MRM Transitions of Analytes for UHPLC-MS/MS Analysis

Compounds	MRM Transition	Frag[a]/Ceb (V)	Surrogates	MRM Transition	Frag[a]/Ceb (V)
Other Hormones (ESI Positive)					
Triamcinolone	395.2 > 375.1	95/4			
	395.2 > 225.1	95/12			
Hydrocortisone	363.2 > 120.9	130/24			
	363.2 > 327.0	130/13			
Prednisone	359.2 > 147.1	95/24			
	359.2 > 171.0	95/36			
Dexamethasone	393.2 > 373.2	87/4	Dexamethasone-d4	397.2 > 359.6	87/5
	393.2 > 355.2	87/5			
Norethindrone	299.2 > 109.1	104/28	Norethindrone-d6	305.2 > 87.1	122/40
	299.2 > 91.1	104/56			
Testosterone	289.0 > 109.0	115/25			
	289.0 > 97.0	115/25			
Norgestrel	313.2 > 91.0	130/60	Norgestrel-d6	319.2 > 91.0	130/60
	313.2 > 77.1	130/75			

[a] Fragmentor (Frag); [b] Collision Energy (CE)

Table 3.6

Table 3.6. MS Source Parameters

Parameter	ESI Positive	ESI Negative
Gas Temp (°C)	300	300
Gas Flow (L/min)	11	10
Nebulizer (psi)	45	45
Sheath Gas Heater Temp (°C)	375	300
Sheath Gas Flow (L/min)	11	11
Capillary Voltage (V)	4000	3500

Table 3.7

Table 3.7. MRLs of Analytes

Compounds	MDLs (ng/L)
ER Agonists	
Estrone	0.1

Table 3.7. MRLs of Analytes

Compounds	MDLs (ng/L)
17β-Estradiol	0.5
17α-Estradiol	0.5
17α-Ethinylestradiol	0.5
Estriol	0.2
Bisphenol A	0.2
AR Agonists	
Testosterone	0.2
PR Agonists	
Norethindrone	0.2
Norgestrel	0.2
GR Agonists	
Dexamethasone	0.1
Hydrocortisone	0.1
Prednisone	0.1
Triamcinolone	0.5

Figure 3.2

R1 Date	R1 G, 1/s	R1 Effluent NH4-N, mg/L	R1 Effluent NO3-N, mg/L	R1 Effluent NO2-N, mg/L	R1 Influent NH4-N, mg/L
1/22/14	298	5.9	24.6	212	233
1/24/14	298	46	25.2	244	340
1/26/14	298	59	33.2	254	340
1/28/14	298	187	21.6	179	407
1/30/14	298	204	25.4	207	407
2/2/14	298	91	19.4	229	339
2/4/14	298	101	15.3	233	339
2/6/14	298	116	12	218	339
2/8/14	298	142	11.5	189	339
2/10/14	298	181	7.9	140	339
2/12/14	298	229	9.5	123	339
2/20/14	298	147			208
2/21/14	298	56			132
2/22/14	298	5.4			132
2/23/14	298	27.7	18.2	159	209

R1 Date	R1 G, 1/s	R1 Effluent NH4-N, mg/L	R1 Effluent NO3-N, mg/L	R1 Effluent NO2-N, mg/L	R1 Influent NH4-N, mg/L
2/24/14	298	45	17.3	136	209
2/26/14	298	24.9	20.2	167	209
2/28/14	298	40	23.1	165	214
3/2/14	298	3.5	26.7	168	214
3/4/14	298	13	26.1	240	314
3/5/14	298	8.8			316
3/6/14	298	12	17	310	353
3/7/14	298	8			327
3/8/14	298	20.6	27.4	310	327
3/10/14	298	90			330
3/12/14	298	90			330
3/13/14	298	16.4	18.8	231	240
3/15/14	298	4.9	29.4	212	240
3/17/14	298	4.5	32.2	197	240
3/19/14	298	22.1	36.8	205	259
3/21/14	298	11.3	35.5	201	259
3/23/14	298	4.6	36	221	259
3/25/14	298	2.8	40.4	220	259
3/26/14	298	3.7			292
3/27/14	298	11.3	48	226	320
3/28/14	298	25.9			379
3/31/14	298	67	48.8	260	372
4/2/14	298	31	43.2	254	340
4/4/14	298	13.3	45.2	278	332
4/6/14	298	12	37.6	283	332
4/8/14	298	45	37.4	265	332
4/10/14	298	10.9	43.2	285	326
4/12/14	298	25.7	38.4	274	355
4/15/14	298	16.9	32.8	270	347
4/18/14	298	174	30.4	148	335
4/19/14	298	155			335
4/20/14	298	135			300
4/21/14	298	39			207
4/23/14	298	3.7	90	80	173
4/26/14	298	2	100	129	173
4/29/14	298	2.2	76	48	173
5/1/14	298	2.4	103.6	86	225
5/3/14	298	3	102	80	225
5/5/14	298	3.3	115.2	95	225
5/7/14	298	20.1	83.7	170	288

R1 Date	R1 G, 1/s	R1 Effluent NH4-N, mg/L	R1 Effluent NO3-N, mg/L	R1 Effluent NO2-N, mg/L	R1 Influent NH4-N, mg/L
5/9/14	298	7.6	137	170	288
5/12/14	298	26.7	78	285	381
5/14/14	298	61	70	213	380
5/20/14	298	66	100	363	363
5/21/14	298	13	100	310	326
5/23/14	298	3	144	159	313
5/26/14	298	3	224	115	358
5/27/14	298	1.8	338	16	358
5/28/14	298	5.7	302	47	387
5/30/14	298	57	182	137	403
5/30/14	298	29	186	254	403
6/2/14	298	13.5	176	113	359
6/5/14	298	7	224	138	382
6/8/14	298	5.7	226	181	387
6/10/14	298	10.6	174	181	400
6/12/14	298	22.5	250	156	400
6/13/14	298	0.6	128	204	447
6/15/14	298	18.9	126	269	447
6/17/14	298	3.9	164	227	447
6/19/14	298	10	132	229	375
6/22/14	298	3	222	115	375
6/23/14	298	2			375
6/25/14	298	50.1	122	139	375
6/26/14	298	23			375
6/30/14	298	3.1	220	143	375
7/1/14	298	12	184	152	375
7/3/14	298	3.2	210	127	375
7/5/14	298	3.3	222	98	375
7/7/14	298	2.1	212	113	375
7/11/14	298	8.6	92	246	390
7/13/14	298	5.4	88	293	384
7/15/14	389	2.5	102	264	384
7/17/14	389	2.7		255	384
7/23/14	298	259			384
7/25/14	298	22.5	50	156	202
7/26/14	298	3.5	70	148	202
7/28/14	298	1.2	154	71	224
7/31/14	298	1.4	238	16	255
8/2/14	298	2.7	249	75	294
8/4/14	298	2	286	62	342

R1 Date	R1 G, 1/s	R1 Effluent NH4-N, mg/L	R1 Effluent NO3-N, mg/L	R1 Effluent NO2-N, mg/L	R1 Influent NH4-N, mg/L
8/6/14	298	0.4	262	118	381
8/9/14	298	100			515
8/11/14	298	1.1	326	1.1	282
9/1/14	298	2.2	130	135	300
9/8/14	298	3.7	132	160	300
9/11/14	298	1.2	182	85	279
9/14/14	298	1.6	201	91	270
9/19/14	298	1.1	201	80	270
9/26/14	298	0.3	201	91	270
10/2/14	298	0.2	200	99	280
10/6/14	298	1.9	296	3	300
10/11/14	298	1.1	250	110	300
10/20/14	298	1.1	200	112	300
10/27/14	298	1.2	201	120	300
11/3/14	298	0.8	12	139	300
11/4/14	298	0.9	177	50	200
11/5/14	298	1.2	178	88	300
11/7/14	298	0.7	110	236	300
11/8/14	298	0.2	82	158	250
11/9/14	298	0.5	92	155	250
11/10/14	298	1.1	90	173	250
11/13/14	298	0.7	94	114	200
11/17/14	298	1	116	110	200
11/19/14	298	1	92	73	170
11/25/14	298	0.5	115	75	170
11/28/14	298	1.5	110	84	170
12/3/14	298	0.1	92	49.4	172
12/7/14	298	0.7	94	8.1	110
12/9/14	298	0.7	99	3	110
12/12/14	298	0.7	98	5	110
12/18/14	298	0.5	89	7	110
12/23/14	298	0.4	91	4.5	110
12/26/14	298	1.2	105	6.1	110
12/29/14	298	0.5	108	4	110
1/2/15	298	0.5	114	4	110
1/8/15	298	0.9	112	3.5	110
1/16/15	298	0.8	163	11.6	160
1/19/15	298	0.8	160	10	160
1/23/15	298	1.2	157	19.6	162
1/27/15	298	0.9	143	28.7	158

R1 Date	R1 G, 1/s	R1 Effluent NH4-N, mg/L	R1 Effluent NO3-N, mg/L	R1 Effluent NO2-N, mg/L	R1 Influent NH4-N, mg/L
1/30/15	298	66	45	186	255
2/2/15	298	41	47	197	255
2/5/15	298	1.1	205	130	300
2/9/15	298	0.6	171	120	300
2/12/15	298	12	141	136	300
2/16/15	298	11	137	164	300
2/18/15	298	1.1	118	172	300
2/23/15	298	7	47	394	448
2/24/15	298	1	50	400	448
3/2/15	298	150	89	340	550
3/7/15	298	90	96	328	515
3/10/15	298	89	95	321	515
3/11/15	298	98	126	354	515
3/15/15	298	46	90	388	515
3/18/15	298	353	63	213	600
3/21/15	298	0.1	140	6	150
3/23/15	298	1.4	170	4	200
3/24/15	298	2.7	152	131	345
3/25/15	298	2.6	158	200	345
3/27/15	298	103	89	239	464
3/31/15	298	158	68	223	512
4/5/15	298	110	92	288	456
4/11/15	298	150	71	219	440
4/14/15	298	93	70	249	440
4/20/15	298	123	65	240	440

Figure 3.3

Dates	G (1/s)	R2 Effluent NH4-N, mg/L	R2 Effluent NO3-N, mg/L	R2 Effluent NO2-N, mg/L	R2 Influent NH4-N, mg/L
1/22/14	298	6.4	7.5	295	304
1/24/14	298	105	9.9	313	434
1/26/14	298	154	10.5	293	434
1/28/14	298	124	13.2	309	434
1/30/14	298	104	8.4	329	434
2/2/14	298	89	4.1	326	415
2/4/14	298	87.2	6.8	340	415
2/6/14	298	66	6.3	368	415
2/8/14	298	82	4.9	351	415
2/10/14	298	71	4.7	357	415
2/12/14	298	51	7.6	401	458

Dates	G (1/s)	R2 Effluent NH4-N, mg/L	R2 Effluent NO3-N, mg/L	R2 Effluent NO2-N, mg/L	R2 Influent NH4-N, mg/L
2/20/14	298	187			459
2/21/14	298	20			339
2/22/14	298	14			370
2/23/14	298	26.1			435
2/24/14	298	29	11.3	417	435
2/26/14	298	107	9.7	377	495
2/28/14	298	88	13.7	368	499
3/2/14	298	94	21.6	340	499
3/4/14	298	72	14.4	345	485
3/5/14	298	86			474
3/6/14	298	63	18.6	377	420
3/7/14	298	8			370
3/8/14	298	15.3	30	344	413
3/10/14	298	40			413
3/11/14	298	39.5	40	321	413
3/12/14	298	33			406
3/13/14	298	11.9	68.1	318	406
3/15/14	298	36.4	80.1	268	406
3/17/14	298	49	75.2	266	406
3/19/14	298	13.9	93.1	265	381
3/21/14	298	8.6	84.9	269	381
3/23/14	298	11.8	94.5	269	381
3/25/14	298	11.5	98.4	238	364
3/26/14	298	6.8			364
3/27/14	298	3.7	172.8	184	364
3/28/14	298	6			392
3/31/14	298	72	115.8	252	431
4/2/14	298	16	109.6	263	415
4/4/14	298	36.7	108	248	419
4/6/14	298	34	81.2	270	419
4/8/14	298	57	83.7	244	419
4/10/14	298	7.8	82	275	373
4/12/14	298	4	86.5	251	358
4/15/14	298	2.6	126.5	200	358
4/18/14	298	7	71.2	200	330
4/19/14	298	8			333
4/20/14	298	8			333
4/21/14	298	3			333
4/23/14	298	6.7	128	188	333
4/26/14	298	3.8	130	159	335
4/29/14	298	2.2	90	118.4	338
5/1/14	298	2.9	118.4	195	339
5/3/14	298	2.8	190	120	343
5/5/14	298	2.6	272.3	65	343
5/7/14	298	1	291.1	68	370
5/9/14	298	3.3	299	66	370
5/12/14	298	10.1	221	163	423
5/14/14	298	3.1	165	153	384
5/16/14	298	14.4	166	173	384
5/21/14	298	2	310	24	343
5/23/14	298	0	350	13	356

Dates	G (1/s)	R2 Effluent NH4-N, mg/L	R2 Effluent NO3-N, mg/L	R2 Effluent NO2-N, mg/L	R2 Influent NH4-N, mg/L
5/26/14	298	3.1	292	151	394
5/27/14	298	1.6	375	28	394
5/30/14	298	8.2	322	100	410
6/2/14	298	6.4		126	410
6/5/14	298	2	400	20	413
6/8/14	298	2.2	390	15.7	365
6/10/14	298	5.9	356	40	374
6/12/14	298	1.4			374
6/15/14	298	1.2	7	360	376
6/17/14	298	1.6	8	380	376
6/19/14	298	1.3	400	5	420
6/22/14	298	10.6	196	195	420
6/26/14	298	2.6	268	145	425
6/30/14	298	2	356	105	425
7/1/14	298	2.1	348	48	425
7/3/14	298	1.9	378	17	425
7/5/14	298	1.9	392	8	425
7/7/14	298	0.9	402	6	425
7/8/14	298	1.3			461
7/11/14	298	69	164	154	459
7/13/14	298	6	196	179	399
7/15/14	298	1.2	374	5	399
7/17/14	298	1.7		6	399
7/19/14	298	0.9		7	399
7/21/14	298	1.8		8	399
7/23/14	298	0.01	190	131	397
7/25/14	298	30.7	174	190	413
7/26/14	298	14	189	205	413
7/28/14	298	4.3	190	195	408
7/31/14	298	6.3	200	221	448
8/2/14	298	11.7	198	259	486
8/4/14	298	5	189	273	493
8/6/14	298	43	168	285	512
8/9/14	298	50			512
8/11/14	298	1.1	326	8.2	324
8/18/14	298	0.8	250	1	242
8/30/14	298	300	209	230	715
9/5/14	298	0.5	244	1.2	242
9/8/14	298	0.5	248	1.1	242
9/11/14	298	0.4	278	1	277
9/14/14	298	0.4	273	7	277
9/15/14	298	0	300	1	277
9/19/14	298	334	180	209	770
10/6/14	298	1.1	242	1	250
10/11/14	298	1.1	250	110	370
10/13/14	298	0.2	256	0	250
10/20/14	298	1.3	240	1.3	243
10/23/14	298	181	187	274	660
10/26/14	298	0.5	246	11	240
11/3/14	298	123	180	288	660
11/4/14	298	138	178	285	660

Dates	G (1/s)	R2 Effluent NH4-N, mg/L	R2 Effluent NO3-N, mg/L	R2 Effluent NO2-N, mg/L	R2 Influent NH4-N, mg/L
11/8/14	298	206	312	113	660
11/9/14	298	0.1	7	234	240
11/13/14	298	1.4	290	6	300
11/17/14	298	1.1	274	7	300
11/19/14	298	0.9	264	9	300
11/28/14	298	1.5	280	22	300
12/3/14	298	0.8	312	0.8	293
12/7/14	298	1.3	310	0.9	316
12/9/14	298	0.7	306	1.2	302
12/15/14	298	0.6	348	0.8	302
12/18/14	298	1.4	312	5	302
12/23/14	298	1.6	350	0.7	350
12/29/14	298	1.3	355	0.8	350
1/2/15	298	0.7	378	0.8	350
1/8/15	298	1.5	458	0.9	400
1/16/15	298	0.6	434	0.8	400
1/19/15	298	0.6	400	0.8	400
1/23/15	298	1.9	340	0.53	280
1/27/15	298	0.8	322	0.46	280
1/30/15	298	131	298	139	600
2/2/15	298	114	165	309	600
2/5/15	298	210	153	305	600
2/9/15	298	84	157	383	600
2/12/15	298	117	186	290	600
2/16/15	298	183	281	187	600
2/18/15	298	149	380	122	600
2/23/15	298	256	360	20	600
2/24/15	298	275	340	17	600
3/7/15	298	310	336	8	604
3/10/15	298	110	434	5	604
3/11/15	298	149	452	7	604
3/15/15	298	165	440	14	604
3/18/15	298	525	67	9	600
3/21/15	298	0.7	150	6	150
3/23/15	298	70	140	6	200
3/24/15	298	50	168	58	345
3/25/15	298	34.6	157	128	345
3/27/15	298	105	132	195	464
3/31/15	298	83	158	192	512
4/5/15	298	60	139	291	456
4/11/15	298	130	107	230	440
4/14/15	298	81	104	217	440
4/20/15	298	123	105	240	440
4/25/15	298	126	110	250	450
5/5/15	298	158	128	150	450
5/6/15	298	125			400
5/7/15	298	80			400
5/8/15	298	82	194	148	400
5/13/15	298	150	139	153	430
5/20/15	298	105	130	137	400
5/30/15	298	1	220	200	400

Figure 3.4

	Concentration (ng/L, ppt)				
			03/08/15		06/05/15
Compound	**4/6/15**	**3/8/15**	**DuP**	**6/5/15**	**Dup**
PFOA	23	<18	<16	<24	<23
Clofibric Acid	<51	<33	<31	<17	30
Ditiazem	100	<210	<190	120	130
Meprobamate	130	140	140	150	150
Primidone	160	100	200	160	200
Triclocarban	310	170	190		
Carbamezapine	220	260	270	280	290
Trimethoprim	210	310	330	330	330
Hydracortisone	<280			370	270
TCEP		<580	<350	450	320
Bisphenol A	<170	<440	560		
DEET	500	220	220	2000	2000
Triclosan	1700	880	810		
Diphenhydramine	270	>2500	>2500	1700	1700
Benzophenone	>2500	<710	790	1200	1700
Atenolol	1200	1700	1200	1100	1200
Sulfamethoxazole	1500	1300	1400	1500	1500
Propylparaben	2200	1500	1700	1200	1200
Gemfibrozil	2100	2200	2200		
TCPP				4400	2300
Naproxen	>2500	>2500	>2500	19000	21000
Caffeine	>2500	>2500	>2500	70000	77000
Propranolol				<34	<34
Fluoxetine	<450			<160	<170
Dexamethasone	<9.1	<540	<790		
Atrazine	<39	<44	<41	<39	<45
PFOS	<14	<14	<14		
Ibuprofen	>2500	>2500	>2500		
Prednisone		<56	<47	<200	<240
Testosterone	<79	<110	<95	<510	<600
Simazine	<16	<18	<16	<16	<18

> over range

< Below detection limit

Figure 3.5

	Concentration (ppt, ng/L) 4/5/06
Fluocinolone acetonide	0.22
Dexamethasone	0.29
Betamethasone	0.57
Progesterone	3.7
Prednisone	4.49
17α-Ethynylestradiol	< 0.5
Methylprednisolone	6.5
Corticosterone	9.8
17α-Estradiol	11.2
Prednisolone	12.3
17-Hydroxyprogesterone	21.2
Triamcinolone acetonide	22.9
17β-Estradiol	29.9
Testosterone	35.8
Estrone	54.1
Hydrocortisone	159
Estriol	166
Cortisone	228
Bisphenol A	395
Norethindrone	< 0.2
Norgestrel	< 0.2

Figure 3.6

	Relative Abundance (Percent) 3/16/15 Synthetic Feed	6/10/15 Primary Effluent Feed
Unclassified; Unclassified; Unclassified; Unclassified	18.69	6.52
Proteobacteria; Betaproteobacteria; Nitrosomonadales ;Nitrosomonadaceae	15.82	2.69
Proteobacteria; Alphaproteobacteria; Rhizobiales; Bradyrhizobiaceae	14.66	4.00

	Relative Abundance (Percent) 3/16/15 Synthetic Feed	6/10/15 Primary Effluent Feed
Proteobacteria; Betaproteobacteria; Burkholderiales; Comamonadaceae	11.86	26.55
Actinobacteria; Actinobacteria; Actinomycetales; Microbacteriaceae	11.15	5.00
Proteobacteria; Gammaproteobacteria; Xanthomonadales; Xanthomonadaceae	5.10	7.28
Bacteroidetes; Flavobacteriia; Flavobacteriales; Flavobacteriaceae	3.42	8.54
Proteobacteria; Alphaproteobacteria; Rhizobiales; Phyllobacteriaceae	1.02	2.05
Bacteroidetes; Unclassified; Unclassified; Unclassified	0.29	4.36
Bacteroidetes; Flavobacteriia; Flavobacteriales; Cryomorphaceae	0.28	8.80
Proteobacteria; Alphaproteobacteria; Caulobacterales; Caulobacteraceae	0.20	0.21
Actinobacteria; Actinobacteria; Actinomycetales; Unclassified	0.03	0.01
Relative Abundance < 4%	17.50	23.99
	Shannon Diversity Index	
	2.58	2.87

Figure 3.7 - 3.8

	time (hrs)	R2A (0 mg/L ATU)	R2B (0.1 mg/L ATU)	R2C (0.4mg/L ATU)	R2D (3 mg/L ATU)
			Effluent Ammonia (mgN/L)		
4/6/15 13:15	0	49.8	51.4	49.4	50.8
4/6/15 14:45	1.5	43.4	47.6	48.2	50.2
4/6/15 16:15	3	37.7	42	46	48.9
4/6/15 17:45	4.5	33.3	42.6	48.6	49.2
4/6/15 19:15	6	25.9	41	49	48.6
			Effluent Nitrate (mgN/L)		
4/6/15 13:15	0	4	4.6	3.1	4.1
4/6/15 14:45	1.5	5.8	6.3	5.4	8.4
4/6/15 16:15	3	7.3	8.3	7	10.8
4/6/15 17:45	4.5	9.5	11.3	8.7	13.9

	time (hrs)	R2A (0 mg/L ATU)	R2B (0.1 mg/L ATU)	R2C (0.4mg/L ATU)	R2D (3 mg/L ATU)
4/6/15 19:15	6	10.9	14.4	9.8	15.4
			Effluent Nitrite (mgN/L)		
4/6/15 13:15	0	8.5	10.3	6.4	11.8
4/6/15 14:45	1.5	13	12.9	5.6	9.1
4/6/15 16:15	3	16.6	12.1	3.4	6.3
4/6/15 17:45	4.5	20.9	10.5	1.8	3.7
4/6/15 19:15	6	24.3	9.9	1	2.1
			Effluent DOC (mgN/L)		
4/6/15 13:15	0	50.32			47.56
4/6/15 14:45	1.5				41.80
4/6/15 16:15	3	40.13			38.19
4/6/15 17:45	4.5				29.40
4/6/15 19:15	6	33.22			23.70

Figure 3.9 - 3.10

	Concentration (ppt, ng/L)			Percent Removal	
	04/06/15 PE	R2A T = 6 hr	R2D T = 6 hr	R2A (Uninhibited)	R2D (Nitrification Inhibited)
Triclosan	1700	450	-	73.5%	
Propylparaben	2200	780	740	64.5%	66.4%
Triclocarban	310	110	200	64.5%	35.5%
Trimethoprim	210	120	210	42.9%	0.0%
Primidone	160	130	170	18.8%	-6.3%
PFOA	23	19	24	17.4%	-4.3%
Ditiazem	100	85	81	15.0%	19.0%
Sulfamethoxazole	1500	1300	1300	13.3%	13.3%
Gemfibrozil	2100	2000	2100	4.8%	0.0%
Atenolol	1200	1200	1000	0.0%	16.7%
DEET	500	500	490	0.0%	2.0%
Meprobamate	130	130	130	0.0%	0.0%
Carbamezapine	220	230	220	-4.5%	0.0%
Diphenhydramine	270	310	590	-14.8%	-118.5%
17β-Estradiol	29.90	< 1.0	< 1.0	96.6%	96.6%
17α-Estradiol	11.20	< 1.0	< 1.0	91.0%	91.0%
Testosterone	35.80	3.10	4.40	91.3%	87.7%
Estrone	54.10	37.50	42.10	30.7%	22.2%
Estriol	166.00	130.50	81.60	21.4%	50.8%

	Concentration (ppt, ng/L)			Percent Removal	
	04/06/15 PE	R2A T = 6 hr	R2D T = 6 hr	R2A (Uninhibited)	R2D (Nitrification Inhibited)
Triamcinolone acetonide	22.90	20.80	21.60	9.2%	5.7%
Hydrocortisone	159.00	147.00	145.00	7.5%	8.8%
Fluocinolone acetonide	0.22	0.21	0.26	4.5%	-18.2%
Bisphenol A	395.00	403.00	397.00	-2.0%	-0.5%
Methylprednisolone	6.50	7.15	8.09	-10.0%	-24.5%
Dexamethasone	0.29	0.33	0.23	-13.8%	20.7%
Betamethasone	0.57	0.65	0.68	-14.0%	-19.3%
Cortisone	228.00	328.00	417.00	-43.9%	-82.9%
17-Hydroxyprogesterone	21.20	31.20	20.20	-47.2%	4.7%
Prednisolone	12.30	28.60	43.20	-132.5%	-251.2%
Prednisone	4.49	11.60	17.20	-158.4%	-283.1%
Progesterone	3.70	15.50	12.10	-318.9%	-227.0%
Corticosterone	9.80	46.60	42.90	-375.5%	-337.8%

Figure 3.11

	Concentration (ppt, ng/L)		
	04/06/15 PE	04/06/15 Continuous Reactor	% Removal
Corticosterone	9.8	< 0.20	98.0%
17β-Estradiol	29.9	< 1.0	96.7%
Cortisone	228	8.87	96.1%
Testosterone	35.8	1.5	95.8%
Hydrocortisone	159	9.44	94.1%
Estriol	166	< 10	94.0%
17α-Estradiol	11.2	< 1.0	91.1%
Estrone	54.1	7.8	85.6%
Prednisolone	12.3	2.56	79.2%
17-Hydroxyprogesterone	21.2	4.6	78.3%
Progesterone	3.7	1.2	67.6%
Dexamethasone	0.29	0.11	62.1%
Prednisone	4.49	2.25	49.9%
Methylprednisolone	6.5	3.32	48.9%
Betamethasone	0.57	0.41	28.1%
Triamcinolone acetonide	22.9	17.8	22.3%
Fluocinolone acetonide	0.22	0.19	13.6%
Bisphenol A	395	368	6.8%

Appendix C: Chapter 4 Data

Figure 4.2

		mg/L-N			mg/L
	Influent Ammonia	**Effluent Ammonia**	**Effluent Nitrate**	**Effluent Nitrite**	**Attached Volatile Solids**
HDPE Reator					
9/12/15	47	33.5	18.8	2.0	
9/14/15	47	43.5	7.1	1.4	
9/16/15	47	43.5	3.2	1.4	
9/18/15	28.7	28.7	2.2	1.4	
9/20/15	28.7	25.1	1.4	1.4	
9/22/15	28.7	23	2.4	3.8	
9/24/15	28.7	22.4	3.4	3.8	
9/27/15	27.6	23.6	4.2	1.5	
10/1/15	27.6	22.7	6.4	0.9	
10/4/15	73	50	12.7	1.0	
10/6/15	73	50	20.0	1.1	
10/10/15	38	10	30.0	2.0	
10/15/15	38	5.4	36.8	3.4	
10/19/15	55	1.2	58.0	0.9	
10/22/15	75.3	1.4	84.5	1.2	
10/26/15	111.2	21.6	92.0	3.3	
10/31/15	111	21.6	106.9	3.3	
11/5/15	111	14.5	114.3	2.3	
11/9/15	111	10	115.0	2.0	147
Nylon Reactor					
9/12/15	47	38	8.9	1.4	
9/14/15	47	45.8	2.3	1.3	
9/16/15	47	46.7	0.8	0.9	
9/18/15	28.7	28.7	0.6	0.8	
9/20/15	28.7	27.7	0.6	1.8	
9/22/15	28.7	23	1.0	2.9	
9/24/15	28.7	24	1.2	3.9	
9/27/15	27.6	24.1	1.5	2.7	
10/1/15	27.6	24.2	2.3	2.3	
10/4/15	73	48	6.5	3.2	
10/6/15	73	44.7	15.1	3.5	

	mg/L-N				mg/L
	Influent Ammonia	Effluent Ammonia	Effluent Nitrate	Effluent Nitrite	Attached Volatile Solids
10/10/15	38	0.9	30.0	3.5	
10/15/15	38	0.9	46.8	0.9	
10/19/15	55	0.7	56.7	2.9	
10/22/15	75.3	0.9	87.5	2.9	
10/26/15	111	8.6	89.1	22.2	
10/30/15	111	3.1	108.5	16.9	
11/5/15	111	19.3	80.1	26.0	
11/9/15	111	15	93.0	20.0	48

Figure 4.3

	% Relative Abundance	
	10/26/15 Nylon	10/26/15 HDPE
Proteobacteria; Alphaproteobacteria; Rhizobiales; Rhizobiaceae	34.3	1.4
Proteobacteria; Alphaproteobacteria; Rhizobiales; Hyphomicrobiaceae	12.6	18.2
Proteobacteria; Alphaproteobacteria; Rhizobiales; Phyllobacteriaceae	5.8	3.8
Proteobacteria; Alphaproteobacteria; Rhizobiales; Bradyrhizobiaceae	5.0	2.8
Proteobacteria; Alphaproteobacteria; Sphingomonadales; Sphingomonadaceae	5.2	6.6
Proteobacteria; Betaproteobacteria; Burkholderiales; Comamonadaceae	8.5	4.9
Proteobacteria; Betaproteobacteria; Nitrosomonadales; Nitrosomonadaceae	3.8	0.6
Proteobacteria; Betaproteobacteria; Rhodocyclales; Rhodocyclaceae	2.5	5.9
Proteobacteria; Gammaproteobacteria; Xanthomonadales; Xanthomonadaceae	1.4	12.9
Actinobacteria; Actinobacteria; Actinomycetales; Microbacteriaceae	6.6	0.8
Bacteroidetes; Sphingobacteriia; Sphingobacteriales; Unclassified	0.9	3.3

	% Relative Abundance 10/26/15 Nylon	10/26/15 HDPE
Bacteroidetes; Flavobacteriia; Flavobacteriales; Cryomorphaceae	0.3	6.6
Relative Abundance < 3%	6.3	24.3
Unclassified	6.8	8.0

Figure 4.4

	Concentration (mg/L-N)			
	Influent Ammonia	**Effluent Ammonia**	**Effluent Nitrate**	**Effluent Nitrite**
HDPE				
6/7/16	8.6	5.3	1.9	1.8
6/9/16	10.0	6.1	1.3	2.3
6/14/16	12.2	5.4	2.4	3.4
6/20/16	16.0	8.8	2.6	3.4
7/4/16	17.2	0.6	17.0	1.1
7/14/16	20.1	0.4	21.4	0.7
7/27/16	20.1	0.4	18.2	0.8
8/4/16	23.4	0.6	23.9	0.8
8/9/16	23.4	0.4	23.1	0.8
8/15/16	23.4	0.4	22.0	0.8
8/18/16	23.4	0.3	24.1	1.0
8/22/16	25.0	0.3	26.5	0.8
8/27/16	48.0	0.5	54.2	1.4
9/7/16	48.0	0.3	40.7	3.6
9/10/16	50.0	1.0	33.0	21.1
9/16/16	50.0	0.3	32.1	23.9
9/22/16	50.0	0.1	53.2	4.9
9/27/16	65.0	0.1	65.9	1.9
10/2/16	65.0	0.3	59.3	2.2
Nylon				
6/7/16	8.6	3	4.8	1.2
6/9/16	10	6.1		
6/14/16	12.2	0.77	18.3	0.6
6/20/16	16	8	7.0	5.3
7/4/16	17.2	0.6	20.9	1.5
7/14/16	20.1	0.3	7.5	3.2
7/27/16	20.1	0.5	17.7	0.8

	Concentration (mg/L-N)			
	Influent Ammonia	**Effluent Ammonia**	**Effluent Nitrate**	**Effluent Nitrite**
8/4/16	23.4	0.4	24.8	0.8
8/9/16	23.4	0.4	24.5	0.7
8/15/16	23.4	0.4	24.4	0.8
8/18/16	23.4	0.2	23.6	0.9
8/22/16	25	0.2	25.6	1.1
8/27/16	48	0.9	54.1	2.9
9/7/16	48	0.2	41.2	1.5
9/10/16	50	0.1	54.0	1.6
9/16/16	50	0.3	54.6	2.5
9/22/16	50	0.4	51.2	3.0
9/27/16	65	0.2	53.4	2.1
10/2/16	65	0.1	77.7	2.2

Triclosan Calibration

Standard Concentration (mg/L)	**Area (mAU*min)**
0	0
5	10363.6
2.5	4535.6
1	2425.5
0.5	1094.9
RSQ	0.9926
Slope (mAU*min*L*mg^{-1})	2023

Caffeine Calibration

Standard Concentration (mg/L)	**Area (mAU*min)**
5	8889.44
2.5	4509.4
1	1928.18
0.25	404
0	0

RSQ	0.9996
Slope (mAU*min*L*mg^{-1})	1778

Figure 4.5

	Removal Rate (ug/L*hr)	
	Nylon Biofilm	**HDPE Biofilm**
Caffiene 200 ug/L Test 1	12.2	2.4
Caffeine 80 ug/L Test 2*	-0.2	-0.5
Triclosan 100 ug/L Test 1	58.9	28.2
Triclosan 100 ug/L Test 2	42.0	31.3

Figure 4.6

Sample	Peak Area (mAu*min)	Concentration Measured (mg/L)	Sample Volume (mL)	Elution Volume (mL)	Calculated Triclosan Sample Concentraion (ug/L)
Before Dose	0	0	100	12	0
After After Dose	1435	0.718	100	12	86.1
After Dose Dup	1294	0.647	100	12	77.6
Rnylon T=1	1017	0.508	100	12	61.0
Rnylon T=61	303	0.152	100	12	18.2
Rnylon T=61 Dup	331	0.165	100	12	19.9
Rhdpe T=1	1218	0.609	100	12	73.1
Rhdpe T=1 Dup	1067	0.533	100	12	64.0
Rhdpe T=61	565	0.282	100	12	33.9
Rhdpe T=61 Dup	679	0.339	100	12	40.7

Time (min)	Average Triclosan Concentration (ug/L)	Removal
Nylon Biofilm		
0	81.9	0.0%
1	61.0	25.5%
61	19.0	76.8%
HDPE Biofilm		
0	81.9	0.0%
1	68.5	16.3%
61	37.3	54.5%

Figure 4.7

	Peak Area (mAu*min)	Concentration Measured (mg/L)	Sample Volume (mL)	Elution Volume (mL)	Calculated Triclosan Sample Concentraion (ug/L)
Before Dose	0	0.000	100	10	0.0
After After Dose	2231	1.115	100	10	111.5
After Dose Dup	2071	1.036	100	10	103.6
Rnylon T=1	1737	0.868	100	10	86.8
Rnylon T=1	1725	0.863	100	10	86.3
Rnylon T=61	1069	0.534	100	10	53.4
Rnylon T=61 Dup	1201	0.601	100	10	60.1
Rhdpe T=1	1783	0.892	100	10	89.2
Rhdpe T=1 Dup	1688	0.844	100	10	84.4
Rhdpe T=61	1626	0.813	100	10	81.3
Rhdpe T=61 Dup	1641	0.821	100	10	82.1

Time (min)	Average Triclosan Concentration (ug/L)	Removal
Nylon		
0	107.5	0.0%
1	86.5	19.5%
61	56.7	47.2%
HDPE		
0	107.5	0.0%
1	86.8	19.3%
60	81.7	24.1%

Figure 4.8

	Peak Area (mAu*min)	Concentration Measured (mg/L)	Sample Volume (mL)	Elution Volume (mL)	Calculated Caffeine Sample Concentraion (ug/L)
Before Dose	0	0.000	100	10	0.0
After After Dose	1454	0.814	100	10	81.4
After Dose Dup	1491	0.834	100	10	83.4
Rnylon T=1	1354	0.758	100	10	75.8
Rnylon T=1	1386	0.776	100	10	77.6
Rnylon T=61	1386	0.776	100	10	77.6
Rnylon T=61 Dup	1391	0.779	100	10	77.9

	Peak Area (mAu*min)	Concentration Measured (mg/L)	Sample Volume (mL)	Elution Volume (mL)	Calculated Caffeine Sample Concentraion (ug/L)
Rhdpe T=1	1329	0.744	100	10	74.4
Rhdpe T=1 Dup	1359	0.760	100	10	76.0
Rhdpe T=61	1344	0.752	100	10	75.2
Rhdpe T=61 Dup	1355	0.758	100	10	75.8

Time (min)	Average Caffeine Concentration (ug/L)	Removal
HDPE		
0	82.4	0.0%
1	75.2	8.7%
121	75.5	8.3%
Nylon		
0	82.4	0.0%
1	76.7	7.0%
121	77.7	5.7%